SAPIENZA
UNIVERSITÀ DI ROMA

IMPROVEMENT OF RAILWAY TRACK DIAGNOSIS USING GROUND PENETRATING RADAR

Francesca De Chiara

Master of Science in Civil Engineering

SUPERVISERS:

Antonio D'Andrea - *Full Professor at "Sapienza" University of Rome-*

Simona Fontul - *PhD, Research Officer at LNEC-*

Eduardo Fortunato - *PhD, Senior Research Officer at LNEC-*

Dissertation partially developed at *Laboratório Nacional de Engenharia Civil* (LNEC), submitted to the *University of Rome "Sapienza"* for the degree of Doctor of Philosophy in Civil Engineering

Francesca De Chiara
Improvement of railway track diagnosis using Ground Penetrating Radar,
May 2014

IMPROVEMENT OF RAILWAY TRACK DIAGNOSIS USING GROUND PENETRATING RADAR

ABSTRACT

The scope of this research is to provide an improved procedure for track railways monitoring, which should be an alternative to the one commonly used in Portugal and in others European countries.

The traditionally approach for track maintenance corrects the track geometry withouth finding out the causes of geometric defects, namely the ones related with the foundation condition. The methodology proposed in this research aims to determining the real causes of track degradation through the application of a non-destructive equipment, the Ground Penetrating Radar (GPR).

The GPR is widely used for road applications while for railways applications it is still under development. Among its advantages, it enables performing measurements in a continuous way, reducing traffic interruptions, and it allows for subsurface layers characterisation in terms of layers thicknesses. On the other hand, as its application is still quite recent in this field, special care is still needed before, during and after tests performance.

In particular, for GPR data intepretation, a calibration study for track materials characterisation is always needed. In situ test pits and laboratory tests are performed and presented in this thesis.

The proposed methodology consists in correlating track geometric parameters with GPR data. It intends to provide an efficient tool for supporting maintenance decisions at network level. In this way, it aims to contribute for the identification of crtical areas and for prediction of track defects, in a more efficient way comparing to the methodology currently performed.

IMPROVEMENT OF RAILWAY TRACK DIAGNOSIS USING GROUND PENETRATING RADAR

RIASSUNTO

Lo scopo della presente ricerca consiste nel proporre una procedura innovativa per il monitoraggio delle sedi ferroviarie, che sia un'alternativa a quella comunemente usata in Portogallo e in altri Paesi Europei.

La metodologia di manutenzione generalmente usata, provvede a correggere la geometria del binario senza interrogarsi propriamente sulle cause dei difetti geometrici, in particolare quelle relazionate con la condizione degli strati costituenti la pavimentazione ferroviaria. La metodologia di indagine proposta nella presente ricerca si pone quindi come obiettivo la determinazione delle cause reali dei difetti geometrici del binario attraverso l'applicazione di una strumentazione non distruttiva, il georadar (GPR).

Il GPR è uno strumento ampiamente usato in campo stradale mentre, nelle applicazioni ferroviarie, è in via di sviluppo. Tra i vantaggi che presenta vi sono le capacità di effettuare misurazioni in continuo, limitando le interruzioni alla circolazione. Inoltre, permette la caratterizzazione della sede ferroviaria, determinando gli spessori degli strati che la compongono. Di contro, dato che la sua applicazione in campo ferroviario è abbastanza recente, attenzioni speciali devono essere prese in considerazione prima, durante e dopo lo svolgimento di ogni test.

In particolare, per effettuare una corretta interpretazione dei dati del GPR, è sempre necessaria la fase di calibrazione al fine di caratterizzare i materiali che costituiscono la sede ferroviaria. A questo scopo, durante la ricerca sono stati effettuati pozzi di sondaggio *in situ* e prove di laboratorio.

Il metodo procedurale proposto consiste nel correlare i parametri geometrici del binario con i dati del GPR, con lo scopo di avere informazioni valide a supportare le decisioni in merito agli interventi di manutenzione della rete ferroviaria. Si vuole pertanto contribuire all'identificazione delle zone critiche e anche prevedere difetti futuri, in un modo più efficiente a quanto normalmente oggi viene fatto.

IMPROVEMENT OF RAILWAY TRACK DIAGNOSIS USING GROUND PENETRATING RADAR

RESUMO

O objetivo da pesquisa consiste em propor uma metodologia inovadora para a monitorização das infraestruturas ferroviárias, que seja uma alternativa à que é geralmente usada em Portugal e noutros países Europeus.

A metodologia de manutençao tradicionalmente usada visa corrigir a geometria da via sem perceber as causas dos defeitos geométricos, em particular os relacionados com a condição da fundação. A metodologia que se propõe tem como objetivo a determinação das causas reais dos defeitos geométricos, através da aplicação de um método não destrutivo, o georadar (GPR).

O georadar è um método que tem sido usado com sucesso nas infraestruturas rodoviárias, mas no domínio ferroviário está ainda em fase de desenvolvimento. Uma das vantagens que tem é a possibilidade de permitir fazer medições em continuo, limitando o número de interrupções na circulação. Permite caracterizar a via em termos de espessuras das camadas que a constituem. Porém, sendo a sua aplicação neste domínio ainda bastante recente, são necessários cuidados especiais antes, durante e depois da execução dos ensaios.

Em particular, para uma correta interpretação dos dados do GPR é necessário desenvolver uma fase de calibração para a caracterização dos materiais que compõem a infraestrutura. Com tal objetivo, durante a pesquisa, foram realizados poços *in situ* e ensaios laboratoriais.

A metodologia proposta consiste em estabelecer relações entre os parâmetros geométricos da via e os dados do GPR, com o objetivo de obter informação que permita apoiar as decisões de intervenção de manutenção, ao nível da rede

ferroviária. Pretende-se assim contribuir para a identificação de zonas críticas e prever defeitos futuros, de uma forma mais eficiente, relativamente ao que tem vindo a ser feito.

To my nephews and sisters Viola, Filippo, Tommaso, Elisabetta and Silvia,

and to my parents Luciana and Antonio

Multa non quia difficilia sunt audemus,

sed quia non audemus sunt difficilia

(Seneca, Epist., 104, 26)

ACKNOWLEDGEMENTS

The present research has been developed and submitted to the University of Rome, under the supervision of Professor Antonio D'Andrea, Full Professor at Department of Civil, Constructional and Environmental Engineering. The aim part of the work was developed and performed at *Laboratório Nacional de Engenharia Civil* (LNEC) of Lisbon under the supervision of Dr. Simona Fontul, Research Officier at LNEC, and Dr. Eduardo Fortunato, Senior Research Officier at LNEC.

The author expresses gratitude to the following Institutions which contributed to the development of this dissertation:

The University of Rome and in particular the Department of Civil, Constructional and Environmental Engineering for the support given to the process and financial assistance;

The *Laboratório Nacional de Engenharia Civil,* in particular the Board of Directors and the Director of Transportation Department, Mr. António Lemonde Macedo, for enabling the possibility of developing/supporting the research constantly and for contributing to the laboratory tests performance;

The REFER Portuguese railways company, in particular Rui Burrinha, for his continuous support in performing in situ tests and for having provided materials.

The author also wishes to express her gratitude to all people who have given help and advice in this research. In particular:

Prof. Antonio D'Andrea for his support, trust and for having allowed the author to work in autonomy.

Dr. Simona Fontul, for her very useful teachings, guidance, encouragement and friendship.

Dr. Eduardo Fortunato, for his expert advices, guidance and support.

The colleagues from Department of Civil, Constructional and Environmental Engineering, for their support and friendship.

The colleagues from LNEC, for their constant support, encouragement and for their precious friendship, in particular Rui Coelho, André Paixao, Sandra Vieria Gomes, Carlos Lima Azevedo, André Lopes, Daniel Filipe, Joaquim Timóteo and technicians of the infrastructure and geotechnical laboratories.

The author acknowledges all the Italian friends, for the continuous support whenever necessary, in particular Giulia, Ciccio, Daniele, Marco, Laura and Raffaella.

Many acknowledgments to all Portuguese or "almost" Portuguese friends, older and newer, for their friendship and encouragements during all these years and for making the author feels at home, in particular David, Tiago, Beto, Raquel, Braghetto, Ana, Francesca and Manila.

A special acknowledgement goes to the author's inseparable family, always united in giving comprehension and serenity.

Last but not least, a special thank goes to Dario for his help and patience, the most special person, friend, and colleague, an exceptional guide in every situation and in every moment.

TABLE OF CONTENTS

LIST OF FIGURES

LIST OF TABLES

LIST OF ABBREVIATIONS AND SYMBOLS

ABBREVIATIONS

GPR – Ground Penetrating Radar;

FWD – Falling Weight Deflectometer;

LNEC - Laboratório Nacional de Engenharia Civil;

AASHTO – American Association of State Highway and Transport Officials;

AREMA – American Railway Engineering and Maintenance-of-Way Association;

ASTM – American Society for Testing and Materials;

GSSI – Geophysical Survey Systems, Inc.;

IDS – Ingegneria dei Sistemi;

LNEC E – LNEC Standards;

ORE – Office de Recherches et d'Essais de l'Union Internationale des Chemins de Fer;

REFER – Portuguese railways company;

UIC – Union Internationale des Chemins de Fer;

AMP – Ataco mecanico pesado (tamping intervention);

EM120 – Track Inspection Vehicle Plasser & Theurer;

RFI - Italian railways company;

RD – Railwaydoctor software.

SYMBOLS

E - electric field (V/m);

σ - conductivity (S/m);

D - displacement current;

ε - absolute dielectric constant of the medium (F/m);

B - magnetic induction;

μ - magnetic permeability (H/m);

H - magnetic field;

ω - angular frequency;

f - excited frequency;

γ - propagation constant;

α - attenuation constant;

β - phase constant;

v - wave velocity (m/s);

Z - wave impedance (Ω);

ε0 - dielectric constant of free space (8.854x10-12 F/m);

μ - absolute magnetic permeability (H/m);

μ0 - magnetic permeability of free space (4πx10-7 H/m);

μr - relative magnetic permeability of the material;

C - wave velocity in the free space (3 × 108 m/s);

T - transmission coefficient;

R - reflection coefficient;

h - layer thickness;

t - travel time;

εr - relative dielectric constant.

Other symbols are defined in the text if necessarily.

1. INTRODUCTION

1.1. BACKGROUND

Today railways have become a very competitive mean of transportation for long distances. During the last decades, they have been subjected to a great development in order to perform and satisfy higher traffic speeds, higher axle loads, higher availability. At the same time, passengers security, comfort and environmental demands have to be maintained to high levels (Anders Ekberg, 2010).

In particular, higher speeds result in an increase of the dynamic effects during operation, and consequently lead to a track quicker degradation. Also, climatic changes enable a faster track deterioration. These aspects result in a worse track performance that can also influence other railway components and it can increase the risk of derailment.

One of the means for reducing track deterioration consists in the construction of new tracks or in their renewal. Then, it becomes necessary to optimize the design of infrastructure, taking into account its entire life cycle, not only the construction phase (Fortunato, 2005). In fact it was shown that the track structural maintenance represents approximately 50% of the total cost of maintenance (Lopez-Pita et al., 2008). Regarding the renewal of the track, some European administrations have invested in the renewal of the existing lines, and, in this way, taking the advantage of using the existing corridors and substructures (Fortunato et al., 2007).

For existing tracks, during monitoring phase, performance parameters should be registered and then evaluated during the track life cycle. This information has to be analysed together with construction data and with maintenance and rehabilitation information, if available.

Today monitoring actions are usually performed by using track inspection vehicles (Esveld, 2001; Lichtberger, 2005), as they can reach speeds between 30 and 300 km/h, enabling an efficient track characterisation at network level and they consist in measuring mainly parameters related to the track layout and rail wearing through diagnostic trains. Inspection vehicles enable the evaluation of track condition and the detection of geometric defects that then are corrected, if needed. They present the main advantage of working at similar speeds and dynamic loads of regular trains, allowing to the track performance assessment in a more realistic way, compared with other methods, manually ones. Moreover, they allow recording measurements, of the longitudinal profile and the cross sections, in a continuous way, without traffic interdictions. Diagnostic trains can be equipped with optional accessories, such as rail and overhead wire recording, or more advanced technologies like GPR or ultrasonic. Data collection and processing is performed by using advanced computer systems that permit to register a great number of data and to simplify their interpretations. In fact, knowing reference values, an "in situ" data analysis can be done: information about quality conditions can be acquired in real time and, consequently, decisions can be made and maintenance plans can be programmed.

Nowadays, railway inspection must be performed more frequently, especially when high-speed trains are involved, in order to guarantee safety and reliability. Anyway, this procedure does not detect the real causes of a rail level deficiency, which can be generated by the presence of ballast pockets, fouled ballast, poor drainage, subgrade settlements and transitions problems (Manacorda et al. 2002; Fontul et al. 2011; Hyslip et al. 2012). Therefore, an important factor for maintenance decision is the substructure condition assessment. With this aim, suitable techniques have to be chosen. Non-destructive tests represent an efficient monitoring tool, as they allow to evaluate infrastructure characteristics in a continuous or quasi-continuous way, saving time and costs, enabling to make changes if tests results do not comply with the project requirements. For example equipment that are used successfully for pavements evaluation, such as Ground

Penetrating Radar (GPR) and Falling Weight Deflectometer (FWD), can be used also for railway evaluation (Fontul, 2004).

The Ground Penetrating Radar (GPR) is now a well-accepted geophysical tool (Jol, 2008) that uses electromagnetic waves to detect objects or interfaces buried under the earth surface (Daniels, 2004). In railways, its application is quite recent. In general, a radar works with two fixed antenna, one transmitter and one receiver, by sending electromagnetic waves into the ground and when a target is detected, part of the wave is reflected; then the receiver, located near the transmitter, picks up the reflected energy and gives information for detection (Jol, 2008). The distance to the detected object is determined by time gap between the moment of pulse emission and the moment of receiving of its echo. It is a versatile instrument that allows obtaining, with high precision, a continuous profile of the medium investigated, such as a natural soil or a road pavement, from which it is possible to acquire a lot of information in a short time. In fact, it can detect layers thicknesses, their variation, any discontinuity in the soil texture, cavities. GPR equipment consists in: a pair of antennas, a transmitter and a receiver, that are classified in different manners; a control unit that enables to collect the data, to control the radar operation, to display and save the results; and others accessories, such as GPS and digital video systems. After the data collection, they are transferred to a computer for processing. The accuracy of GPR results is related to velocity estimation that depends on the dielectric properties of materials, but generally these are not very easy to be determined, as they are influenced by several factors such as water content and, for railways studies, also ballast fouling. GPR data calibration is a crucial phase and for pavement studies, it can be performed with both the execution of cores/tests pits or GPR laboratory tests. In the last years, the development of new GPR systems with higher antenna frequencies, better data acquisition systems, more user friendly software and new algorithms for calculation of materials properties have been leading to a regular use of GPR, also for railways. In some countries, GPR tests have been performed along tracks with the aim of detecting zones with problems at both ballast level (fouling) and subsoil. First results have shown that GPR is a reliable technique to

assess track geometry problems and consequently to improve maintenance planning.

Most of European railways are old tracks where design has not been optimized and subgrade has been ignored for years. A better knowledge of these tracks through their investigation is required, with the aim to establish an acceptable level of quality and capacity (Anders Ekberg, 2010). For this scope, GPR may help to detect not only track characteristics, but also track defects, such as a soft subsoil layer, ballast fouling conditions, ballast pockets and trapped water (Hyslip et al., 2003).

A recent and innovative approach for improving track monitoring can consist in combining two non-destructive techniques: the diagnostic train and the GPR. Some countries have started to perform this procedure and to interpret data by using specific software, enable to create real datasets in which is possible reporting and representing all gathered information in a multiple sub-windows screens. Also in the present research, an alternative combination of the two approaches is presented.

1.2. OBJECTIVES

The main Ph.D. research scope consists in proposing an alternative and innovative procedure to the traditional monitoring procedure followed in Portugal. As the actual procedure treats the effects of track defects but not the causes, maintenance interventions can result inadequate and the maintenance intervention is limited to tamping. On the other hand, the proposed procedure aims to be a useful tool for detecting the causes of track defects at network level and, depending on them, maintenance interventions can be chosen ad hoc.

The new methodology aims to combine inspection vehicle geometric parameters with GPR data. For this scope, longitudinal profile and alignments are the two main parameters to be studied for detecting track defects, as referred by Portuguese Standards, namely their standard deviation values. Some upgrades are

proposed by the new methodology, as a continuous trend of standard deviation values that can be more useful than "punctual values" for a more accurate localisation of defects. In addition, the new procedure aims to study more consecutive campaigns with a systematic increment of standard deviation values, even if Standard limits for maintenance decision interventions are not overcome.

The most important innovation presented by the new methodology is the use of Ground Penetrating Radar. It was used as an additional but very important tool in correlation with the EM120 inspection vehicle. For data interpretation, an accurate calibration is necessary. Therefore, during the research, several tests were performed. Even if GPR limits the number of cores and test pits, for railways studies tests pits are strongly recommended. On the other hand, for new pavements GPR data interpretation can be done by considering dielectric constant values found in bibliography or determined with laboratory tests. In this thesis both laboratory tests and test pits are presented. In the first case, the aim is to test several materials, commonly used in Portuguese and European tracks, with GPR and dielectric constant values are determined. The dielectric constant values for different materials conditions, recreating the in situ conditions (dry, wet, clean, fouled), are compared and also the respective trends with their gradually variation. Test pits, performed along Portuguese tracks, are analyzed with the scope of determining clean and fouled ballast thicknesses and GPR responses in terms of reflections. A third alternative procedure is developed for a renewal track, which aim consists in determining different materials dielectric constant values, by knowing project thicknesses, for different climatic conditions.

It can be confirmed that, for the new procedure, laboratory tests and test pits results represent a helpful tool. By giving dielectric constant values to the interpreted layers, stretches with problems can be localised, not only longitudinally, as actual procedure defines, but also in depth. The knowledge of the depth of intervention is fundamental. In this way, the most appropriate intervention can be selected depending on the layer to be restored.

It can be concluded that the new methodology can be a useful tool for track maintenance policy along the entire life-cycle, as it enables:

- the identification of critical areas (longitudinally and in depth) and detection of the causes of geometric defects, such as subgrade settlements and fouling ballast at network level;
- the prediction of the defects: control of the increase of geometric parameters in different campaigns for studying the evolution of track degradation with improvement of the maintenance policy (cost management);
- the choice of the best intervention;
- the evaluation of the quality of the interventions;
- the decrease of interventions number, resulting in cost savings and less traffic interruptions.

1.3. OUTLINE OF DISSERTATION

The PhD thesis is composed by 7 chapters, including the Introduction presented in Chapter 1.

Chapter 2 presents the state of the art of GPR non-destructive test. The first section is dedicated to its application fileds: from the older to the more recent. Then, a presentation of the components, in particular of antennas, is done. The principles of electromagnetic theory, on which GPR is based, is described. Also, materials characterisation through GPR and the concept of dielectric constants are mentioned as they represent a key aspect for the entire research. Finally, GPR data collection, processing and interpretation phases are addressed.

Chapter 3 regards railway monitoring procedure and track assessment. The traditional method, represented by the diagnostic train, is addressed. Several equipment are presented and in particular the inspection vehicles used on the Italian railways are presented. Then, a wider section is dedicated to EM120 diagnostic train performed in Portugal: its components and their functions are

described. GPR equipment is one of the last improvements for the EM120. A specific paragraph is addressed to the GPR application on railways. Considerations about the test preparation and data interpretation, together with the last software for data acquisition and interpretation are made. Finally, the specific software used in this research for data interpretation is explained in detail.

A great part of the research was developed in laboratory and presented in Chapter 4. First, a state of the art of materials classification, in particular ballast material, GPR laboratory tests and results in terms of dielectric constant values for road and railway materials is presented. Then, a description and characterisation of the materials tested at LNEC is made. Different antenna systems were used and their functions and characteristics are described. Finally, GPR tests preparation for three different materials and respective results are presented and compared.

Chapter 5 addresses the in situ calibration. In the first part, particular attention is dedicated to ballast material characterisation with GPR, that represents still a challenge. The latest developments presented in literature are reported. Then, a Portuguese case study is described for determining the dielectric constant values of different materials existing in a renewal track and an alternative procedure is developed for this scope. Test pits execution and their interpretation with GPR is described, together with a verification analysis of results.

In Chapter 6 track maintenance is described. First, the track degradation phenomenon focused on ballast, sub-ballast and subsoil layers problems is mentioned and then the suitable interventions depending on the causes of the degradation. In a second part, maintenance policy and European Standards are presented. A particular section is dedicated to actual Standards, monitoring procedure and maintenance interventions decisions followed in Portugal. Some peculiarities are mentioned and then the reason of developing a new methodology for monitoring by using GPR, that is presented in the third part. Three case studies are analysed with the actual and new procedure and compared.

Finally, Chapter 7 reports the conclusions of the research, together with some future developments.

2. GROUND PENETRATING RADAR

2.1. GENERAL PRESENTATION

The Ground Penetrating Radar (GPR) is now a well-accepted geophysical tool (Jol, 2008) that uses electromagnetic waves to detect objects or interfaces buried under the earth surface (Daniels, 2004). The word "Radar" comes from an English denomination "RAdio Detecting And Ranging" used to indicate equipment able to make measurements of objects position by transmitting electromagnetic waves. In general, a radar works with two fixed antenna, one transmitter and one receiver, by sending electromagnetic waves into the ground and when a target is detected, part of the wave is reflected; then the receiver, located near the transmitter, picks up the reflected energy and gives information for detection (Jol, 2008). The distance to the detected object is determined by time gap between the moment of pulse emission and the moment of receiving of its echo (Figure 2.1).

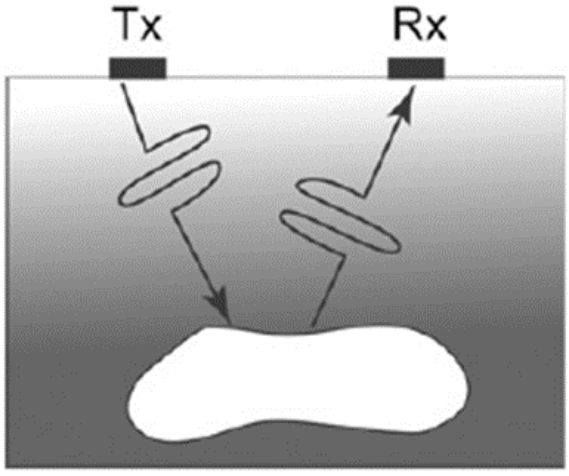

Figure 2.1 - GPR operation (Jol, 2008)

GPR is based on the same principle of conventional radars, but there are some differences:

In conventional radar, the emitted electromagnetic wave propagates in air; while in the radar applied for ground introspection, wave propagates in soil or other solid materials (Peters Jr et al., 1994):

- In general, conventional radars use a single antenna while most GPR systems use two separate antennas (Jol, 2008);
- Unlike conventional radars that identify targets at long distance (some kilometers), GPR presents only a limited penetration (centimetres or few meters) (Jol, 2008; IDS, 2013);
- Resolution also changes: for conventional radars it can reach up to some hundreds of meters, while GPR can detect with precision some centimetres (IDS, 2013).

It is a versatile instrument that allows obtaining, with high precision, a continuous profile of the medium investigated, that can be either a natural soil, or a road pavement, or a wall, from which it is possible to acquire a lot of information in a short time. In fact, it detects and localises the presence of objects, buried structures, cavities, or of any discontinuity in the soil texture.

2.1.1. Historical background

The first GPR experiment was made by Hülsmeyer in 1904 with the scope of detecting metal objects (Daniels, 2004). In the 1920s radar was commonly applied for military use, with the objective to detect non-metallic mines, but it was necessary waiting more 30 years, for the first successful measurements related to earth science problems. Moreover, after the 2ndWar, its use grew quickly and extensively, especially by using technology of war origins such as metal detector, electromagnetic detection systems and radar. In the 1960s applications in Arctic and Antarctic areas with pulsed radar altimeters showed very good results in terms of dielectric characteristics, loss factors, scattering of thick ice (Waite and

Schmidt, 1962). This represented an important event as consecutive experiments were performed for sounding soils and rocks (Jol, 2008). In the 1970's the first infrastructure applications occurred, in particular in tunnels and on bridge decks (Saaranketo, 2006).

During '50 and '60 equipment and devices were complex, bulky and required a long time for data acquisition. Recently, the significant technological developments of electronics and computers have permitted innovative applications also in the geophysics investigation area, in particular applied to geological and archaeological fields and also to building and civil ones. Modern equipment have reduced dimensions, are portable and easy to use. Then, they are characterised by organization and automatic control of data acquisition process and also by electronic memories able to create a database of registered values. Through simple operations, measured data are directly transferred to a computer for automatic processing and graphic reconstruction, where trend and morphology of the curves, or different coloured samples, displayed several buried structures.

2.1.2. GPR applications

The GPR is used in various areas ranging from civil engineering to geology, archaeology to environment (The Finnish Geotechnical Society, 1992), therefore equipment have to be built "ad hoc" for its different uses, enabling the user to make the best choice (Daniels, 2004).

The main applications of GPR nowadays are presented below.

In civil engineering:

- Studies of transportation infrastructures in terms of layer thicknesses or changes in structure (road, railways and airfields);
- Location of various types of underground utilities (metal or plastic pipes, electric cables, optical fiber cables, sewers, cuniculi, etc.);

- Structural controls on artifacts, identifying cracks, detached surfaces, areas of materials degradation;
- Detection and recognition of types of reinforcements and inspection of structures (such as tunnels, viaducts, bridges, dams, etc.);
- Research and identification of buried structures for planning excavation and reconstruction works.

In geology:

- Determination of subsoil nature and geometry, localisation of rocky masses, rocky boulders, karst cavities, etc.;
- Measurement of ice sheet thickness;
- Identification of numerous discontinuities (faults, fractures, joints, etc.).

In archaeology:

- Discovery of masonry structures, artifacts, burial chambers, findings of different types;
- Testing and evaluations for licenses granting in archeological restricted areas.

2.2. EQUIPMENT

2.2.1. General considerations

GPR systems present different characteristics depending on the area where are applied. First, the choice of the antennas, such as their frequency and configuration, is a crucial aspect in survey planning. This choice depends on several factors: target dimensions, electrical properties of the medium, characteristics of the surface and the testing zone. Best results are obtained considering a suitable: signal to clutter ratio, signal to noise ratio, spatial resolution and depth resolution of the target (Daniels, 2004).

Moreover, a lower frequency enables to achieve a greater depth of penetration but presents a reduced resolution. Table 2.1 presents the relationship between penetration depth, frequency and suitable application.

The GPR system is usually composed by: one or more antennas, a control unit, a computer, and accessory equipment. Figure 2.2 presents a general scheme of radar functioning.

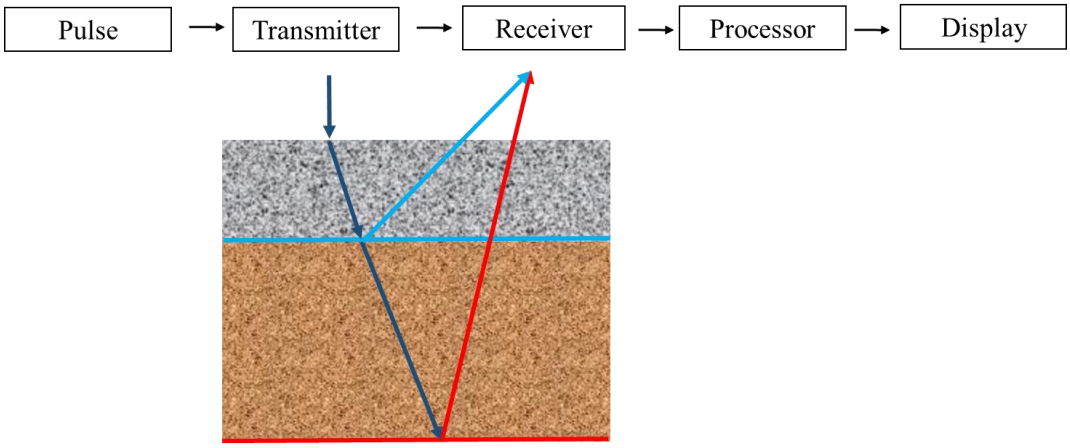

Figure 2.2 - General scheme of radar system

Generally, the GPR antennas consist of a transmitter and a receiver and they are classified in different manners. One classification is based on their location relative to the ground, for example: ground-coupled and air-coupled. They have different ranges of frequencies and consequently different penetration depths and resolutions, given that a higher frequency reaches a lower penetration but provides a higher resolution (Fontul, 2004). They present also several sizes and dimensions. These systems are similar in terms of operating principles.

Another antennas classification is based on their operation: monostatic, bistatic (Figure 2.3) and cross-polarized. The monostatic mode is when transmitter and receiver are joint in a single structure, enabling to obtain information of the entire zone and to detect targets depth; with bistatic operation the two antennas are separate, at a certain distance, depth penetration is higher but there is loss of

information in a gap "d" function of the two antennas; in a cross-polarized scheme transmitter and receiver are perpendicular and it is efficient for detecting sloping target relatives to the antennas operation direction.

Table 2.1 - Frequency antennas, penetration depths and applications (Leucci, 2008)

Approximate Depth Range	Primary Antenna Choice	Secondary Antenna Choice	Appropriate Application
0 - 0.5	1600 MHz	900 MHz	Structural Concrete, Roadway, Brdige, Decks
0 - 1 m	900 MHz	400 MHz	Concrete, Shallow Soils, Archaelogy
0 - 9 m	400 MHz	200 MHz	Shallow Geology, Utilities, UST's, Archaelogy
0 - 9 m	200 MHz	100 MHz	Geology, Environmental, Utility, Archaeology
0 - 30 m	100 MHz	Sub-Echo 40	Geologic Profiling
≥ 30 m	MLF (80, 40, 32, 20, 16 MHz)		Geologic Profiling

Then, a control unit enables to collect the data, to control the radar operation, to display and save the results. After the data are collected, they are transferred to a computer for processing (Figure 2.4).

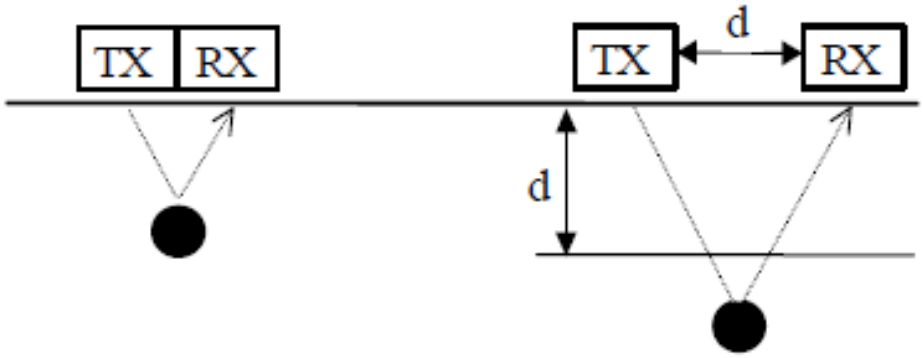

Figure 2.3 - Antennas configuration: monostatic (left) and bistatic (right) (IDS, 2013)

(a) (b)

Figure 2.4 - GPR equipment: (a) antennas (Fontul et al., 2011) and (b) control unit

Among the accessory equipment, the most used are a global positioning system (GPS) and digital video systems. The first is very important because results have to be related with the survey line and a distance correction is often necessary also if different lanes have to be compared. In general, GPS coordinates are linked with

GPR scan numbers and modern software allows for distance adjustment during data processing.

Digital video recording enables a better visualization of survey area and therefore a better interpretation, identifying particular structures, such as switches and culverts. Recently, advanced systems like thermal cameras and laser scanner technology have been used for detecting moisture content in materials and cracks in asphalt pavements (Saarenketo et al., 2012). Also infrared thermography has been performed on railways (Max Clark et al., 2004) and on concrete bridge decks for identifying air pockets in the material (Hing and Halabe, 2010).

2.2.2. Ground-coupled antennas

Ground-coupled antennas present a frequency ranging from 80 to 1500 MHz, their signal is very strong enabling to achieve greater depth of penetration, up to 30 m (Highways Agency, 2001; Saarenketo, 2006). In transport infrastructures studies, frequencies between 400 MHz and 1500 MHz are generally used with good results (TRB, 1998).

During surveys, the ground-coupled antennas are in contact with pavement, or very close to its surface, reaching a maximum test speed of about 15 km/h (Saarenketo and Scullion, 2000). This may represent a disadvantage and, to overcome this aspect, antennas can be suspended achieving a maximum speed test of about 20 km/h. In this latter case, special attention should be paid to the gap between the antenna and the surface, as the smaller the air gap the better are the results (Fontul et al., 2012a).

Among the advantages of ground-coupled antennas is, on one hand, a high signal penetration even if the presence of surface coupling and antenna ringing require signal processing. However, they are usually used in geological investigations, for discovering cavities, stratigraphy and fracture zones. On the other hand, these antennas presents a better vertical feature resolution, such as crack detection,

comparing with the air-coupled antennas, and this permits to detect pavement cracks and cables (Scullion and Saarenketo, 1998).

Ground-coupled antennas main manufacturers for road and railway infrastructures assessment are GSSI (USA), IDS (Italy), MALA (Sweden), Penetraradar Corporation (USA), Sensors and Software (Canada) and UTSI Electronics (United Kingdom) (Sebesta et al., 2013). Figure 2.5 presents the GSSI ground-coupled antennas used in this study.

2.2.3. Air-coupled antennas

Air-coupled antennas operate in the range between 500 and 2500 MHz and, in general, their signal can penetrate up to 0.9 m and 0.5 m, respectively. During data collection they are suspended at about 0.3-0.5 m above the pavement surface and can be installed on a trailer or directly on the survey vehicle. In this way, higher test speeds can be achieved (up to 80-120 km/h) allowing the evaluation of the substructure at traffic speed. This factor represents a great advantage. For this reason, they are suitable for pavement studies at network level (Fontul et al., 2012a).

These antennas show a quite consistent signal and the main advantage consists in its repeatability, as coupling is constant for different pavement properties (Saarenketo, 2006).

The main manufacturers of air-coupled antennas are GSSI, Penetraradar, Pulse Radar and Wavebounce, all from USA, and Euradar systems have also been used in pavement surveys in the Netherlands (Sebesta et al., 2013).

LNEC's equipment has two GSSI horn antenna pairs, namely with 1000MHz and 1800 MHz frequencies (Figure 2.6).

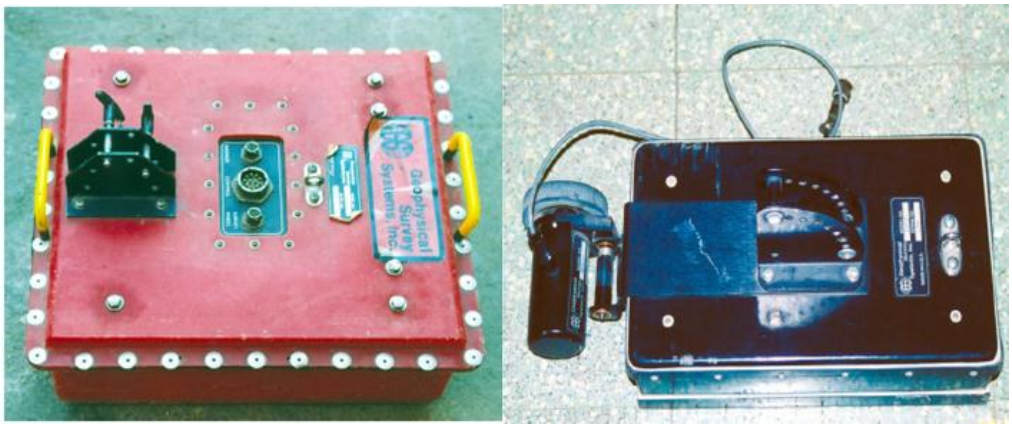

Figure 2.5 - Antennas of 500 MHz (left) and 900 MHz (right) (Fortunato, 2005)

Figure 2.6 - LNEC's GSSI air-coupled antennas

2.3. THEORETICAL PRINCIPLES

2.3.1. Introduction

GPR operation principle is based on electromagnetic theory, its functioning consists in sending short electromagnetic pulses into a medium and when pulses achieve an interface they are reflected back partially and collected by the receiving

antenna (Figure 2.7). The reflected energy is displayed in waveforms and the greatest amplitudes represent the interfaces between layers with distinct dielectric characteristics (Daniels, 2004; Saarenketo, 2006). Therefore, GPR measures the travel time between the transmission of the energy pulses and its reception.

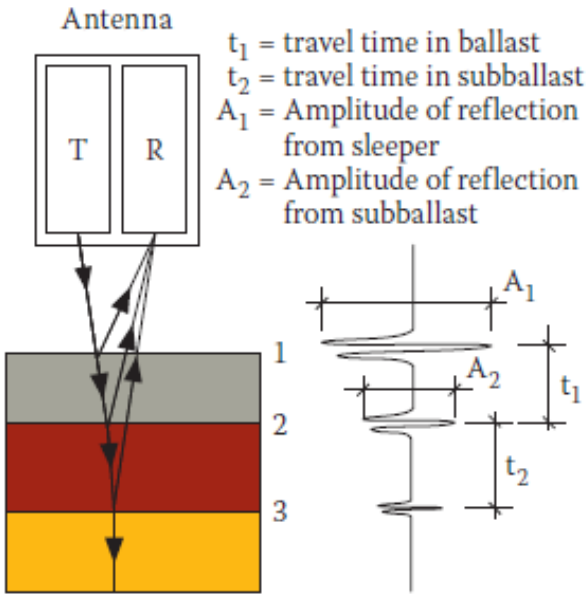

Figure 2.7 - GPR principles (Saarenketo, 2006)

Transmission and reception of radar pulses are performed from one or more antennas that are moved on the investigated medium (Sussmann et al., 2003; Hyslip et al., 2003). The collected data are processed and saved on a control unit, that is also used to generate the necessary pulses for the operation of the antennas (Fontul, 2004).

For a better understanding of equipment functioning, from electromagnetic waves transmission to their reflections displayed into colour or grayscale hues, it is necessary to describe the physical principles behind GPR operation.

2.3.2. Electromagnetic waves theory

GPR signals are electromagnetic waves. Maxwell's equations mathematically describe electromagnetic physics while constitutive relationships quantify medium properties: their combination enables a GPR signals description in a quantitative way (Annan, 1992).

Maxwell's Laws state that a dipole excited from a high frequency voltage generates an electric field parallel to the dipole. Electric charges, in motion inside the electric field, produce a magnetic field perpendicular to the dipole.

Constitutive laws allow describing a medium response to electromagnetic fields. For GPR, the electrical and magnetic properties are of importance.

There are two different types of current: conduction current and displacement current (Jol, 2008). The first one is produced by moving charges attracted by the electric field. The characteristic parameter is the conduction current intensity J_c, correlated to the electric field as presented bellow (Eq. 2.1):

$$J_c = \sigma \cdot E \qquad \text{Eq. 2.1}$$

Where:

- E is the electric field (V/m);
- σ is the conductivity (S/m), which is a measure of material's ability to conduct an electric current.

Displacement current depends on the distance between charges and it is directly proportional to the applied electric field through the absolute dielectric constant of the medium, as follows:

$$D = \varepsilon \cdot E \qquad \text{Eq. 2.2}$$

Where:

- D is the displacement current;
- ε is the absolute dielectric constant (permittivity) of the medium (F/m).

The dielectric constant of the material is a characteristic which describes how it affects any electric field set up in it and this capacity is also influenced by water content. A high dielectric constant value tends to reduce any electric field present (Daniels, 2004).

The third constitutive law describes the relationship between the magnetic field and the magnetic induction:

$$B = \mu \cdot H \qquad \text{Eq. 2.3}$$

Where:

- B is the magnetic induction;
- μ is the magnetic permeability, that represents a measure of the degree to which a material can be magnetized (H/m);
- H is the magnetic field.

Displacement current intensity J_P is given by:

$$J_p = \frac{dD}{dt} = \varepsilon \frac{dE}{dt} \qquad \text{Eq. 2.4}$$

The current that flows into a medium during a GPR test is the sum of conduction current and displacement current (Annan, 1992), as follows:

$$J = J_c + J_p \qquad \text{Eq. 2.5}$$

This relationship, expressed in frequency domain, becomes:

$$J = (\sigma + i\omega\varepsilon) \cdot E \qquad \text{Eq. 2.6}$$

Where:

- ω = 2πf is the angular frequency;
- f is the excited frequency.

An antenna, stimulated by an electric impulse, generates an electromagnetic field: electromagnetic waves penetrate into a medium, and their amplitudes decrease, depending on the travelled distance.

Maxwell's equation that expresses the propagation of electromagnetic field, along z direction, in a homogeneous medium, can be expressed as:

$$E = E_x e^{\gamma x} \qquad \text{Eq. 2.7}$$

Where:

- γ is called propagation constant, it is a parameter that describes the change of a wave amplitude as it propagates in a given direction.

It is defines as:

$$\gamma = \alpha + \beta \cdot i \qquad \text{Eq. 2.8}$$

Where:

- α is the real part, and it is called attenuation constant;
- β is the imaginary part, and it is the phase constant.

They both depend on conductivity, dielectric constant and permeability of the investigated medium.

When the medium is lossless, conductivity is null and, consequently, also the attenuation is constant; therefore the propagation constant can be rewritten as (Del Conte, 2004):

$$\gamma = \beta \cdot i \qquad \text{Eq. 2.9}$$

The most important wave properties are velocity (v), attenuation (α) and impedance (Z) (Jol, 2008).

Velocity is expressed as:

$$v = \sqrt{\frac{1}{\varepsilon\mu}} \qquad \text{Eq. 2.10}$$

Where:

- $\varepsilon = \varepsilon_0 \cdot \varepsilon_r$ is the absolute dielectric constant;
- ε_0 is the dielectric constant of free space (8.854×10^{-12} F/m);
- ε_r is the relative dielectric constant of material;
- $\mu = \mu_0 \cdot \mu_r$ is the absolute magnetic permeability (H/m);
- μ_0 is the magnetic permeability of free space ($4\pi \times 10^{-7}$ H/m);
- μ_r is the relative magnetic permeability of the material.

If C is defined as the wave velocity in the free space, it can be represented as:

$$C = \sqrt{\frac{1}{\varepsilon_0 \cdot \mu_0}} \qquad \text{Eq. 2.11}$$

And then:

$$v = \frac{C}{\sqrt{\varepsilon_r \cdot \mu_r}} \qquad \text{Eq. 2.12}$$

It can be supposed that relative magnetic permeability is 1 for non-magnetic materials and, therefore, the velocity (v) will be affected only by the dielectric constant of material (ε_r).

The wave impedance Z (Ω) depends on dielectric constant, conductivity and magnetic permeability, as follow:

$$Z = \sqrt{\frac{i \cdot \omega \cdot \mu}{i \cdot \omega \cdot \varepsilon + \sigma}} \qquad \text{Eq. 2.13}$$

When an electromagnetic wave penetrates a medium, composed by different materials, it is in part reflected, scattered and refracted at the interfaces of layers with different electromagnetic properties (Sussmann, 1999). The reflected and transmitted portions are represented by two coefficients: the reflection coefficient (R) and the transmission coefficient (T), that are related to wave impedance of different materials (1 and 2):

$$R = \frac{Z_2 - Z_1}{Z_2 + Z_1} \qquad \text{Eq. 2.14}$$

$$T = \frac{2 \cdot Z_1}{Z_2 + Z_1} \qquad \text{Eq. 2.15}$$

The wave impedance Z (Ω) depends from dielectric constant, magnetic permeability and conductivity, as follow:

$$Z = \sqrt{\frac{i \cdot \omega \cdot \mu}{i \cdot \omega \cdot \varepsilon + \sigma}} \qquad \text{Eq. 2.16}$$

However, assuming a low conductivity and a low magnetic permeability, it can be affirmed that impedance depends from the dielectric constant of materials (ε).

2.3.3. Waves propagation

GPR energy develops in a conical way as it travels into the ground, which apex is the transmitted antenna (Figure 2.8). The approximate size of the radiation footprint at a defined depth in the ground can be calculated, as it depends on the antenna frequency and the dielectric constant value of the ground through which the energy passes (Conyers, 2013).

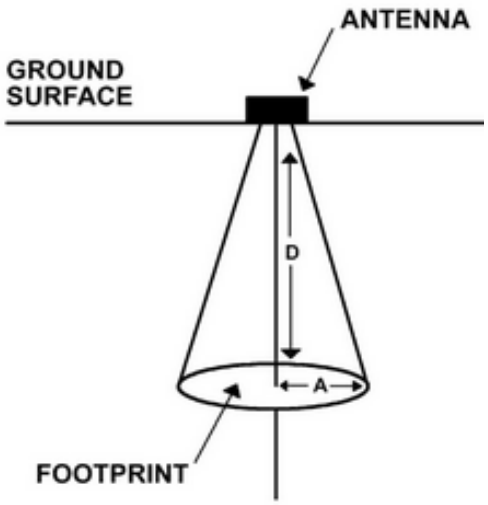

Figure 2.8 - GPR radiation footprint (Conyers, 2013)

As already referred, when an electromagnetic wave encounters a boundary between two materials with different properties, various phenomena can affect its behaviour, such as: reflection, dispersion, refraction and diffraction.

Wave reflection is the most important aspect because GPR is able to detect only the reflected wave. The reflected signal has variable amplitude, depending on the difference between the relative dielectric constants of different media. This aspect is express through a parameter, called reflection coefficient (R). In the following equation ε_{r1} represents the dielectric constant of the upper medium and ε_{r2} is the dielectric constant of the lower medium.

$$R = \frac{(\sqrt{\varepsilon_{r1}} - \sqrt{\varepsilon_{r2}})}{(\sqrt{\varepsilon_{r1}} + \sqrt{\varepsilon_{r2}})} \qquad \text{Eq. 2.17}$$

So, the higher the reflection coefficient, the higher the signal amplitude and therefore, a stronger signal will be obtained if the difference between two dielectric constants is higher.

2.3.4. Signal velocity computing

The accuracy of GPR results is related to velocity estimation that depends on the dielectric properties of materials, but generally these are not very easy to be determined, as they are influenced by several factors (see 2.4.2).

The main methods to calculate the signal velocity are described herein.

One of the most important is the "common mid-point" (CMP) (Figure 2.9) and it is used in seismic reflection (Ulriksen, 1982; Annan, 1992). It requires a transmitting antenna and a receiving one and consists in determining the velocity through the propagation depth, by varying the distance between them (S_i). Therefore, starting from a common mid point, antennas are moved in opposite directions and, at each fixed distance x_i, the time gaps t_i are registered. In this way, the average velocity is determined as follows:

$$v = \sqrt{\frac{x_a^2 - x_b^2}{t_a^2 - t_b^2}} \qquad \text{Eq. 2.18}$$

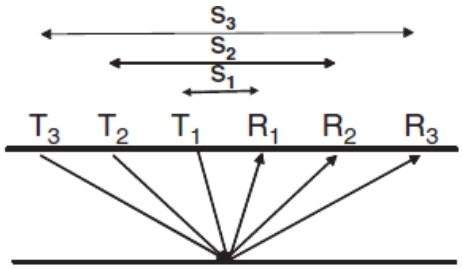

Figure 2.9 - Common mid point method (Annan, 1992)

A second method, called "wide angle reflection and ranging" (WARR) (Figure 2.10), consists in maintaining fixed the transmitting antenna while the receiving antenna moves away. Therefore, the wave crosses various mediums and therefore various signals are registered, such as the air wave (A), the direct wave through the upper medium (G) and the reflected waves from the interfaces (R) (Fontul, 2004). These are registered by the receiving antenna at different time intervals (Figure 2.10).

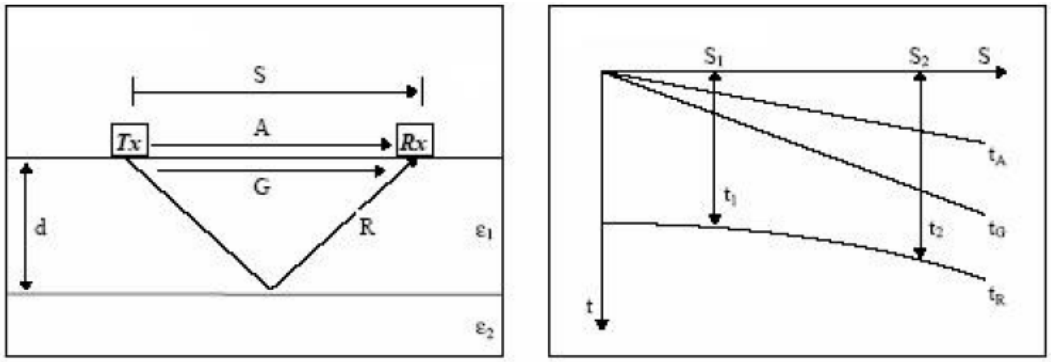

Figure 2.10 - Graphic representation of WARR method Davis and Annan, 1989 referred by Fontul (2004)

Finally, the commonly used method for air couples antennas, also applied by LNEC, is the "amplitude estimation method" (Figure 2.11). It is a velocity estimation technique but also an automated velocity calibration for air-launched antenna. The first part of procedure consists in obtaining a reflection by using a metal plate placed on the pavement surface, as the metal is considered a perfect reflector. Then, this signal is compared with the one obtained for various interfaces (i.e. surface and deeper layers).

The wave velocity on the first layer (v_1) depends on the metal plate's reflection (A_m) and on the pavement surface reflection (A_1), and can be calculated using the next equation:

$$v_1 = \frac{C}{\frac{(A_m + A_1)}{(A_m - A_1)}} \qquad \text{Eq. 2.19}$$

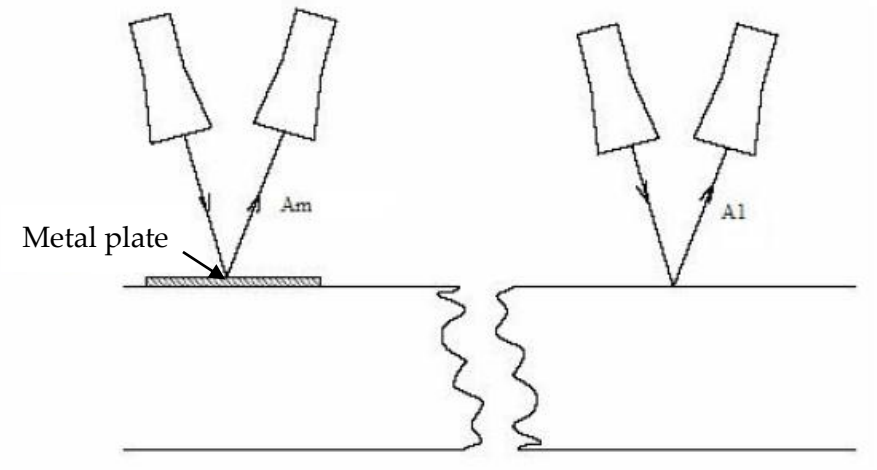

Figure 2.11 - Schematic representation of amplitude estimation method (Highways Agency, 2001)

This method is also used to remove the part of the wave that corresponds to its travel through the air from the GPR data, in order to shift the "zero level" to match the pavement surface.

For a better interpretation of data, calibration must be performed before each survey and when test conditions change; antenna elevation must be constant and checked periodically

The last method for velocity computing is "multiple antennas on surface" and it is similar to the common mid-point (Fontul, 2004). It is an automated method and it uses several receiving antennas, located near the pavement surface, that pick up the signal emitted by a single transmitting antenna. The velocity is determined by analysing differences in travel time for different paths.

The advantage of the last two methods is the continuous estimation of velocity while in the first two the calculation is made at discrete position.

2.4. CHARACTERISTICS OF MATERIALS

2.4.1. General aspects

The most important characteristics of a medium are the dielectric constant and the conductivity, as they influence the radar signal. They are affected by materials water content, namely its increase results in an increase of the dielectric constant and the conductivity.

Conductivity is a measure of a material ability to conduct an electric current. All materials are conductive, and the vacuum is the only medium considered as a perfect conductor. They can be divided in: conductors, that are perfect reflectors with a strong wave loss, such as metals; insulators, that do not conduct an electric current; and semiconductor, that have an electrical conductivity between and insulator, and in this group almost all materials are included.

Ground Penetrating Radar is most suitable for low-electrical-loss materials (Jol, 2008), in fact, if a medium is characterised by null conductivity, GPR signals can penetrate to greater depths. In practice, these conditions are rare. Clayey and

sandy materials limit the GPR signal penetration. In addition, conductivity grows with materials water content increasing.

Earth materials are mixtures, constituted by many others materials or components, except water and ice that are composed exclusively by a single component. In this context, for GPR interpretation is very important to know their physical properties (Jol, 2008).

Anyway, in the case of road materials, their conductivities are typically low, and they are considered insulators (Saarenketo, 2006).

2.4.2. Dielectric constant

The relative dielectric constant is the most significant parameter that affects electromagnetic waves. It is dimensionless and it is given by (Ulriksen, 1982; Saarenketo, 1997):

$$\varepsilon_{r=}\frac{\varepsilon}{\varepsilon_0} \qquad \text{Eq. 2.20}$$

The relative dielectric constant influences the wave propagation velocity (v) into a medium, and depends on the light speed in vacuum (c), as follows:

$$\varepsilon_r = \left(\frac{c}{v}\right)^2 \qquad \text{Eq. 2.21}$$

Therefore, wave pulse changes passing through materials with different dielectric characteristics and part of it is reflected and refracted at their interface.

The typical method for determining the dielectric constant is in laboratory (Chapter 4) or through drills or test pits (Chapter 5). Another method was introduced in part 2.3.4 for velocity calculation. By replacing the velocity with the dielectric constant Eq. 2.19, the following expression is obtained for the surface layer dielectric constant:

$$\varepsilon_1 = \left(\frac{1 + \frac{A_1}{A_m}}{1 - \frac{A_1}{A_m}} \right) \qquad \text{Eq. 2.22}$$

While, for deeper layers, located immediately beneath the surface layer, the procedure is the same but the dielectric constant value is calculated as follows:

$$\varepsilon_2 = \varepsilon_1 \left[\frac{1 - \left(\frac{A_1}{A_m}\right)^2 + \left(\frac{A_2}{A_m}\right)}{1 - \left(\frac{A_1}{A_m}\right)^2 - \left(\frac{A_2}{A_m}\right)} \right]^2 \qquad \text{Eq. 2.23}$$

Where:

- A_2 is the reflection amplitude from the second interface.

These relationships have shown to be efficient for homogeneous asphalt pavements and most concrete pavements, in particular for the Eq. 2.23 signal attenuation was supposed null (Saarenketo, 2006).

New processing techniques were developed for improving GPR results in order to estimate the dielectric properties of surveyed structures (Lahouar, 2003a; Al-Qadi and Lahouar, 2005).

Namely reflected signals amplitudes were considered, as they depend on the contrast of the dielectric constants of the adjacent layers. It was determined that the relative reflection amplitude at the nth layer interface is given as follow (Eq. 2.24):

$$\frac{A_n}{A_m} = \frac{\sqrt{\varepsilon_{r,n}} - \sqrt{\varepsilon_{r,n+1}}}{\sqrt{\varepsilon_{r,n}} + \sqrt{\varepsilon_{r,n+1}}} \left[\prod_{i=0}^{n-1} (1 - \gamma_i^2 \right] e^{-\eta_0 \sum_{i=0}^{n} \frac{\sigma_i d_i}{\sqrt{\varepsilon_{r,i}}}}$$

Eq. 2.24

$$n = 0, 1, \ldots\ldots, N-1,$$

Where:

- N is the number of pavement system layers;
- A_n is the reflection amplitude at the n^{th} layer interface;
- $\varepsilon_{r,n}$ is the relative dielectric constant of the n^{th} layer;
- σ_i is the conductivity of the n^{th} layer;
- γ_i is the reflection coefficient at the i^{th} interface;
- η_i is the wave impedance of free space;
- A_m is the amplitude of the metal plate reflection.

Then, dielectric constant value for each layer can be obtained by substituting the Eq. 2.24 into the Eq. 2.22 and Eq. 2.23. It should be considered that for this formulation the pavement layers were assumed to be homogeneous and then the dielectric constant of each layer is assumed to be constant (not variation into the layer thickness) (Al-Qadi and Lahouar, 2005).

Regarding the typical values of dielectric constants, they range between 5 and 10 for dry geological materials. Air value is 1 and water value is around 80, representing an important aspect because just a little water content may influence significantly the dielectric materials properties (Fontul, 2004). In bibliography, same materials present different dielectric values that are resumed in Table 2.2. This is due to the fact that local materials were studied and also because different mixtures, for example for concrete and asphalt, were considered.

Table 2.2 - Range of dielectric constant (εr) for various materials (Fontul, 2004)

Material	Cd	R1	R2	R3	R4	R5	R6	R7	R8	R9
Air		1	1		1	1	1	1	1	1
Water		81	81		80	80	80-81	81	81	81
Asphalt	dry	2-4	4-10*	3-5*		3-6*	5-10*		3-6*	3-8*
	wet	6-12		4#						
Concrete	dry	4-10	5-9*	6-11*		6-11*	4-10*		6-11*	6-9*
	wet	10-20		9#						
G.M./Gravel			6-18	5-9						4-6
				7#						
Sand	dry	4-6		2-6*	3-5	3-5	4-25	4-6	3-5	
	wet	20-30		4#	20-30	20-30		30	20-30	20-30
Silt	dry					5-30*	9-23*		5-30*	
	wet							10		
Clay	dry	10-40			5-40*	5-40*	4-16*		5-40*	
	wet							8-12		
Rock:				6-12*			4-10*			
				9#						
- granite	dry	5			4-6*			5	4-6*	5-6
	wet	7						7		7-8
- limestone	dry	7			4-8*			7	4-8*	5-7
	wet	8						8		8
- basalt	wet							8		
- shale	wet	6-9								
Cement. treated soil										16
Cement. treat GM										13
Lean concrete			6-9							

Table codes:

- Cd. – material condition;
- R1 to R9 – bibliography reference number, see Table 2.3;
- * – condition not specified;

- # – average value for dielectric constant;
- G.M.– granular material.

Table 2.3 - List of references presented in Table 2.2 (Fontul, 2004)

Number	Reference
R1	The Concrete Society, 1997
R2	Highways Agency, 2001
R3	ASTM, D 4748–98; 1998
R4	Annan, A.P. and Cosway, S.W., 1991
R5	CROW, 2000
R6	The Finish Geotechnical Society,1992
R7	Ulriksen, P.; 1982*
R8	Parry, N.S. et al, 1992**
R9	Cimadevilla, E.L, 1996

As already referred, material dielectric properties change also with moisture content. Several approaches that have been developed during years regarding the influence of soil moisture content, reported by Sussmann (1999) , are presented in Figure 2.12.

Also Okrasinki (1978) studied the effect of porosity, water content and volumetric moisture content on three soils (sand, silt and clay), with different dielectric constants, during a laboratory experience. The idea of the study was that the propagation velocity through a medium is slower than through air. For materials with higher porosity, it was obtained a lower value of dielectric constant; even if it depends from the type of soil, the trend is almost similar, as it is represented in Figure 2.12.

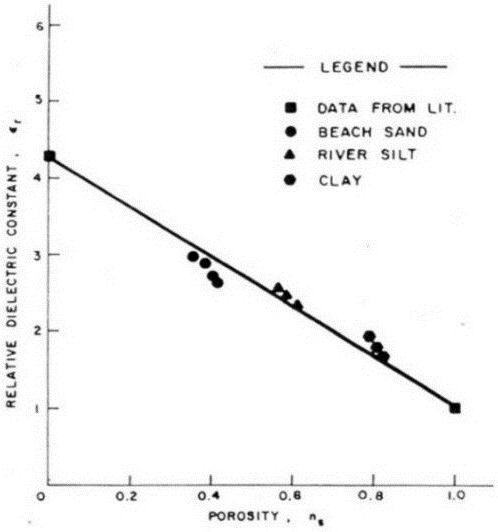

Figure 2.12 - Relationship between porosity and dielectric constant, Okrasinski et al. (1978) referred by Sussmann (1999)

Then, for the same types of soils, the effects of the moisture content on dielectric constants are represented in Figure 2.13. Two different trends can be identified, namely one for the sand and the other one for the silt and the clay: this may depend from an increased water absorption.

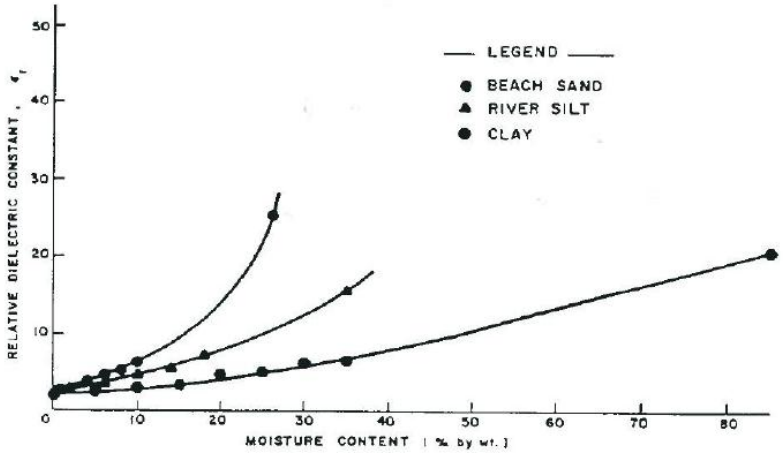

Figure 2.13 - Relationship between moisture content and dielectric constant, Okrasinski et al. (1978) referred by Sussmann (1999)

2.5. DATA COLLECTION

2.5.1. Introduction

GPR testing procedure setup depends on several factors starting with the aim of the survey (Fontul et al., 2007; Yelf, 2007). Therefore, it is necessary to make a plan in order to define several aspects, such as: when and where carrying out the tests, the test velocity, spacing, etc.

During testing, location information is an essential factor for relating GPR data with others, i.e. test pits. For this reason distance measurement devices that control sampling interval should be used (Saarenketo, 2006), and any event location (bridges, mileposts, culverts etc.) should be marked (Fontul, 2004). Also GPS and digital video systems are generally installed.

It is necessary to check if there are signal interferences from some sources, such as radio and television, electrical cables, and metal bridges. The operator that performs GPR tests should limit interferences as much as possible or indicate them for helping the interpretation phase. In addition, videos are a good mean of support for a better analysis of data.

After collection, data are saved on a computer and they are ready to be processed.

2.5.2. Testing preparation and recommendations

GPR surveys with air-coupled antennas may be performed whenever, except when the weather is rainy or when the surface is still wet. In fact the presence of water causes loss of wave energy, affecting GPR results (Annan, 1992; Daniels, 2004; Saarenketo, 2006; Jol, 2008).

In general, GPR tests are undertaken when traffic is interdicted, in order to avoid interferences on the GPR signal, for example, when metal lorries pass near the antennas. For roads and railways with a high volume of traffic, and for airports, tests are generally performed during the night.

Regarding the survey location, test alignments depend on the scope of the study and on the type of infrastructure. In roads surveys, generally, the alignment adopted is coincident with the most loaded wheelpath, namely the exterior one. In railways, the most common situation is to consider three parallel lines, a central one between rails, and the other two outside the rails, on each side; in the case that only one alignment can be performed, the central one has to be chosen. In bridges, the number of lines depends on the bridge width but, in general, it is recommended to consider distances between alignment up to 0.5 m (Saarenketo, 2006).

If load tests with Falling Weight Deflectometer (FWD) are performed, for bearing capacity evaluation, layer thicknesses are required for back-calculation process; for this reason GPR tests are carried out along the same longitudinal profile as the FWD surveys.

Tests can also be performed in transversal direction, obtaining a 3D profile view that provides a better analysis in order to solve more difficult problems (Slob et al., 2003).

Another important parameter to be defined before data collection is the test speed: a slower speed enables a better accuracy but it is not always possible because it generates traffic interruptions (Saarenketo, 2006). Moreover, it depends on the type of antennas: ground coupled antennas placed on the surface are used at speeds no higher than 20 km/h while horn antennas can reach speeds up to 80-120 km/h (Fontul et al., 2012a). Nowadays, ground coupled antennas can reach speeds higher than 100 km/h if they are suspended above the surface up to 30 cm and in these cases they are considered as semi air-coupled antennas.

Also sampling distance has to be defined. It depends on several factors: the type of structure, data storage capacity of the equipment and the test speed (Andreas Loizos and Plati, 2007b). This latter decreases with the increase of scans per meter. Generally, in road and airfield surveys, one scan per meter is enough for detecting continuous layers interfaces and it enables to perform tests at high speed and does not require a big storage capacity. On the other hand, in the case of rigid pavement,

cement treated materials are characterised by a high wave absorption, therefore scans number should be higher (Turtschy et al., 2004). In particular, at LNEC, in most project studies, the number of scans per meter used is 4 (Fontul, 2004). Saarenketo (2006) refers that on roads, airports and railways a good sampling density is 10 scans per meter for both ground coupled and air coupled antenna, as it allows to obtain important information such as crack propagation and segregation. In railway surveys, a high number of scans per meter, and therefore a low speed test, is required in order to determine the in situ condition of track bed ballast. But it is not always possible as it influences traffic interruptions, then new GPR systems have been developed permitting a high speed data collection (Max Clark et al., 2004). REFER (Portuguese railways company) surveys have a sampling density of about 10 scans/m. As example, Figure 2.14 shows results obtained for different scan densities, during a track substructure evaluation performed by LNEC, namely 20 scans per meter (on left) and 50 scans per meter (on right) and it can be seen that, in the second case, one more layer can be detected.

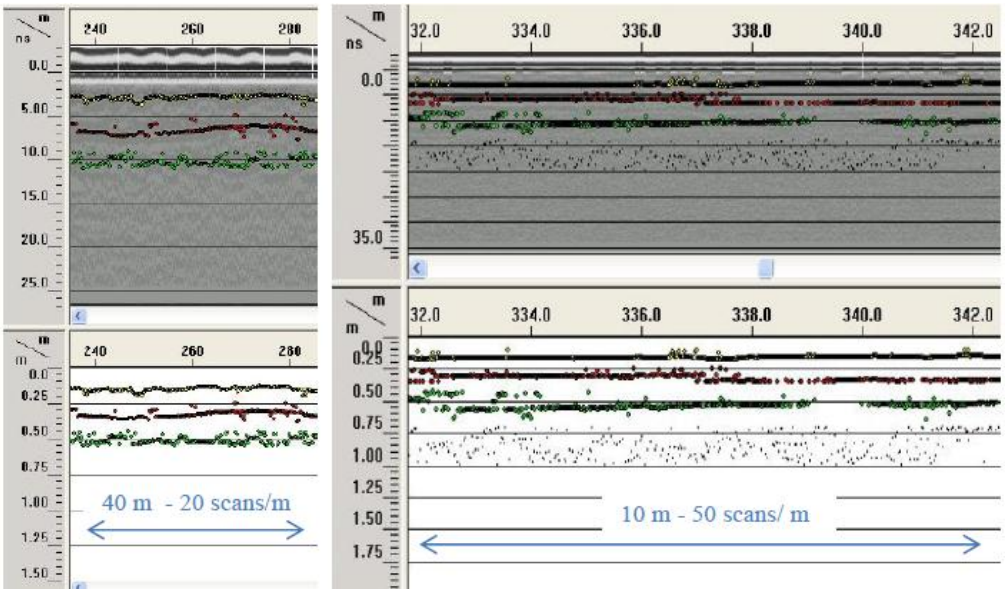

Figure 2.14 - Different scan densities: 20 scans per m (on left) and 50 scans per m (on right) (Fontul et al., 2012a)

Another parameter is the depth of penetration (time window). In general, for high frequency antennas, 12 ns and 20 ns time windows are chosen. For ground coupled antennas, with 400-600 MHz frequencies, time window varies between 60 and 90 ns. For lower frequency antennas it depends on the maximum depth that has to be studied. Saarenketo (2006) recommends that the window should be at least one-third longer the target depth. In Figure 2.15 two results files, measured on the same section, are presented: one with 20 ns and the other one with 30 ns time window. It can be observed that the interface highlighted in the figure is located almost at the bottom of the 20 ns time window. In this situation, it is important to increase the window in order to detect deeper features and to avoid losing information.

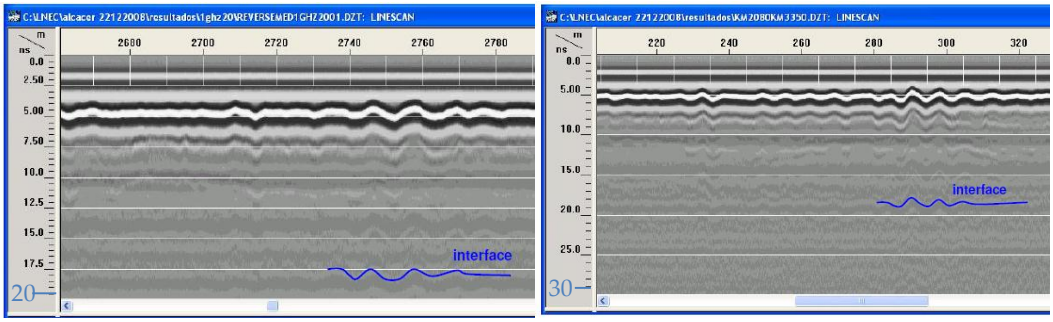

Figure 2.15 - Time window: 20 ns gain window register (on left) and 30 ns gain window register (on right) (Fontul et al., 2012a)

Not only the maximum time but also the position of the time window is important, as the surface reflection has to be in the time window. This represents a crucial aspect for ground-coupled antennas, as it is difficult to be detected, for this reason an antenna lifting is always recommended for checking the correct position of the surface reflection. On the other hand, for air-coupled antennas, coupling pulse on air should be collected because, for some GPR software, it is considered as a reference pulse (Saarenketo, 2006), while surface reflection is detected through the calibration with a metal plate.

About the scan density, as new GPR system are characterised by a higher storage capacity, for infrastructure tests, 512 scans are used (Saarenketo, 2006).

Together with GPR, cores or test pits are always required for layer thickness calibration (Phillips et al., 2006). In order to improve the reliability of the results, thicknesses are re-calculated in order to adjust the wave velocity, based on sample information, and, in this way, to obtain reliable values of dielectric constants. Special care is required for core location's choice: more than one point should be considered along the studied line, as a variation of thickness may occur. In addition, cores are extracted after GPR test and based on the collected data, namely where the files are clear and the signal is continuous (Fortunato, 2005).

2.6. DATA PROCESSING

2.6.1. Introduction

GPR data processing consists in modification of GPR signal in order to obtain well-defined results, improving the image of the data collected, such as a better resolution, and it may be developed during data collection or after it (Sussmann, 1999). It is composed by several stages as represented in the black picture in Figure 2.16: data editing, basic processing, advanced processing, and visualization/interpretation processing (Annan, 1999; Jol, 2008).

Editing is the first action after data collection, consisting in the reorganisation of the files, i.e. joint, scaled and cut. Data basic processing consists in some operations in order to create a more satisfactory product for initial interpretation and data evaluation; in some cases it is applied during GPR survey with the aim of having a first feedback, however it is better after survey when a higher precision is guaranteed. Advanced data processing are chosen by the operator and their scope is to facilitate data interpretation, then processed data will result different from raw data; operations include spatial and temporal filtering, deconvolution and background removal. Visual processing is the last step in which the operator transforms the product in order to be easy to interpret, by increasing some features and reducing others, depending on the final objective. However, this fact may

induce to error, simplifying extremely the problem and missing important information (Annan, 1999).

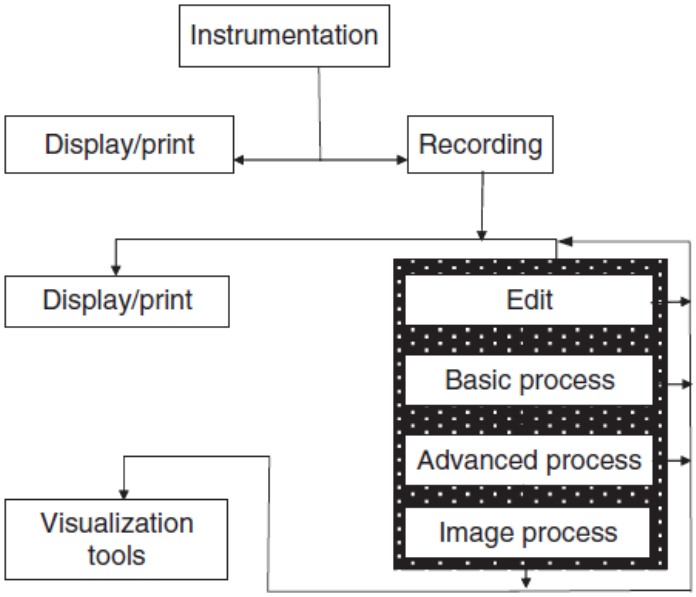

Figure 2.16 - GPR stages (Jol, 2008)

For pavements studies, GPR processing remain a crucial and time-consuming phase, despite new computer processors and software (Saarenketo, 2006).

2.6.2. Data editing and basic processing

For a first interpretation of data, some processing of data can be helpful with the scope of improving GPR data visualization (Leucci, 2012) and for detecting possible errors and then repeating the survey.

In a first phase, several editing actions are usually performed on the raw data. Initially, files are reversed, if necessary, in order to compare different lanes of the same road or railway track (left and right) and if they present different lengths, the operator can decide to cut or join one or more files.

Sometimes, file distance is scaled, depending on the initial and final coordinates. The scans are scaled using a constant scale parameter (scan m^{-1}).

Also polarity and colour scales are adjusted, in order to guarantee the same aspect during the data interpretation. In a grey scale, positive reflections should be represented in white and negative in black; for example, for air-coupled antennas, the first and maximum positive reflection is represented by the surface reflection. For ground-coupled antennas polarity is the same, in particular positive reflections appear when the upper layer has a dielectric constant value lower than the lower layer and vice versa (see layer 2 and 3 in Figure 2.19).

Basic processing phase provides a rapid output of data and can include various steps such as zero-level application, time gain and filtering adjustments.

Zero-level should correspond with the surface of the infrastructure to be studied. When air-coupled antennas are used, the air pulse should be removed, on the other hand metal plate reflection is sufficient for identifying time zero level. For ground-coupled antennas, the zero level can be identified for example by antenna lifting operation and some software enables to create a lifting file for this scope.

Time gain is another setting, it has historically been very subjective and also very dependent on the display device (Annan, 1999). It consists in increasing the signal amplitudes at deeper depths. Wave attenuation may cause some problems for data interpretation. In fact, if for the top layers the signal amplitudes are well detected, at deeper layers the detection may be very difficult. Moreover, attenuation is very variable, depending on the medium (Figure 2.17).

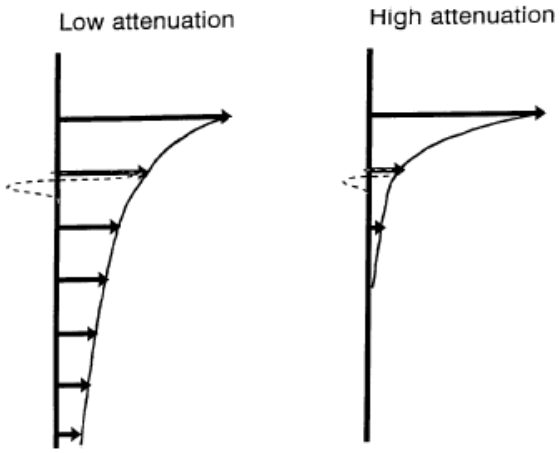

Figure 2.17 - Wave attenuations for different media (Annan, 1999)

The idea of the application of time gain is to amplify radar signal whenever it presents a drop (attenuation) (Figure 2.18). There are different ways for applying gain settings, in general for air coupled antennas one-point gain (flat gain) is used; while for ground coupled antennas, different gain points should be selected at intervals of minimum 20 ns, but limiting their number, as signal can result smoothed. Generally, the software allow to apply an auto gain setting but has to be used with care (Saarenketo, 2006).

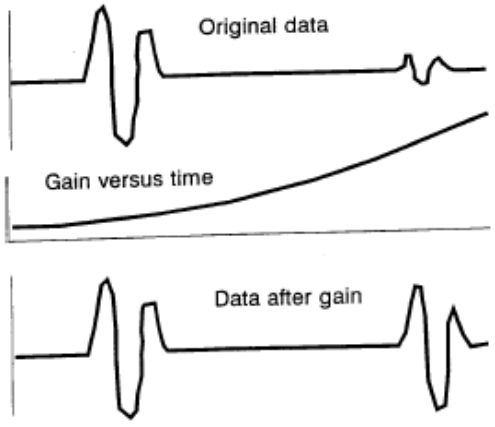

Figure 2.18 - Concept of time varying gain where signal amplification varies with time (Annan, 1999)

The next step in basic processing is filters application. A filter is a system that performs mathematical operations to reduce or enhance certain aspects of a signal, in particular the presence of noise. A filter is evaluated based on the type of action that imposes to the passing signal and it can be considered in both time and spatial domain.

A common type of filter is represented by frequency filtering. Even if GPR data are collected with a specific dominant frequency, the recorded signal includes a band of frequencies around the dominant frequency component (Leucci, 2012). In this group, band pass filtering are distinguished. In this case, the main parameter to define is characterised by two cut-off frequency values, in order to avoid that the signal passes above (low-pass filter) and below (high pass filter). For this kind of filters, it is necessary to have a good knowledge of the signal spectrum. In fact, it must be applied if noise is detected or if the signal is disturbed, in order to prevent loss of data. In particular, a low pass filter enables to remove the higher frequencies in the passing signal. On contrary, a high-pass filter deletes the lower frequencies and emphasizes the higher ones.

A combination of the previous filters generates another common filters, named as band-reject and band-pass filters. In the first case, the passing signal is blocked at a certain frequency band while continues in lower and higher frequencies. In the second one, it is blocked in both lower and higher frequencies and it passes in a specific frequency band.

As a general rule, during basic processing, data should be adjusted in an intelligent way in order to improve some aspects and, at the same time, to maintain intact the data, avoiding the distortion of information (Annan, 1999).

2.6.3. Advanced processing and visual processing

After an initial and fast improvement of raw data, a more sophisticated data processing may be required, depending on the application and on the target of interest.

First, an advanced data processing can be performed aiming to improve the data interpretation. This includes a series of algorithms that may be time consuming. Some of the most used are background removal and deconvolution (Annan, 1999).

Then, visual processing is performed in the final stage. It may be applied only if a certain number of information is known, given the fact that the data are completely changed as result of this process. Therefore, special care is required in order to avoid losing information. One of the most common processes is migration.

All the referred processes include well-known seismic processing operations (Yilmaz, 2001).

Background removal enables the horizontal band removal, visible in GPR sections, that can represent the reflection of objects placed to a certain constant distance to the antenna. In general, noise is quite consistent along the GPR section (Kim et al., 2007), for this reason, it can be supposed to remove the horizontal appearance of ringing with a simple arithmetic average, namely by summing the amplitudes of reflections generated at each time and along the entire section, and dividing them for the number of traces. In this phase, attention must be paid to not remove real linear events and time window must be specified in order that filter is not applied after the surface wave (Leucci, 2012).

In pavements surveys with air-coupled antennas, the calculation of background signal should be done in special points, in particular where layers thicknesses change in order to avoid the loss of structural data. For ground-coupled antennas, background removal filter is generally used for detecting layers interfaces near the surface. Figure 2.19 shows an example, the upper figure represents 400 MHz raw data and the lower figure the same image after background removal application. It is evident that the interface 1, near surface, is visible only after filtering process (Saarenketo, 2006).

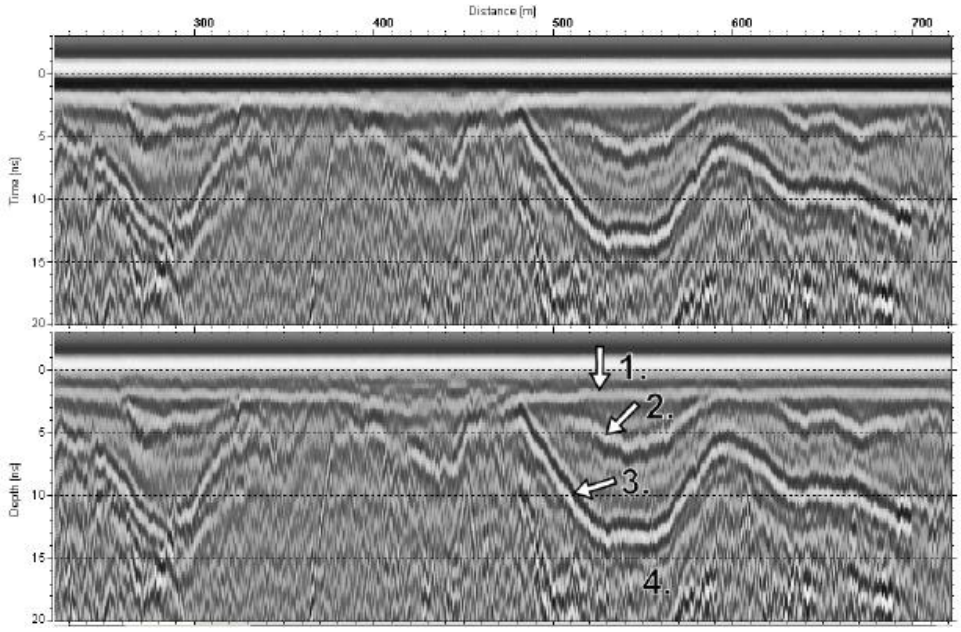

Figure 2.19 - Example of background removal filter application in 400 MHz GPR data (Saarenketo, 2006)

Deconvolution is the opposite action of convolution. Convolution is the physical process that describes how GPR wavelet interacts with the earth filter (the reflection and transmission response of the subsurface). On the other hand, deconvolution removes the effect of the source wavelet for a better GPR interpretation (Lee et al., 1992; Leucci, 2012). It is a very useful signal processing technique (Kim et al., 2007), as improves the signal resolution compressing the wavelet and removing, in part, multiples similar to noise.

Migration is an image processing, and is a technique that enables to show the inclined reflectors, such as sloping layers, in their real subsurface position and to eliminate diffractions in the registered data. A GPR section does not have unidirectional information due to the effect of radiation conical lobe and therefore parts of reflections obtained may be generated by objects positioned laterally to the antenna. This omnidirectional aspect is represented by generation of hyperbolas that may cause serious problems during data interpretation. Migration

solves this kind of problem bringing back energy to its real reflection point. However, this technique is expensive and it is applicable only when GPR data satisfy the same conditions applied to seismic reflection data. The possible benefits of migration are data-dependent and attention is suggested in its application, in fact it is recommended to use it only when results show a better accuracy and resolution of data (Fisher et al., 1992). In GPR processing, Kirchoff migration and difference migration are commonly used (Sussmann, 1999).

For pavement materials, in wet conditions, GPR signal changes continuously in shape and phase, due to dielectric dispersion, therefore deconvolution and migration application may represent a problem (Saarenketo, 2006).

The final product of the processing phase is a cross-section of the subsurface wave properties, displayed in terms of the two-way travel time, namely the time of the wave from when it is emitted to when it is received (Leucci, 2012).

2.7. DATA INTERPRETATION

2.7.1. Introduction

After processing, GPR data have to be interpreted. First, they are displayed in images representative of the studied structure conditions, as single trace, two dimensional and/or three-dimensional dataset (Daniels, 2000). In the single trace, spatial coordinates are fixed (x,y) and the only variable is the time (Figure 2.20). This configuration is rarely used but it is very suitable for studying anomalies and determining objects locations.

Bi-dimensional configuration is the most used, even because test pits or core data can be displayed for GPR calibration. Data are represented in a vertical section of the tested structure that is given as sum of single traces by moving GPR antennas along a definite direction (i.e. x), therefore distance (x) and time are both variables.

The result image can be represented by a grey or a colour scale, where the intensity of each colour is representative of wave amplitudes (see 2.6.2) (Figure 2.21).

Then, if GPR is moved also along a second direction (i.e. y), a three dimensional image can be represented, as a sum of single traces collected in y direction (Figure 2.22).

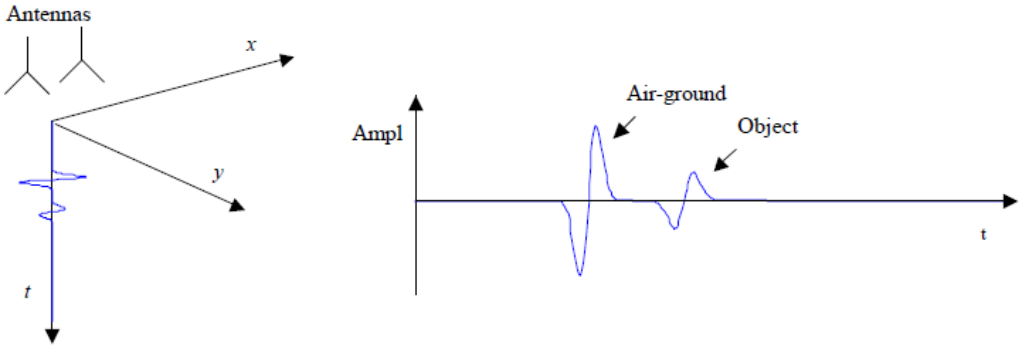

Figure 2.20 - GPR single trace scan (Scheers, 2001)

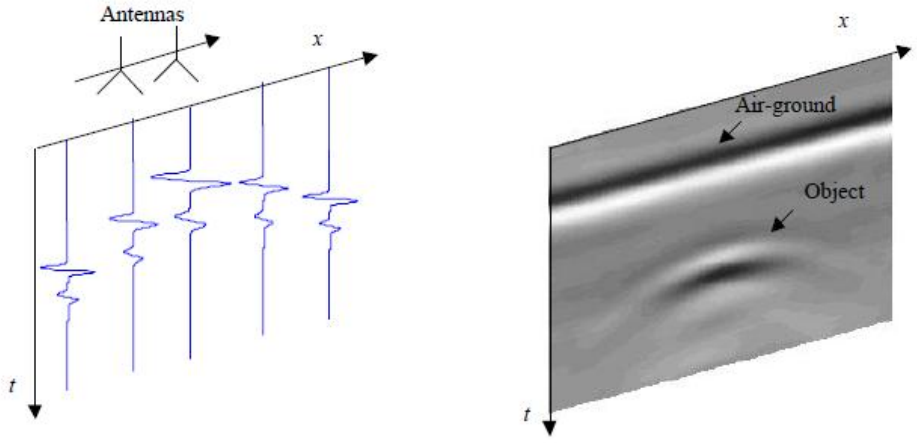

Figure 2.21 -Two-dimensional scans (Scheers, 2001)

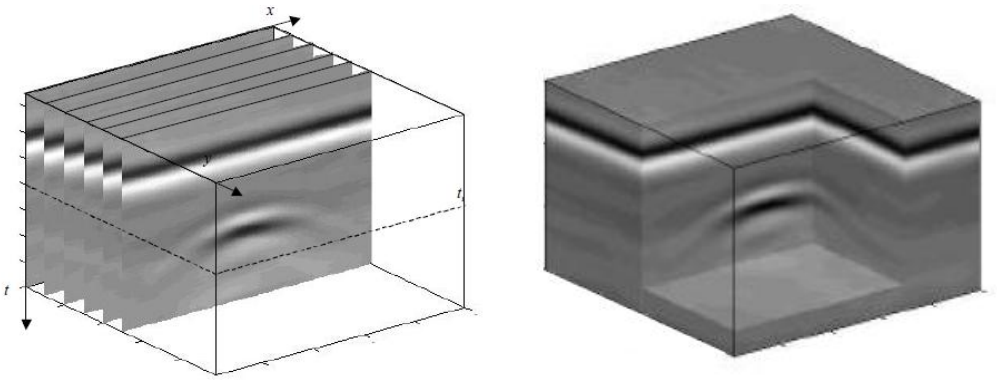

Figure 2.22 - Three-dimensional scans configuration (on left) and an example of arbitrary cut in the 3D volume (on right) (Scheers, 2001)

2.7.2. Procedure

GPR interpretation has to be performed by a person with a specific training (Phillips et al., 2006). Annan (1992) enhances critical aspects and recommendations that should be taken into account, such as:

- Knowledge of the final objective of the survey;
- Data organization and correlation with site maps;
- Velocity or dielectric constant values (laboratory or tests pits) estimation for the studied media;
- Correlation of GPR data with core, test pits;
- Anomalies location indication.

In particular, for transport infrastructure studies, the person that analyse the data must have a great knowledge of the structure to be studied and its condition.

Layers materials properties assessment, in terms of signal velocity or dielectric constant values (see 2.3 and 2.4), has to be well performed, as the higher the precision the more reliable the interpretation; their calculation is necessary for determining and verifying layers thicknesses and their variation (Fontul et al., 2007), moisture content (Plati and Loizos, 2013; Alani et al., 2013), asphalt air voids,

segregation, defects (Scullion and Saarenketo, 1998), geosynthetics (Carpenter et al., 2004).

It is important, for a better interpretation, to collect all available information about the surveyed site, for example, test pits, cores or layer thickness information, anomalies in the signal, caused by ballast fouling, cavities or trapped water; punctual objects, like pipes. In addition, the presence during survey of the person that will analyse the results, it is desired for a better understanding of the relationships among the GPR profile, the investigated site, and the external conditions (i.e. weather).

During pavement surveys, the main scope of the interpretation is to detect different layers in the GPR continuous profile and to determine their thicknesses.

In GPR profiles it is not simple to define the location of layer interfaces because many reflections occur, creating several maximum amplitudes (positive and negative) and during data analysis it has to be established which of them should be considered for the study.

There are two different operations for detecting layers interfaces:

- Picking the maximum reflection amplitude, that is the most common and accurate technique even if extra care is required with polarity changes;
- Picking the zero amplitude level, immediately before the maximum reflection amplitude. It prevents the difficulties in detecting polarity changes but it is less accurate and may induce to error if there are thin layer reflectors that cause overlapping reflections (Saarenketo, 2006).

Different software have been developed in order determine peaks automatically. They present good results if they are applied in new infrastructures. In case of old infrastructures, as they present many discontinuities in longitudinal, vertical and transverse directions, the best solution is the semi-automatic interpretation (Saarenketo and Scullion, 2000).

In a new structure, the interfaces of different layers can be detected almost immediately. On the other hand, on an older structure, traffic loads and climatic factors may cause several problems such as cracking, in roads, and ballast fouling, in railways. For this reason, an accurate interpretation, complemented by cores and test pits, may be helpful for detecting existing distresses and possible future problems, such as predicting pavement pumping (Tosti and Benedetto, 2012). This is important for the management of pavement design and rehabilitation (Phillips et al., 2006).

For example, in road infrastructures, the main features that have to be detected are (Saarenketo, 2006): bottom of the bound layers, bottom of unbound base, bottom of the entire pavement structure and bottom of the embankment (if it exists). In addition, bedrock, bridges, damaged sections and their possible causes, cables and pipelines can be detected.

Through travel time (t) and material characteristics (ε_r) (Figure 2.23), it is possible to calculate infrastructure layers thicknesses (h), as follows:

$$h = \frac{v \cdot t}{2} \qquad \text{Eq. 2.25}$$

Where:

- v is the wave velocity (m/s) (see 2.3 and 2.4);
- t is the two-way travel time from the surface to the interface depth.

Then, layers thicknesses can be used for dimensioning new pavement structures and for determining infrastructure bearing capacity through back-calculation, based on Falling Weight Deflectometer tests (Scullion and Saarenketo, 2000; Parrillo and Roberts, 2006; Fontul et al., 2012).

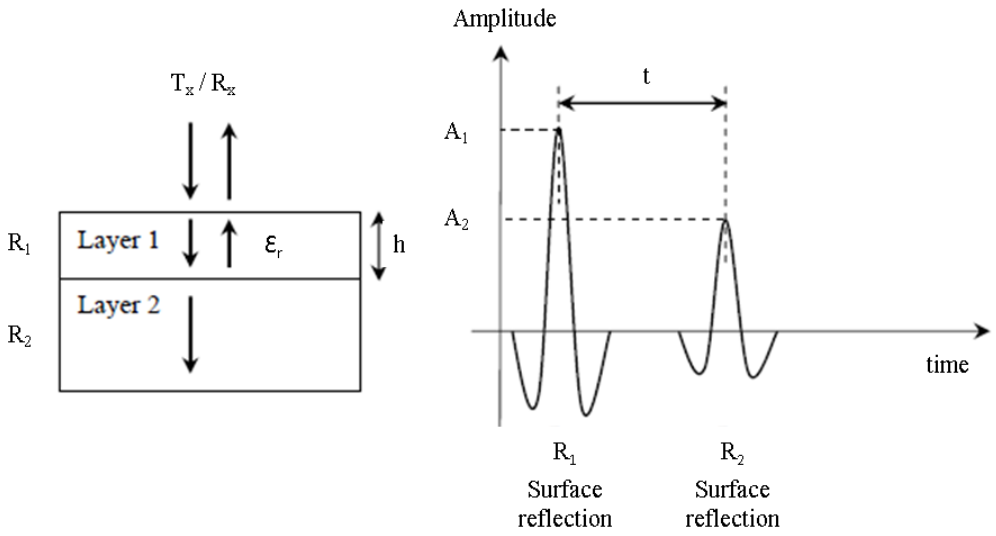

Figure 2.23 - Wave transmission (left) and signal response (right) of a two-layer system (Lahouar, 2003)

2.8. CONCLUSIONS

The Ground Penetrating Radar (GPR) technique, in particular its application in infrastructures studies is presented in this Chapter.

GPR consists generally in two antennas, a transmitter and a receiver antenna. The first send electromagnetic waves into a medium. When there is a change of medium dielectric properties, i.e. in correspondence of the interface between two infrastructure layers, wave is partially reflected. Then it is picked up by the receiver antenna. Based on the travel time, between the moment of pulse emission and the moment of wave receiving, and the materials properties, layer thickness can be determined.

The main medium characteristics are the dielectric constant and the conductivity and their knowledge is essential, as they influence the radar signal. They are affected by materials water content, and if it increases also dielectric constant and conductivity tend to increase. The ideal conditions occur when low-electrical-loss

materials are tested, as GPR signals can penetrate to greater depths. In practice, these conditions are rare and clayey and sandy materials limit GPR signal penetration.

There are different GPR systems, depending on the application area. Frequency and configuration of the antennas are chosen in order to obtain better results, taking into account that a lower frequency allows a higher depth of investigation but a lower resolution.

GPR testing procedure depends on the aim of the survey and before starting several aspects should be defined, such as test speed, sampling density, and alignments to be performed. It is necessary to control if there is a risk for interference problems, such as radio and television, electrical cables, and metal bridges and in this case to limit their influence. Climate conditions are also crucial, in fact, during rain is not recommended to perform GPR, as water decreases the wave intensity.

During survey, data are collected and a pre-processing operation is recommended. Then data are saved on a computer, processed and interpreted. In this phase, in particular, a good experience of the person that analyse the data is required for obtaining good results, avoiding the risk of removing key information.

Moreover, for a better interpretation, calibration through laboratory tests or test pits/cores is necessary. For relating GPR data with cores, location data must be recorded with distance measurement devices or with GPS, and digital video systems. Also other kinds of additional information, such as the locations of bridges, mileposts, switches should be marked.

The bibliography studied has shown that GPR is an efficient tool for infrastructures studies, as it enables to collect data in a continuous way. It is not time-consuming, limiting traffic interruptions, and also results are helpful for determining construction quality, pavement layers thickness, and pavement defects, such as moisture content and cracks.

3 RAILWAY ASSESSMENT DURING MONITORING

3.1. INTRODUCTION

As all types of infrastructures, railways have to maintain a proper behaviour during the entire life cycle. During the railway infrastructures operation, some track components have to be replaced while others can remain the same, in particular the substructure (Berggren, 2009; Esveld, 2001).

A correct and regular maintenance policy, that guarantee high safety standards, has to be established (Sussmann et al., 2001) and, at the same time, costs and time of traffic interruptions have to be limited.

Presently, two crucial aspects have to be taken into account. On one hand, the increase of load traffic speeds and axle loads on existing structures, initially designed for lower speeds. On the other hand, the climatic changes are important factors that can damage the structure, due to intense precipitation or higher temperatures. These result in a faster track deterioration, and, consequently, in a worse track performance, that also can influence other railway components, such as rails, fastenings, switches and train wheels, increasing derailment risk.

One of the means for reducing track deterioration consists in the construction of new tracks or in their renewal. Regarding this latters aspect, some European administrations have invested in the renewal of the existing lines, and in this way were taken advantage of using the existing corridors and substructures (Fortunato et al., 2007).

In addition, performance parameters should be registered during monitoring, to be evaluated during the track life cycle. This information has to be analysed together with construction data and with maintenance and rehabilitation information, if available.

This is important for studying the evolution of the geometric parameters, making a prevision of track degradation and to identify zones with different behaviour (Fortunato et al., 2007).

Nowadays, the track monitoring consists in measuring mainly parameters related to the track layout and rail wearing. This monitoring procedure does not detect the real causes of a rail level deficiency, which can be generated by the presence of ballast pockets, fouled ballast (Figure 3.1), poor drainage, subgrade settlements and transitions problems (Manacorda et al., 2002; Fontul et al., 2011; Hyslip et al., 2012). Therefore, an important factor for maintenance decision is the substructure condition assessment.

Figure 3.1- Example of degradation caused by fouling for a track formed by ballast and subsoil layers (Fortunato, 2005)

In order to perform an efficient railway assessment, suitable techniques have to be chosen. Non-destructive tests represent an efficient monitoring tool, as they allow to evaluate infrastructure characteristics in a continuous or quasi-continuous way, saving time and costs, enabling to make changes if tests results do not comply with

the project requirements. For example equipment that are used successfully for pavements evaluation, such as Ground Penetrating Radar (GPR) and Falling Weight Deflectometer (FWD), can be used also for railway evaluation (Fontul, 2004).

In this chapter, two non-destructive techniques and their applications for railway monitoring surveys in Portugal are presented: a traditional one, represented by the diagnostic train, and an innovative one, the Ground Penetrating Radar.

3.2. RAILWAY INSPECTION

3.2.1. General methodology

For a better and faster railway characterisation, equipment has been developed in the last years, aiming to evaluate one or more parameters at the same time.

Today monitoring actions are usually performed by using track inspection vehicles, as they can reach speeds between 30 and 300 km/h, enabling an efficient track characterisation at network level. A detailed description of these equipment can be found in Esveld (2001) and Lichtberger (2005).

The first manufacturers are Plasser & Theurer and Amberg, but recently railway operators performed track vehicles by using custom assembled solutions.

Inspection vehicles enable the evaluation of track condition and the detection of geometric defects that then are corrected, if needed. They present the main advantage of working at similar speeds and dynamic loads of regular trains, allowing to the track performance assessment in a more realistic way, compared with other methods, manually ones. Moreover, they allow recording measurements, of the longitudinal profile and the cross sections, in a continuous way, without traffic interdictions.

The traditional system for track measurement is contact based, namely it is a chord measuring system, based on telescopic measuring axles and measuring bogies (Esveld, 2001). This kind of system is limited in terms of measured length. For this reason, it has been replaced by a non-contact system or, in some vehicles, the two systems can coexist and are used at the same time. The modern system is characterised by an inertial system (IMU), that record a spatial curve (Wenty, 2007) and it allows to register both short-wave and long-wave deviations, that is an essential aspect for high speed lines. Often, it is integrated with a GPS system.

Diagnostic trains can be equipped with optional accessories, such as rail and overhead wire recording, or more advanced technologies like GPR or ultrasonic.

Data collection and processing is performed by using advanced computer systems that permit to register a great number of data and to simplify their interpretations. In fact, knowing reference values, an "in situ" data analysis can be done: information about quality conditions can be acquired in real time and, consequently, decisions can be made and maintenance plans can be programmed.

Nowadays, railway inspection must be performed more frequently, especially when high-speed trains are involved, in order to guarantee safety and reliability.

In some European countries, such as Portugal and Finland, rail inspection is performed with Plasser & Theurer EM120 equipment (see 3.2.2).

In Italy, railway monitoring has been largely developed by the infrastructure operator RFI. There are many diagnostic trains used for different functions, such as Archimede ("Treno Misure"), Galileo, Talete, Euclide and Aldebaran (RFI, 2013). In 2012, a new diagnostic train "Dia.Man.Te" (ETR 500Y1 and ETR 500Y2) was constructed (Figure 3.2). It represents the first train in the world able to run at a top speed of 300 km/h. It measures, in each moment, more than 200 parameters relating to track, energy, signalling (ERTMS system) and telecommunications.

Figure 3.2 - Dia.Man.Te train (RFI, 2014)

Archimede is functional since 2003 and it is also dedicated to the high speed monitoring. When it was introduced, it was considered a great innovation as its speed could reach 220 km/h, comparing with the oldest diagnostic trains that run at 160 km/h. Archimede enables to determine simultaneously 119 parameters, such as track geometry, rail profile and corrugations, surface defects, ride quality, overhead line measurements (geometry, contact wire wear, pantograph interaction, arcing measurement, electric parameters), telecommunications and signalling monitoring. One of the key advantage is that different parameters can be correlated and analysed in an integrated mode (Moretti et al., 2004).

Then, Galileo performs ultrasonic rail inspections, Talete is specific for rail geometry and profile, Caronte is a vehicle equipped with signalling diagnostic systems and track surface inspection systems, Euclide is a combination of these last three trains, includes a laser technology and it is mostly used for rail wearing measurements. Finally, Aldebaran uses a laser technology to measure all parameters of contact line and interaction between pantograph and wires.

3.2.2. Equipment: EM120

In this PhD research, the data used for the track geometric characterisation were obtained by a Track Inspection Vehicle Plasser & Theurer EM 120, used in Portugal (Figure 3.3 and Figure 3.4).

It is able to travel and record continuously at a top speed of 120 km/h.

The geometric parameters collected are:

- Longitudinal profile (left and right rail);
- Alignment (left and right rail);
- Track gauge;
- Superelevation/crosslevel;
- Twist;
- Curvature, radius;
- Gradient;
- Measuring Speed;
- Distances;
- Events.

Figure 3.3 - EM120 diagnostic train

Figure 3.4 - Part of EM120 interior

EM 120 is composed by an inertial system, where geometric parameters are defined through three-dimensional rails position. Moreover, during the analysis of the parameters defined by geometric chords (alignment and longitudinal profile), it is also possible to select and study only some of them by filtering their wavelengths (REFER, 2001).

The inertial system is composed by:

- an Inertial Measuring Unit (IMU), composed by three accelerometers and three gyroscopes;
- an Optical Gauge Measuring System (OGMS), that consists in a laser range measuring system, which measures the displacement of each rail from a reference point, such as the centre of the posterior bogie;
- a GPS, for vehicle positioning indication;
- an encoder, that registers the travelled distance by the vehicle.

Measurements are performed with a 200 Hz frequency, every 0.005 seconds, and then a new track position is established. This process can be done in two different ways, namely through a gyroscope system or accelerometer system, and if necessary, results are compared and corrected using GPS information characterised by 1 Hz frequency recordings (Fortunato et al., 2007).

EM 120 can present different optional measuring systems, namely Portuguese EM120 presented:

- Track geometry inspection system;
- Rail transversal inspection system;
- Cross level inspection system;
- Catenary Wire Geometry Measuring;
- GPR (see 3.3).

Figure 3.5 - Computer systems

During survey, data are collected in computers (Figure 3.5) and control units mounted on EM120 and graphs are created and plotted for each parameter. An operator has the task of reporting and marking events, such as: PK, traffic speed and special points, such as stations, switches and bridges (Figure 3.6).

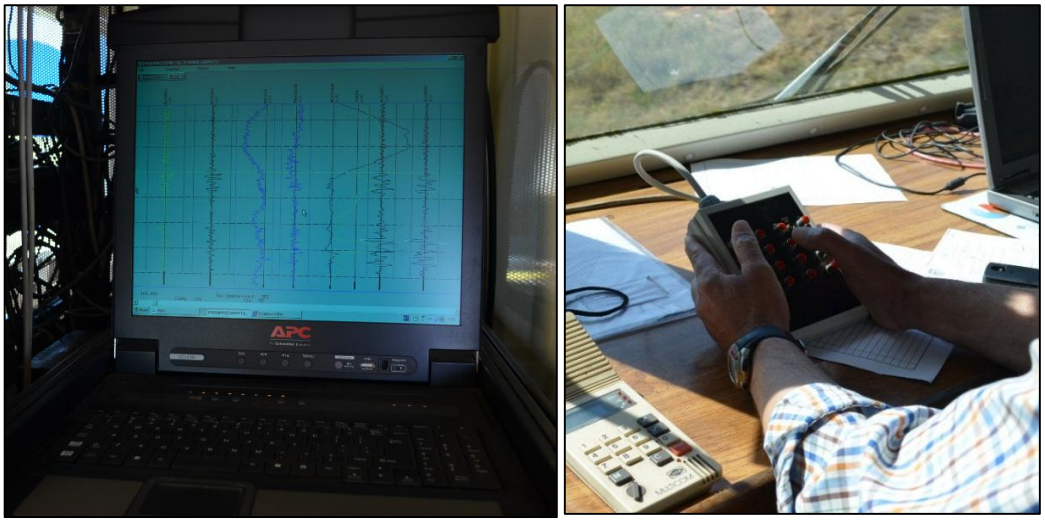

Figure 3.6 - Plotted geometric parameters (left) and events marked by the operator (right)

Post-data analysis is resumed in a final report. This phase allows evaluating critical segments of the track, their length and related location, where one or more parameters values are higher than tolerance values, the type of defect and its maximum amplitude. Also, track performance parameters are determined, based on acceleration variations, taking into account the maximum admissible traffic speed of the track (Fortunato et al., 2007).

Moreover, as an auxiliary help in track assessment, EM 120 is equipped with video cameras that make a detailed video record of the track.

One of the last improvements was done in 2009, when a GPR system was mounted on EM120 (Figure 3.7).

Figure 3.7 - Portuguese monitoring equipment: EM120 and GPR

3.3. GPR TEST

3.3.1. Overview

GPR application to railways, during construction and monitoring phase, is relatively recent. The first tests started in Finland in 1980's but they presented problems in terms of data collection and processing. In Germany, Göbel et al. (1994) referred by Saarenketo (2006) performed GPR tests for determining: ballast thickness, layers interfaces, ballast pockets and mudholes location. Jack and Jackson (1999) studied ballast layer along a track using two antennas with different frequencies, good results were found: clearer ballast interfaces indicating a clean ballast, and vice versa, and thickness variations, affirmed GPR as a useful tool for identifying track sections with urgent necessity of rehabilitation. Gallagher et al. (1999) research found positive results for survey of ballast/subgrade interface, such as anomalies detection. Hugenschmidt (2000) reports a study developed on different lines, namely the evaluation of ballast thickness, fouled zones and ballast/subgrade interface depth.

GPR has been used in most of Europe countries and in the rest of the world. In Europe, in particular in Finland (Saarenketo, 2006; Silvast et al., 2006), UK (Clark et al., 2004; Eriksen et al., 2006), Sweden (Smekal et al., 2003), Greece (Loizos and

Plati, 2007a), Italy and Germany (Manacorda et al., 2002). In North America (Sussmann et al., 2001; Olhoeft and Selig, 2002), in China (Liu and Zhang, 2012) and Australia (Manacorda and Simi, 2012).

During time, GPR studies have been focused on different issues, i.e. for geotechnical investigations and for ballast surveys. The development of new GPR systems with higher antenna frequencies, better data acquisition systems, more user friendly software and new algorithms for calculation of materials properties can lead to a regular use of GPR.

GPR procedure for railway monitoring at network level is one of the last challenges (Manacorda et al., 2002; Silvast et al., 2006; Loizos et al., 2007; Manacorda and Simi, 2012; Liu and Zhang, 2012; De Chiara et al., 2013). New high speed equipment are developed in order to promote a fast track inspection, such as ZAAR (Eriksen et al., 2004) and SafeRailSystem (SRS) developed by IDS Ingegneria dei Sistemi. As example, the latter includes an array of 3 or 4 antennas, a high speed radar control unit, a data logger and visualisation system, a doppler radar position-encoder, a video camera and a GPS synchronized to the radar data. Data collection speed with this configuration can be up to 300 km/h (Manacorda and Simi, 2012).

3.3.2. Test preparation

GPR surveys are more complicated in railways than in roads, in fact they present various particularities that require special attention during tests.

For GPR applications at railway network level, air-coupled antennas should be used, in order to perform survey at traffic speeds (Hyslip et al., 2007). As already referred in Chapter 2, the most common situation is to consider three parallel lines, a central one between rails, and the other two in correspondence of both rails sides; in the case that only one alignment can be evaluated, the central one has to be chosen.

Antennas configuration must be defined in terms of elevation, orientation and polarization. Antennas elevation over the surface should not influence GPR signal

and the optimal elevation should be chosen taking into account various features. First, the presence of different metal elements such as rails, sleepers (Gallagher et al., 1999). Rolling stock and catenaries may also create interference in the results, therefore antennas disposition should be accurately studied for reducing noise signals. Olhoeft et al. (2005) presents a study about the best antennas configuration, in terms of orientation, positioning and polarization by using 1 GHz air-coupled antennas. Then, during surveys, antennas can hit the sleepers and other objects, i.e. switches, ballast between sleepers (Fontul et al., 2007; Loizos and Plati, 2007a), for this reason, their disposition may change depending on the in situ conditions.

Antenna orientation should be defined in order to irradiate more energy parallel to the direction of the rails and less energy to the sides: this effectively decreased the interference of rail reflections (Al-Qadi et al., 2010).

In addition, antenna frequency should be chosen suitably, in accordance with the scope of the test (Figure 3.8), and several studies have been developed along the years in this matter. Gallagher et al (1999) confirmed that antennas with frequency lower than 900 MHz should be used for investigating deeper layers while that with frequency higher than 900 MHz are recommended for obtaining better resolution. A study promoted by Sussmann et al. (2003) includes both ground-coupled, 100 MHz and 400 MHz, and air-coupled antennas, 1 GHz. It yielded that first type provides good results in detecting different layers interfaces and zones with trapped water. Same results were obtained with 1 GHz antennas by Hyslip et al. (2007), plus ballast and sub-ballast variation, and ballast pockets detection; especially as a system of 3 antennas were mounted, one in the centreline and two at the end of the sleepers, outside the rails, enabling a complete substructure survey along and across the track. Roberts et al. (2006) presented an advanced study for a more complete interpretation, not only based on layers reflection, but also focused on scattering analysis for detecting fouled ballast by using a high frequency antenna, namely 2 GHz. Silvast et al. (2006) used 400 MHz antenna, mounted on the Finnish railway maintenance vehicle, for railway structures and subgrade soil inspections; and solving ballast fouling problem detection by using

Fourier Transform analysis (Shihab et al., 2002). In order to obtain more reliable results, multi-channel systems characterised by antennas with different frequencies are preferred, as demonstrated for pavements surveys by Loizos and Plati (2007b). Then, in Roberts et al. (2008), GPR surveys are presented, namely along a track of over 400 km of length using both 2 GHz and 500 MHz antennas, and concluding that the first enables distinguishing clean ballast from fouled ballast and the second one is necessary for mapping reflections associated with sub-ballast and subgrade layers.

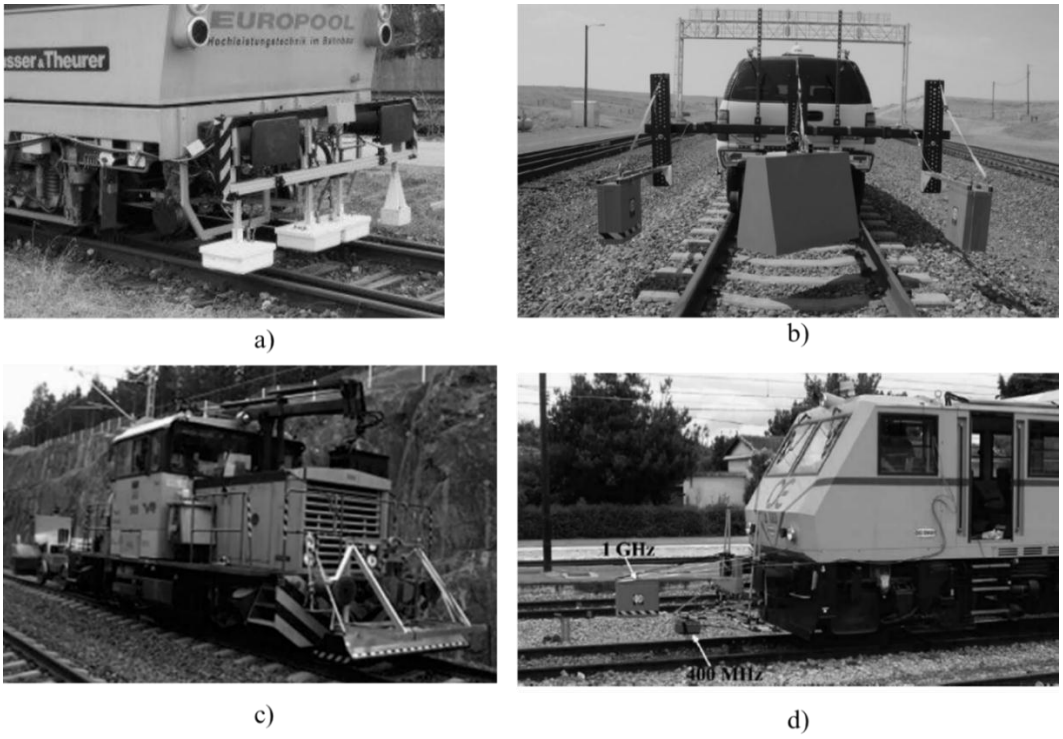

a) b) c) d)

Figure 3.8 - Multi-channel and multi-frequency GPR antennas: a) Italy and Germany (Manacorda et al., 2002); b) USA (Olhoeft, 2005); c) Finland (Silvast et al., 2010); d) Greece (Plati et al., 2010)

Then, other parameters must be defined before survey starting:

- the sampling density: for performing GPR at network level, limiting traffic interruptions, a high speed data collection is required;

- the time window: based on frequency antenna, the appropriate time window is different;
- the sample/scan density: for new GPR systems, characterised by a high storage capacity, 512 scans are generally used.

In this research, 400 MHz IDS antennas are used. These antennas are originally ground-coupled, but they can be used as semi-air-coupled when lifted about 30 cm above sleeper level. GPR surveys are performed with a sampling density of 8.6 scans/m, the time window is 90 ns and the sample/scan density is 512.

3.4. DATA INTERPRETATION

3.4.1. Introduction

GPR data interpretation depends from the type of structure. In railways the interpreter should identify: ballast layer, sub-ballast layer and, eventually, capping layer; subsoil can be detected in some case by using antenna with lower frequency.

As referred in Chapter 2, interpretation can be done in an automatic or manual mode. Different software have been developed in order to determine peaks automatically but they are not always confident as several factors cannot be included or exact, except for new structures. For example, if the thickness of a certain layer it is known and also its water content, and if both do not vary significantly along the track, the interpreter can use GPR automatic process for studying ballast fouling phenomenon. On the other hand, in an old railway line, thickness, water content and ballast fouling are very changeable and the automatic technique is not recommended. In the last case, the interpreter experience is crucial for a better interpretation of the encountered problem.

Many GPR manufacturers, such as GSSI, IDS and MALA, are also software packages producers, i.e. RADAN and GRED HD. Also special packages specific

for road, bridge and railway surveys, exist, for example Roaddoctor by Roadscanner and GeoExplorer (Kathage et al., 2005).

For railways, software packages, such as Railway Doctor by Roadscanners (see 3.4.2), SRS DPA by IDS, BallastVue by GSSI, have been created.

In particular, the first two enable to create real datasets in which is possible reporting and representing all gathered information in a multiple sub-windows screens.

SRS DPA is composed by a data processor (DP) and a data analyser and reporting (DA). Beyond typical interpretation with detection of layers interfaces, it enables, for example, the elimination of disturbance due to sleepers, an automatic calibration of radar velocity with core/test pits, insertion of events; then, output data can be represented at the same time, such as ballast fouling, ballast moisture distribution, special events (bridges, switches, crossings, etc.) (IDS, 2014).

BallastVue is a GSSI-RADAN module that provides information about ballast conditions, namely it permits an automatic calculation of fouling degree (GSSI, 2008).

3.4.2. Railway Doctor: General presentation

In the present research, data processing and interpretation was done with Railway Doctor (RD), that is a complete software package for GPR-based analysis of railways ((Roadscanners, 2000). It is one of the ROADSCANNERS software products, which include all features specifically developed for road and railway data analysis, maintenance and rehabilitation planning.

RD enables to view, interpret and analyse simultaneously multiple datasets that use the same coordinates such as GPR data from different antennas, maps, digital video, railway databases and condition measurements (Figure 3.9). This kind of multi-parameter analysis allows locating problematic railway sections and defining the origin causes of the defects. It is also possible to plan track bed

maintenance and renewal procedures using the rehabilitation planning toolbox (Roadscanners, 2000).

The following data can be linked to a RD project:

- Ground Penetrating Radar (i.e. GSSI, IDS, MALÅ, 3d-Radar, Sensors & Software);
- Reference data (i.e. sample cores);
- Digital video, photos, and maps;
- Railway databases (ASCII tables, MS Excel, MySQL, dBase, Oracle, MS Access, Paradox);
- Railway condition data (ASCII tables, MS Excel, MySQL, dBase, Oracle, MS Access, Paradox);
- Falling Weight Deflectometer data (Dynatest, KUAB, Carl Bro).

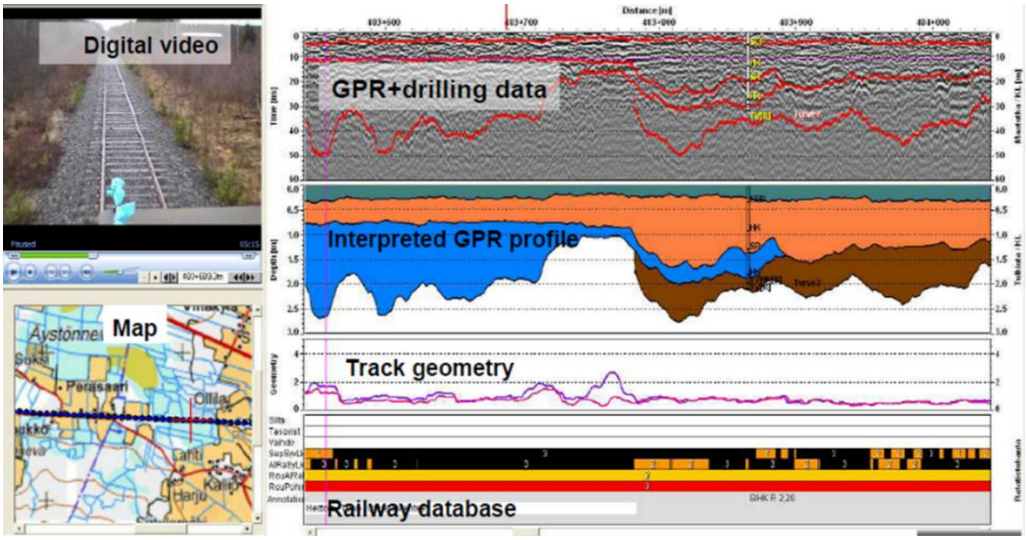

Figure 3.9 - A data view from Railway Doctor (Roadscanners, 2000)

Interpretations are most reliable in a combined view: data can be attached to the software and displayed in an integrated manner where various types of datasets are synchronized with each other. A maximum of 15 different types of data can be opened in different sub-windows in a view. Within the sub-windows many datasets of the same type from different years, for example, can be open simultaneously.

GPR data display

RD can display GPR data in a number of ways. The Y-scale of the GPR display view is adjustable to a time scale (ns) and, after giving a fixed ε_r value, to a depth scale (m). The user can affect the data imaging by changing the colour table, its transforms and threshold. The program also allows the user to display GPR data measured with different antennas in the same window, as overlapping profiles, or in separate windows.

Structure Analysis

Analysis can be used to detect defects in rail tracks, to determine their causes and to suggest suitable rehabilitation measures. Examples of analysis tools are visual inventory based on the video from the investigated site, multi-parameter automatic data classification, bearing capacity calculation from FWD data and GPR interpreted layer thicknesses.

External Map and Printing

All data in the software can be exported with coordinate and/or position information. The possible output formats are suitable for use in other software such as CAD programs, ArcGIS, MapInfo, etc. RD has an effective tool for making theme maps of analysed results directly from various types of open datasets. In addition, images can be created from large files such as video and GPR data to save disk space. *GPR data Processing*

The software can pre-process both ground coupled and air coupled GPR data. Pre-processing operations common to both data types are cutting, joining, reversing, normalization of horizontal scale and channel splitting. In addition, pre-processing

operations for air-coupled data include background removal and surface elevation correction.

Signal processing can be done also on-screen. This makes data handling faster and saves disk space. Possible operations are for example: background removal, DC-level correction, signal gain, horizontal and vertical filtering, Kirchoff migration, Hilbert transform, correlation filters and arithmetic operations.

Interpretation of GPR data

The program includes manual interface tracking and semi-automatic interface tracking tools. The interpreted interface can be drawn with different styles to indicate a clear / apparent / weak interface. Each interpreted interface gets a layer code, which attaches predefined information to each interpreted point, such as layer name and dielectric constant value (ε_r). Based on the given ε_r, the program can calculate the depth of the interpreted interface or object. It is also possible to insert annotations in the GPR profile.

3.4.3. Project Procedure

For creating a new RD project, the first thing to do it is opening the Project Handling dialog. This shows a tree view of the projects created and consists in four levels of divisions:

1) Projects;
2) Survey lines;
3) Data groups;
4) Individual data.

Then, it is necessary to create a "*.RDP" file in order to manage the different datasets that will be attached to the new project. In this phase, a dialog box is opened where some information must be defined, such as: the project type, the location and the region country. If there are many projects, it is possible to simplify the work by grouping them for example by contract, by region, by year or by survey method.

Once the project is defined, datasets are linked in the "Linking New Data" dialog. First, a survey line file is created to which the measurement data are bound. The line-based linking allows viewing datasets on the same distance axis in the same view. If the distance of the survey line is not known, it is possible to use the same length used with the GPR files by clicking "Read Distance Info from GPR-file" button, as it was done in this study.

After the "Line file" is created, other datasets can be linked, such as digital map picture data. Oriented and un-oriented map picture files (.jpg, .tif, .png, etc.) are supported by the program.

When GPR file is linked to the survey line, the program reads header information and binary settings of the GPR file and displays them in the "GPR Data Information" dialog. In addition, the measurements settings are displayed, such as:

- The horizontal scale (scans/meter) of the current GPR data file, this value can be edited and, therefore, the program will calculate the new length automatically;
- The time window (nanoseconds) of the current GPR data file;
- The time zero level (nanoseconds) of the surface in the current GPR data file;
- The gain settings, and then signal amplification values used during measurement;
- The number of scans in the GPR file;
- The length (meters) of the GPR profile with the current horizontal scale, and if it is changed, the program changes the horizontal scale value automatically;
- The creation date of the measurement;
- The starting location of measurement, that can be edited;
- The type of antenna.

When the information parameters are accepted, the program proceeds to a view of the GPR data. Here it is possible to scroll the data, to set the new data zero level, and change view settings.

In particular, some of the view options are:

- Set minimum and maximum values for the y-axis by entering the desired values in the Y-Scale Minimum and Y-Scale Maximum edit boxes. The values are in nanoseconds as default but it is possible to enter the scale as meters;
- The axis can be named and their placement can be chosen;
- The drawing colour of the interpreted line, the text and the background colour can be chosen;
- From the "Output Window" drop-down list, it can be chosen if data is outputted in a new window or in the same window, i.e. 400 MHz ground-coupled antenna data and 1 GHz air-coupled can be displayed in the same window or not;
- A secondary axis can be enabled giving name and unit multiplier, for example the multiplier can be entered as ε_r value (m/ns).

Then "GPR Data Output" options include the possibility to choose the data to be displayed, namely GPR data, interpretations, topography profile and markers. Also data representations can be changed by changing the colour table and its transforms.

In this phase, more parameters can be viewed and edited, namely the measurement equipment, the antenna centre frequency, the unit number (if available) and the type of antenna (ground-coupled or air-coupled).

The "Linking New Data" dialog also includes other two command buttons:

- Edit file, it opens a dialog for editing the currently selected GPR data file. Operations included are: file reversal, file cutting, files joining and rescaling;

- Pre-process file, it opens a dialog that enables pre-processing of the currently selected GPR data file. Operations included are: filtering, stacking and gaining of the GPR data.

Ground truth data can also be linked. There can be a maximum of 10 samples per ground truth point. In this section, reference points are created and respective parameters are defined, such as point number, distance, coordinate, etc. Other options can be defined, such as name, code, depth, thickness, ε_r value etc. The program displays the ground truth depth reference data on the screen, in a separate window or overlaying GPR data.

As referred in 3.4.2, database sets, digital videos, image files and other types of data, such as Roughness and Falling Weight Deflectometer data, can be linked in the RD project.

For a faster analysis, a useful tool ("Unbound GPR- data view)" can be used, as it permits a quickly GPR data preview without first linking them to a project. In this case, all the view properties and processing settings can be modified. In addition, another tool ("Unbound GPR Line and Interpretation View") enables also all the interpretation and output options.

After all data are linked, GPR data "on screen" processing starts; it has to be highlighted that it can be done also before linking the data to the project. It includes most of the basic processing operations, such as horizontal and vertical low pass, high pass and band pass filtering, background removal, DC-level (data-offset) removal, signal amplitude recovery and arithmetic operations. On screen processing operations can be done for both ground-coupled antenna data and air-coupled antenna data. However, usually air-coupled antenna data processing needs also special pre-processing for removing the antenna elevation bouncing and possible interfering end reflection. The on-screen processing has been developed to simplify and make the process of GPR data processing more effective and faster (Figure 3.10). The operations can be applied in any order to any scan

and sample sections and they can be applied several times. The maximum number of operations is limited to 63.

They are one and two dimensional. In the first group there are:

- Amplitude DC-Level Correction;
- Background Removal – Calculated from Data Itself;
- Background Removal - Remove Existing Background;
- Signal Amplification;
- Vertical Filtering;
- Arithmetic operations;
- Hilbert Transform;
- Bouncing Removal Operation.

The two dimensional operations are:

- Horizontal High Pass and Low Pass Filtering;
- Migration;
- Mute Trace Section;
- Mute Single Traces.

After processing phase, GPR data interpretation must be done. In Railway Doctor two kinds of interpreting tools, namely manual interface tracking and semi-automatic interface tracking can be used. The program can also overlay data from different antennas in the same view. This is a useful feature when, for example, the survey line has been measured with 1.5 GHz and 500 MHz antennas. The lower frequency data show the whole rail track structure but a lower resolution while the higher frequency data show a partial depth but a higher resolution.

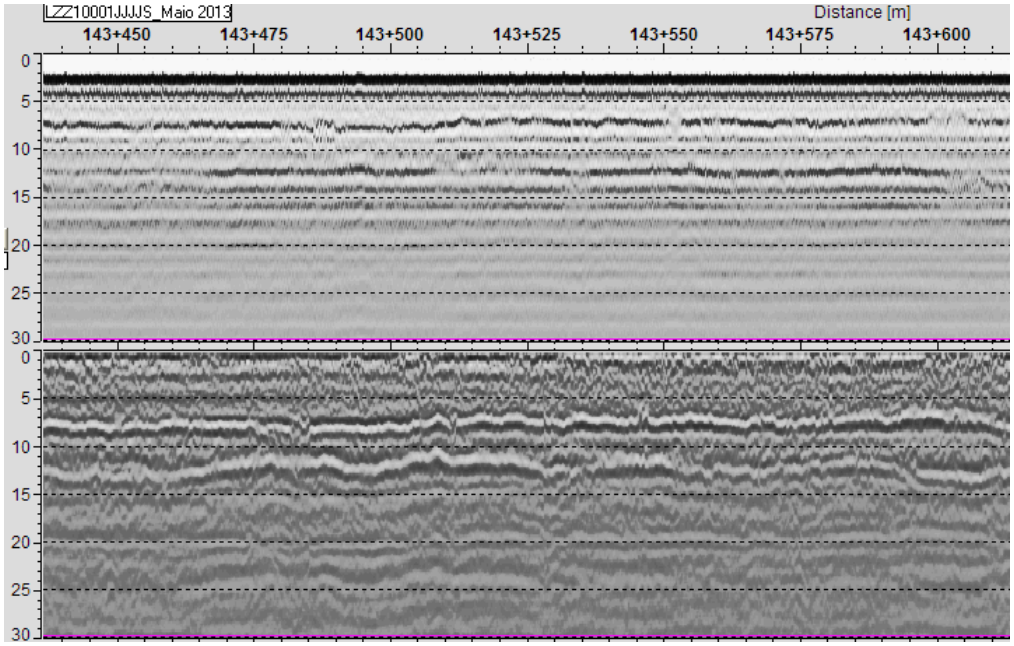

Figure 3.10 - Data processing: before the application of some filters (up) and after (down)

Before starting, some recommendations regarding the interpretation of GPR data are necessary.

Therefore:

1) The GPR data time zero level must be defined, for accurate thickness calculations;
2) If topographical corrections are required, location coordinates must be attached to the data;
3) The horizontal scale of measurement data must also be balanced or made constant through the data profile before starting the interpretation.

On the other hand, it is also possible to start the interpretation directly from the original data, if the following conditions have been satisfied:

1) The time zero-level is set;
2) Distance scale has been balanced and it is not necessary to attach elevations or coordinates to the data;

3) There are no interferences in the data that cannot be filtered or removed using on-screen processing.

Then interpretation starts. The first thing to do is to set the layer code and name, ε_r value, quality and interface type. Each interface layer must have a single code so that it is distinguishable from other layers in later operations.

Successively, in general, manual interpretation is used for ground coupled antenna data and semi-automatic for air coupled antenna data. Once interface tracking is completed (Figure 3.11), the program saves all the interpreted points in random access files in the order they are saved. If the points have been removed or added afterwards, the displayed lines will be scattered. The updating operation cleans the data and rearranges the points in the correct order and it also calculates the correct depths for multi-layer structures.

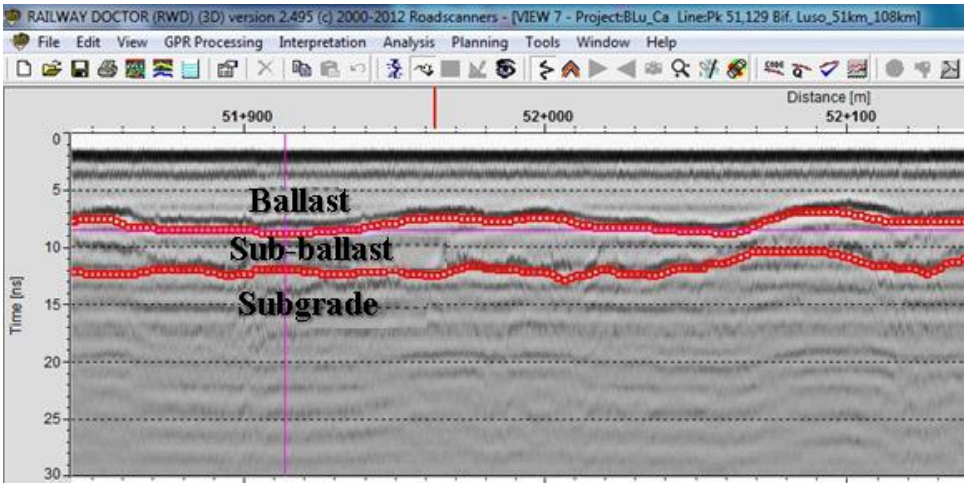

Figure 3.11 - Example of interpretation

Then, data analysis can be done. In case of railways (Figure 3.12), it includes operations for calculating:

- the Ballast Fouling Index;
- the ballast moisture content.

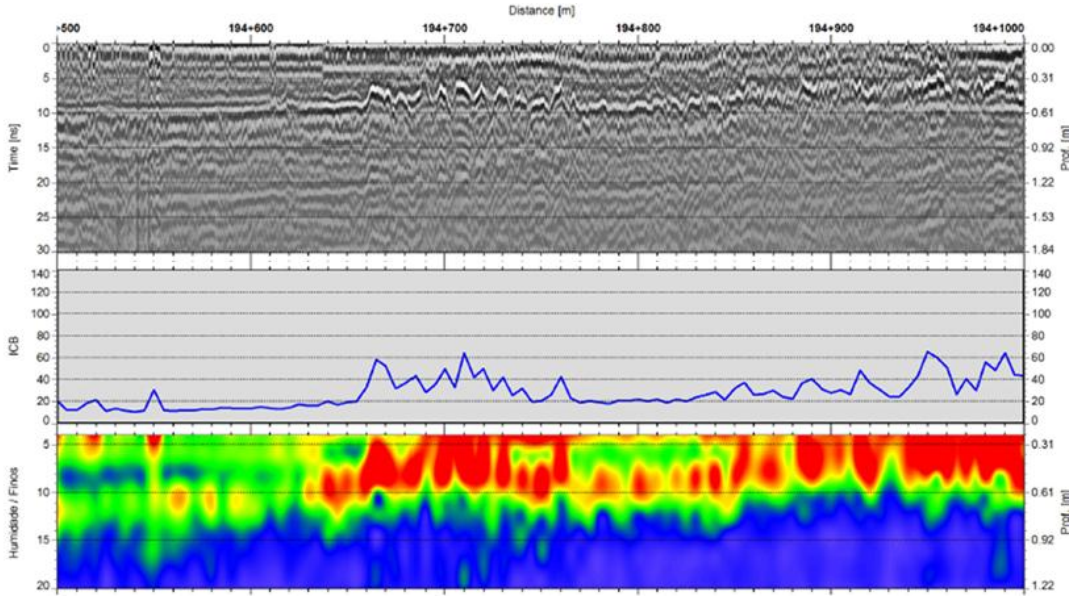

Figure 3.12 - Example of ballast fouling index and moisture content

In the RD Program the ballast fouling index was calculated from the GPR signal using a special frequency spectrum analysis algorithm, where the windowed Fourier transform was used (Silvast et al., 2010). The Fouling Index is depending on the ballast type and on the measuring equipment. Therefore, calibration data are needed to match the results correctly.

3.5. CONCLUSIONS

Chapter 3 presented a new methodology for determining the real causes of track defects, in Portugal, and it has been developed combining two non-destructive tests: the track geometry measurement performed with EM120 inspection vehicle and the infrastructure condition assessment performed by Ground Penetrating Radar.

Track inspection vehicles are used all over the world and they enable to measure a series of parameters together for determining infrastructure condition. New

technologies have permitted to construct high performance inspection vehicles, in terms of speed, track measurement systems, number of collected parameters, data acquisition and data processing. It is becoming more and more frequent the additional installing of devices, for different scopes, such as GPR, ultrasonic, laser scanners.

In Portugal, rail inspection is performed with Plasser & Theurer EM120 equipment. Its enables a survey up to 120 km/h speed. A system of computers and control units perform data collection, every 25 cm for track geometry, and their trend is represented on graphs created in real time. At the same time, also PK, traffic speed and special points, such as stations, switches and bridges are reported by the software or the operator. In the last years, various systems were mounted on EM120 for improving track monitoring, and recently GPR antennas were installed on it.

GPR application in railways is quite recent. It has been demonstrated to be a useful tool for the evaluation of infrastructure condition in terms of thicknesses and structural changes, during construction and monitoring phase. Some actions have to be taken before starting a survey, as railways components may create different kinds of problems, namely signal noise; and antennas should be chosen accurately, in particular their frequency and their elevation over the surface.

Recently, GPR has been used for improving railway monitoring and for determining different types of defects, such as the presence of ballast fouling, ballast pockets, lack of drainage, etc. New testing methodology has been developed by assembling on the track inspection vehicle a GPR with high performance characteristics.

For interpretation, many software programs have been created specifically for railways, providing a confident data processing by remove sleepers and rails noise, or integrated with new frequency analysis technique for distinguish zones with clean and fouled ballast. A more accurate description was made for "Railway Doctor" software, that is the one used in this PhD research.

4. LABORATORY TESTS FOR DIELECTRIC PROPERTIES ASSESSMENT

4.1. INTRODUCTION

Before starting the GPR interpretation, a series of information about tested materials are required, in particular their dielectric properties. In this Chapter the assessment of dielectric properties in laboratory for railway infrastructures materials, mainly ballast, is presented for different material conditions and GPR antennas. This assessment is crucial for a confident interpretation of data measured in situ.

Dielectric properties affect GPR signal propagation, reflection and data resolution. It is important to study which factors influence the dielectric constants and in which degree, with the aim of improving GPR data analysis through an appropriate interpretation phase.

Dielectric constants are very sensitive to water content and, for this reason, GPR tests are not recommendable during rainy conditions. On the other hand, soils have to be tested in wet conditions, as water can be retained into the material for days, depending on the type of material. Therefore, it is important to study the variation of the dielectric properties with the variation of its water content.

Also, many studies have shown dielectric properties variation, not only with water content, but also with temperature (Evans et al., 2008).

Another important aspect to take into account in railways studies is the evolution of ballast condition, mainly the grading and fouling (see Chapter 6). Depending on the track structure, ballast may be subjected to aggregate breakdown and subgrade soils pumping due to traffic loads; in some countries coal dust from cargo trains has been the main source of ballast voids filling. Over the time, all these aspects can lead to fouling conditions that produce track instability and change ballast dielectric properties, even more with higher water content values.

Then, for ballast material, it is necessary to study its dielectric constant value variation for different levels of fouling, in order to improve management maintenance planning. Several studies were conducted for defining ballast conditions based on the quantity of fines in ballast (see 4.1).

Therefore, GPR data calibration is a crucial phase, as it improves results reliability through a manual interpretation based on the adjustment of wave velocity or of the dielectric constant, allowing GPR signal to pass from a time scale (ns) to a depth scale (m).

For pavements studies, calibration can be done using different approaches (Fontul et al., 2012b). The simplest, but also the less accurate, is to use default values for materials dielectric constants (see Table 2.1). The traditional method is to extract cores and/or to open test pits in situ (Chapter 5), and samples should be carried to laboratory for performing traditional tests, such as sieve test, determination of water content, determination of ballast fouling level, etc. Signal velocity can also be measured in situ with portable instruments, such as a Percometer, or it can be performed in laboratory (Saarenketo, 1998; Andreas Loizos and Plati, 2007b), in alternative also a network analyser can be used (Berthelot et al., 2010).

Another way consists in measuring the dielectric properties through GPR laboratory tests, under controlled conditions of water content (w), density and knowing the layer thickness. Laboratory tests for determining the dielectric properties of infrastructure materials have been performed along the years in different countries, as materials characteristics may change based on project standards (see 4.3).

In this thesis, both laboratory tests and test pits were performed in Portugal.

4.2. BALLAST FOULING INDEX

Fouling Index was introduced in literature for the first time by Selig and Waters (1994) and it is the result of a study developed in North America. It is calculated

as the sum of the percentage of fine aggregates passing the number 4 sieve (4.75 mm) and the number 200 (0.075 mm). The fines that passed the Nº. 200 sieve are accounted for twice in this index due to the significance of the size of fine particles in decreasing the drainage capacity.

$$FI = P_4 + P_{200} \qquad \text{Eq. 4.1}$$

The higher is the number of fine particles, the greater FI, then a higher ballast void volume will be occupied and a poor drainage and resilience capacity will occur.

Another index for ballast fouling detection is the "Percentage Void Contamination" (PVC) by Feldman and Nissen (2002) cited by (Indraratna et al., 2011). It is determined as follows:

$$PVC = \frac{V_2}{V_1} \times 100\% \qquad \text{Eq. 4.2}$$

Where:

- V2 is the total volume of re-compacted fouling material with particles passing 9.5 mm sieve;
- V1 is the void volume of re-compacted ballast material, taking into account the total ballast depth.

Limit values are represented in Table 4.1, however others PVC limits are considered for different track standards and ballast depths.

Table 4.1 - Ballast fouling categories based on PVC (Indraratna et al., 2011)

Category	PVC (%)
Clean ballast	0 - 20
Moderately fouled ballast	20 29
Fouled ballast	> 30

The disadvantages of FI and PVC indexes are explained in Indraratna et al (2011). In particular, FI does not distinguish among the various fouling materials, which may present different characteristics such as the specific gravity that is different between a coal dust and a pulverized rock. On the other hand, PVC presents a difficulty in terms of calculation, as the measurement of ballast void volume occupied by fouling particles takes a lot of time. Also, the gradation of fouling material is not considered in the formula. Nevertheless, it represents an important aspect: if the number of voids of fouling aggregates is quite high, like for coarse particles (from 4.75 mm to 9.5 mm), a certain number of voids exists and drainage is still permitted.

Considering the previous indexes, the new index proposed is the "Relative Ballast Fouling Ratio"(Indraratna et al., 2011), that represents the ratio between solid volume of the ballast particles (passing a 9.5 mm sieve) and ballast particles (retained on a 9.5 mm sieve):

$$R_{b-f} = \frac{M_f \left(\frac{G_{s-b}}{G_{s-f}}\right)}{M_b} \qquad \text{Eq. 4.3}$$

Where:

- M_f and M_b represent the dry mass of fouling and ballast material;

- $G_{s\text{-}b}$ and $G_{s\text{-}f}$ are the specific gravities (density) of fouling and ballast material.

Then, in comparison with FI and PVC, it can be observed that $R_{b\text{-}f}$ calculation will be faster than PVC calculation and also, the solid volume and specific gravities of fouling aggregates will be taken into account.

In order to avoid an incorrect determination of PVC that may overestimate the fouling level, Indraratna et al (2011) suggests considering the solid volume of fouling aggregates instead of the total volume.

Therefore, PVC can be expressed as:

$$PVC = \frac{M_f \left(\frac{G_{s-b}}{G_{s-f}}\right)}{M_b} \frac{(1+e_f)}{e_b} \times 100\% \qquad \text{Eq. 4.4}$$

Where:

- e_b is the ballast void ratio;
- e_f is the fouling material void ratio.

$R_{b\text{-}f}$ can be expressed as:

$$R_{b-f} = PVC \frac{e_b}{(1+e_f)} \qquad \text{Eq. 4.5}$$

Generally, in several samples, e_f may be very different, while e_b, on contrary, does not change significantly. For higher values of e_f, fouling is poorer and, consequently, drainage is better. Then $R_{b\text{-}f}$ increases while PVC decreases, and this shows that $R_{b\text{-}f}$ takes into account the fouling gradation, in opposition with PVC.

Relative Ballast Fouling Ratio values and respective fouling categories are showed in Table 4.2, in comparison with FI and the Percentage of fouling.

Table 4.2 - Categories of FI, % fouling and Rb-f (Indraratna et al., 2011)

Category	FI (%)	R_{b-f} (%)
Clean ballast	< 1	< 2
Moderately clean ballast	1 - 10	2 - < 10
Moderately fouled ballast	10 - 20	10 - < 20
Fouled ballast	20 - 40	20 - < 50
Highly fouled ballast	≥ 40	≥ 50

4.2.1. Case study

During a ballast renewal intervention, performed along some stretches of a Portuguese old railway track, part of the retired ballast was collected in two different locations, one that presented a definitely high content of fines and the other one with a lower content.

The aim was to characterise the two materials in laboratory, namely defining their grading distribution and the corresponding fouling level, by using both FI and R_{b-f} indexes (Figure 4.1).

The grading curves were determined by using the NP EN 13450 (2005) and they are represented in Figure 4.2 and Figure 4.3. In these curves, three ASTM sieves were included for determining fines distribution and then fouling indexes (FI and Rb-f), in particular: #3/8" (9.5 mm), #4 (4.75 mm) and #200 (0.074 mm).

Comparing both curves, it can be observed for the first a high percentage of fines passing 9.5 mm sieve, of about 35%, in comparison with the second type that are about 15%.

Figure 4.1 - Sieve analysis

These curves were then compared with a grading envelope Figure 4.4 obtained from 114 fouled ballast grading curves, which samples were extracted from a Portuguese line and represented in a previous study (Fortunato, 2005).

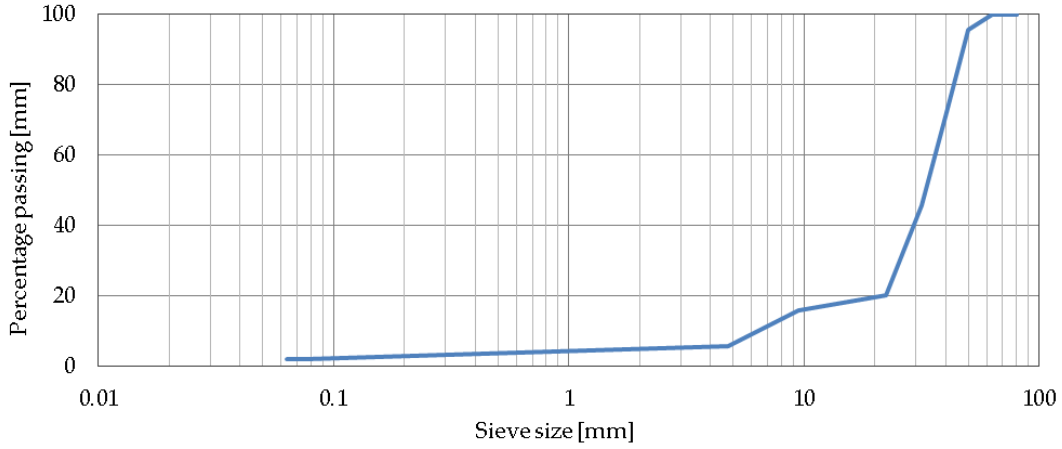

Figure 4.2 - Fouled ballast grading curve

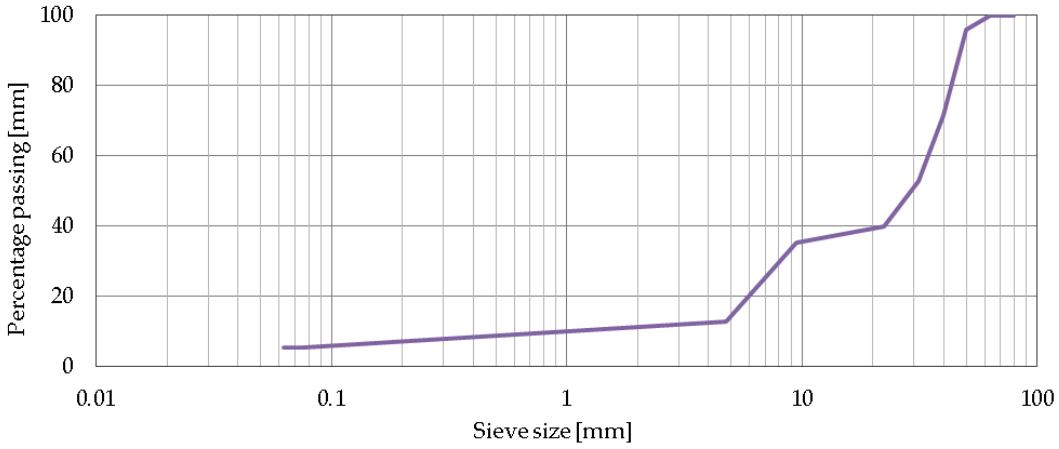

Figure 4.3 - Highly fouled ballast grading curve

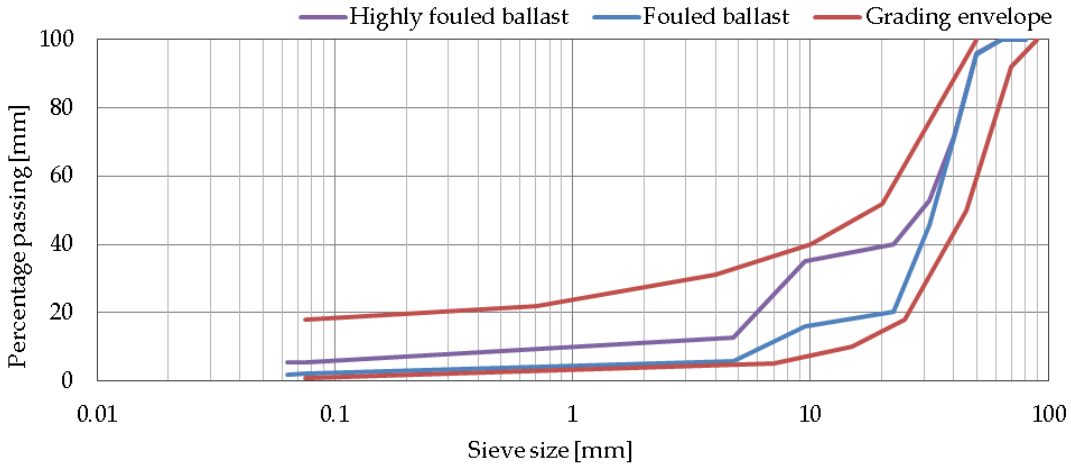

Figure 4.4 - Grading envelope of fouling ballast

For calculating $R_{b\text{-}f}$, as referred previously, density has to be determined. Due to the presence of different fractions, aggregates were divided into four groups and different standards were applied for their analysis, namely for particles with dimensions:

- < 9.5 mm, NP EN 581 (1969);
- between 9.5 mm and 22.4 mm, LERO PE-01 based on NP EN 1936 (2001);

- between 22.4 mm and 31.5 mm, LERO PE-01 based on NP EN 1936 (2001);
- between 31.5 and 63 mm, NP EN 1097- 6 (2003).

Table 4.3 presents the values obtained for each fraction and the weighted average values calculated respecting the percentage of each fraction in the global distribution. This latter value was used for calculating the $R_{b\text{-}f}$ of the two types of ballast collected *in situ*.

Table 4.3 - Dry density of ballast aggregates, measured and weighted average values

Fraction (mm)	Fouled ballast		Highly fouled ballast	
	Measured	Weighted average	Measured	Weighted average
31.5 - 63	2.66		2.64	
22.4 - 31.5	2.66	2.65	2.64	2.64
9.5 - 22.4	2.66		2.64	
< 9.5	2.66	2.61	2.64	2.64

FI and $R_{b\text{-}f}$ indexes were calculated with Eq. 4.1 and Eq. 4.3 and then compared (Table 4.4).

According to Table 4.2, the classifications of both ballast are different for the two indexes, namely, FI tends to characterise both materials with lower fouling levels, estimating an inferior percentage of fines. This is reasonable, as FI, in comparison with $R_{b\text{-}f}$ index, does not take into account the fraction between 4.75 mm and 9.5 mm as fouling materials. As example, in this case study, this percentage is significant moreover for highly fouled ballast in which it is about 25 %.

Table 4.4 - FI and Rb-f indexes for the two types of ballast

	Fouled ballast	Highly fouled ballast
$R_{b\text{-}f}$ (%)	19	54
FI (%)	8	18

4.3. PREVIOUS LABORATORY TESTS

Laboratory tests for determining the dielectric properties of infrastructure materials have been performed along several years in different countries, as materials used in the infrastructure are different for different design procedures.

Several studies carried out, have shown strong differences between clean and fouled ballast, even more in wet conditions. The first laboratory measurements were done by Gobel et al. (1994) cited by Sussmann (1999), that found a dielectric range value between 2 and 6 for clean ballast, and between 6 and 14 for fouled ballast.

Moreover, Clark (2001) studied dry, wet and saturated ballast conditions and Sussmann (2002), cited by (Saarenketo, 2006), as well (Table 4.5).

Table 4.5 - Dielectric constant values for different ballast conditions (Saarenketo, 2006, adapted)

	Dielectric Value of Granite Ballast	
Material	Clark et al (2001)	Sussmann et al. (2002)
Dry clean ballast	3	3.6
Moderately clean ballast	3.5	4
Dry fouled ballast	4.3	3.7
Wet fouled ballast	7.8	5.1
Saturated fouled ballast	38.5	7.2

In Portugal, railway tracks present different structures. Old lines are in general composed by a granite ballast layer, that has replaced the limestone ballast used in the past, a limestone fouled ballast layer and subsoil. New and renewed lines include a capping layer between ballast and subsoil and, right in some stretches, they include a rockfill layer between capping layer and subsoil (see Figure 5.4). Also they may include granite sub-ballast layers, between capping layer and ballast.

At LNEC, various tests have been performed for the assessment of railway infrastructure materials dielectric constants along the years, presented by Fortunato (2005). Several tests were performed along the Portuguese Northern Line, at its rehabilitation, from loading tests to materials characterisation and also GPR tests were performed for the first time in Portugal on railway tracks. Therefore, calibration tests in laboratory were carried out. With this aim, various samples were built in order to perform tests on the track materials. In this way, not only the in situ materials like limestone ballast were tested but also the new materials used during rehabilitation, like granite ballast and granite and limestone sub-ballast. During tests, the water content of materials was changed, and in case of limestone ballast, also the fouling level was studied (low, medium and high level) aiming to reproduce the in situ fouling condition. A wooden cubic structure with a volume of 0.70x0.70x0.70 m^3 was constructed. Materials were placed consecutively and they were compacted with a vibratory compactor, varying the final thickness between 0.45 and 0.65 m. Different water contents were used during compaction, according to the material type, and in case of fouled limestone aggregate this value was adopted in order to obtain a suitable mixture of material. Then, GPR tests were performed in dry and in wet conditions, considering different water contents and after that fouled ballast had been wetted for 10 hours. Two ground coupled antennas were used, namely of 500 MHz and 900 MHz frequency (see also 4.5.2), except for granite sub-ballast aggregate for which only 900 MHz antenna was applied. Dielectric constant values have shown higher values for 500 MHz than for 900 MHz, and in particular the difference was about 5 % for limestone dry ballast and of about 25% for granite wet ballast. The lowest dielectric values correspond to granite dry ballast (between 3.7 and 4.3) and the higher ones to limestone ballast fouled with fine particles (between 13.2 and 16).

Table 4.6 - Dielectric constant values (Fortunato, 2005, adapted)

Material	Condition	Dielectric values	
		Antenna 500 MHz	Antenna 900 MHz
Limestone clean ballast	dry	5.3	5.0
	wet	7.2	6.4
Granite clean ballast	dry	4.3	3.7
	wet	4.8	3.8
Limestone ballast fouled with fine particles	dry	15.4	12.5
	wet	16.0	13.2
Limestone ballast fouled with medium particles	dry	10.0	9.6
	wet	11.2	11.2
Limestone ballast fouled with coarse particles	dry	7.6	6.4
	wet	8.6	7.5
Granite sub-ballast	w=1.7 %	-	6.4
	w=1.7 %	-	7.1
	w=1.7 %	-	8.5

A similar study was developed by Leng and Al-Qadi (2009). It consisted in measuring dielectric constant values for limestone and granite ballast material, simulating different water contents and also different fouling levels, by using a dry clay material. Measurements were done with 2 GHz air-coupled antennas and

materials were placed into two wooden container boxes of 1.5x1.5x1.2 m. First, 300 mm of dry clean ballast was tested with GPR and air void volume was measured. After, different fouling conditions were simulated and surveyed with GPR, namely dry clay was applied at four fouling levels: 10%, 25%, 40% and 50% of the air void volume. In addition, 600 mm of ballast material was placed above the 50% fouled ballast and water content was changed, namely 10%, 25%, 40% and 50% of the air void volume, and GPR was performed. Results have shown first, as Fortunato (2005), that granite ballast has a smaller dielectric constant than limestone ballast; second, for each material, dielectric values increase with the increase of fouling level; third, a linear relationship occurs between dielectric constant values and both fouling levels and water contents (Figure 4.5).

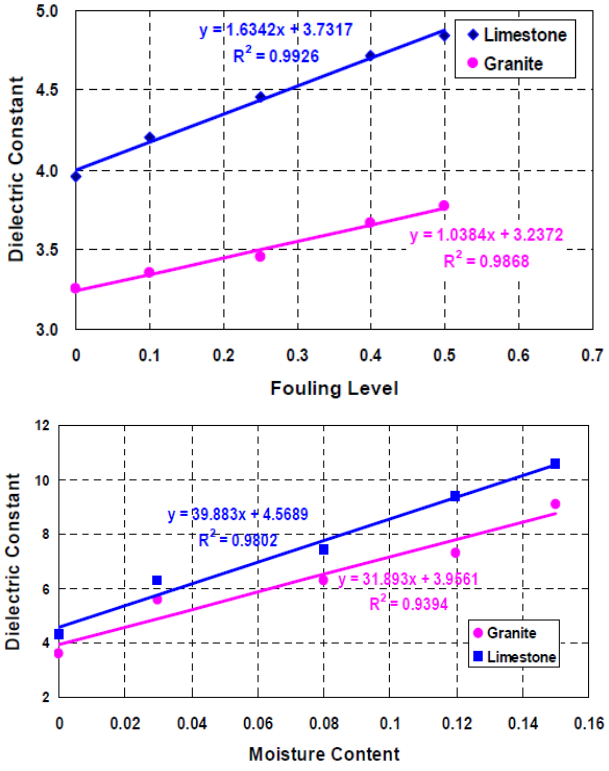

Figure 4.5 - Ballast dielectric constants for various fouling levels (up) and moisture contents (down) (Leng and Al-Qadi, 2009)

Pedrosa (2009) reports a LNEC laboratory study for sub-ballast materials, performed on experimental sections constructed in a physical model, under controlled conditions. For this scope, a rectangular section with a square area of about 2 m^2 and a depth of 0.30 m was created. Two different materials were considered, namely granite and limestone, and also variations of water content. GPR surveys were performed in each section with GSSI horn antennas of 1 GHz and 1.8 GHz (see also 4.5.1) and RADAN software was used for data processing. Results (Table 4.7) have shown for granite material satisfactory values, as they are equivalents for both antennas; on the other hand, for limestone material, 1.8 GHz antenna values are higher than that obtained with 1 GHz antenna although the difference is small.

Table 4.7 - Laboratory values obtained for wave propagation velocity, layer thickness and dielectric values (Fontul et al., 2011)

Material	Antenna frequency [GHz]	Layer thickness [m]	Wave velocity [m/ns]	Dielectric values
Granite aggregate	1	0.32	0.107	7.86
	1.8	0.32	0.107	7.86
Limestone aggregate	1	0.29	0.096	9.77
	1.8	0.29	0.096	10.63

Zhang et al. (2011) tested four ballast samples collected from rail infrastructures, characterised by different material, gradation and shape. A 1.2 GHz antenna was used and dielectric constants were calculated (Table 4.8): results have shown that the two samples with the highest volume of smaller particles also have the highest dielectric constant values and highest levels of signal attenuation.

Table 4.8 - Dielectric constant and relative attenuation values for different types of ballast

Sample	Velocity (mm/ns)	Dielectric constant	Relative attenuation (db)
Ballast 1	135.48	4.9	2.3
Ballast 2	145.25	4.3	0
Ballast 3	126.55	5.6	8
Ballast 4	125.64	5.7	13.7

4.4. MATERIAL CHARACTERISATION

4.4.1. Presentation

Dielectric value is a good parameter of ballast quality, and with this aim, during the research several tests were carried out and presented in this thesis.

The laboratory tests carried out can be divided in three main case studies:

1) clean ballast characterisation;
2) fine soil characterisation;
3) fouled ballast characterisation.

And many sub-cases, that include:

- tests with five GPR antennas with different frequencies;
- different water content values;
- four levels of fouling.

In particular, two materials were used and a mixture of them for simulating a third material, and they were characterised in laboratory. The materials are:

- a clean granite ballast;
- a silt soil;
- a fouled ballast.

4.4.2. Ballast

Ballast material, extracted by an authorized quarry and provided by REFER, satisfies Portuguese requirements NP EN 13450 (2005) in terms of physics and mechanical characteristics, such as particle size distribution, shape, flakiness, abrasion resistance (micro-Deval), fragmentation resistance (Los Angeles), freezing and thawing, etc.

As this material was also used for ballast fouling composition, some features were taken into account. For simulating various fouling conditions, the most recent index found in bibliography was used, namely Rb-f (see Eq. 4.3). The peculiarity of this index is that the fouling material is considered as material passing a 9.5 mm sieve (Australian Standards) that is not considered in European sieve distribution. Moreover, EN 13450 European Standard defines as "fine particles" that passing the 0.5 mm sieve and "fines" that passing the 0.063 mm. For this reason, in the ballast distribution also the 9.5 mm sieve was considered (Figure 4.6).

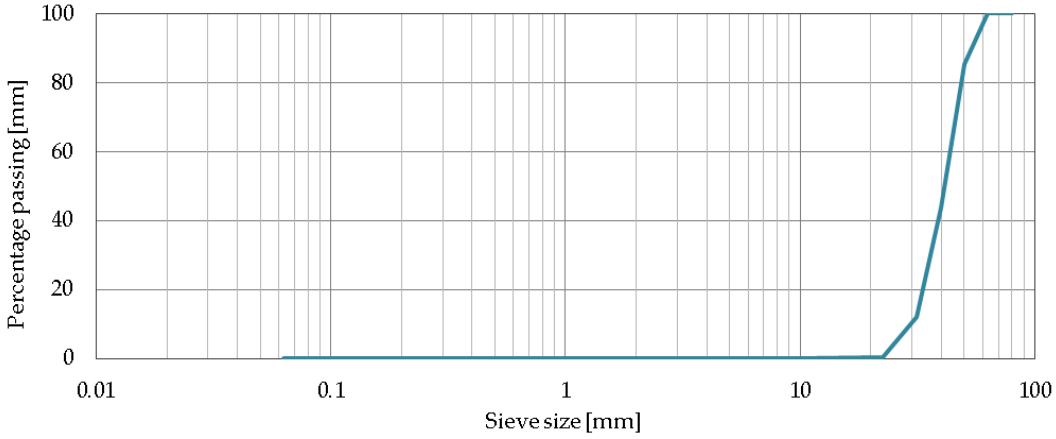

Figure 4.6 - Ballast grading

European Standard EN 13450 "Aggregates for railway ballast" define 6 categories for ballast size distribution (A-F) and in this case study ballast can be classified as type A (Table 4.9).

Table 4.9 - Grading European Standard (De Bold, 2011, adapted)

Sieve size [mm]	Railway ballast size 31.5 mm to 50 mm			Railway ballast size 31.5 mm to 63 mm		
	Percentage passing by mass					
	Size distribution category					
	A	B	C	D	E	F
80	100	100	100	100	100	100
63	100	97 to 100	95 to 100	97 to 99	85 to 99	93 to 99
50	70 to 99	70 to 99	70 to 99	65 to 99	55 to 99	45 to 70
40	30 to 65	30 to 70	25 to 75	30 to 65	25 to 75	15 to 40
31.5	1 to 25	1 to 25	1 to 25	1 to 25	1 to 25	0 to 7
22.4	0 to 3	0 to 3	0 to 3	0 to 3	0 to 3	0 to 7
31.5 to 50	≥ 50	≥ 50	≥ 50	-	-	-
31.5 to 63	-	-	-	≥ 50	≥ 50	≥ 85

Then, for ballast material, particle density and water absorption property were determined by using NP EN 1097- 6 (2003) and obtaining the following values:

- density or specific gravity (Gs): 2.62 Mg/m^3;
- water absorption: 0.35%.

For this material, a plastic box with 1.10x0.94x0.47 m^3 of volume was used. For keeping the box intact during compaction, the box was confined with a metal grid, in order to allow a proper compaction without breaking and, at the same time, limiting metal reflections during GPR tests (Figure 4.7).

After ballast characterisation in laboratory, a sample of 670 kg of material was calculated to be needed in order to obtain a final thickness of 40 cm. Then, it was oven dried until the constant mass, at 100°C.

Before laying the material into the box, aluminum sheets were placed at the bottom of the box with the aim of obtaining a high reflection amplitude, as metal is the ideal reflector, and for enabling a better GPR analysis.

Two hand compactors, a lighter and a heavier, were used during these tests. For ballast compaction the lighter one was used. The physical sample was constructed by compacting three sub-layers of 10 cm each, during about 15 minutes/sub-layer, and obtaining a final thickness of 38.8 cm.

Figure 4.7 - Aluminium sheet placed on the bottom of the box (left) and ballast compaction (right)

4.4.3. Fine soil

This soil was used during this study in order to simulate the fouling particles, that in the fouling index used, correspond to particles below 9.5 mm. This material

came from an earthen dam, and presented also aggregates greater than 9.5 mm. For this reason, before grading analysis, a selection of particles with dimensions passing the 9.5 mm sieve was performed, in order to respect $R_{b\text{-}f}$ formula (Eq. 4.3).

Then, soil grading curve was done taking into account the LNEC E 196 (1967) and it is represented in Figure 4.8.

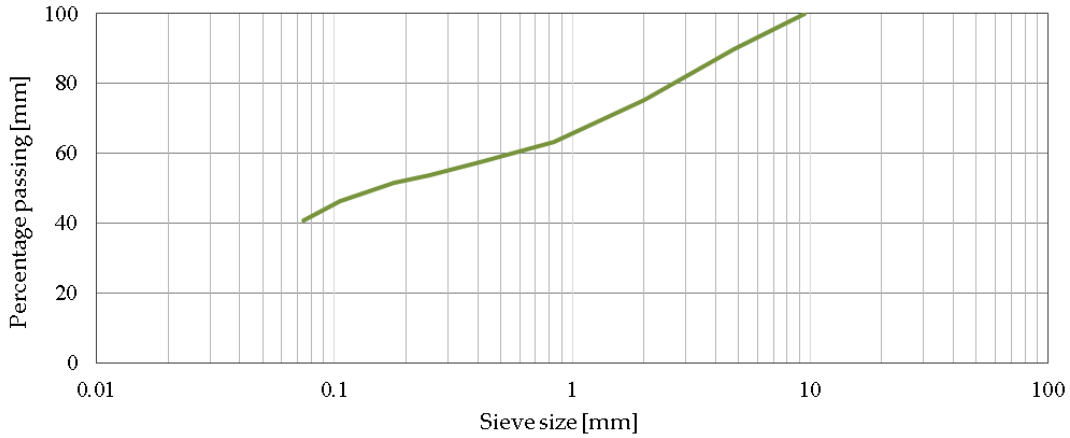

Figure 4.8 - Soil grading

Due to the fact that the percentage of particles passing the 0.074 mm sieve is greater than 35%, soil can be classified as a silt-clay soil in AASHTO classification (AASHTO M 145, 1995). In particular, as Atterberg limits have given the follows results:

- Liquid limit w_L=27.8%;
- Plastic limit w_P=0%.

Then soil can be classified as silt (A_4).

Density was determined considering the NP 581 (1969) and for the determination of the optimum water content, the LNEC E 197 (1966) was used:

- density or specific gravity (G_f): 2.71 Mg/m^3;
- optimum water content: 8.4%.

The silt soil was tested in a second plastic box which dimensions were 0.53x0.41x0.40 m^3.

As one of the scopes of these tests was to study the variation of dielectric constant values by changing water content, four water content values were assumed, in particular two lower and two higher than the optimum value (8.4%):

- 6%;
- 8%;
- 10%;
- 12%.

Before placing the material into the box, it was put on metal trays for adding water and mixing (Figure 4.9). As in the previous case study, aluminum sheets were placed at the bottom of the box.

The amount of material needed in order to obtain the required level after compaction was calculated by considering a fixed value for the final density of each sub-layer. For compaction, in the first sub-case (w=6%) the compactor with less energy was initially used. It took 10 minutes for compacting the first sub-layer but it was observed that the performance was poor, therefore it was decided to use the heavier compacter for the rest of the physical model construction (Figure 4.9).

Then, four physical models were constructed compacting five sub-layers of 6 cm for 6 minutes each one. After a sub-layer construction, in correspondence of the inner sub-layers, surface was grooved for avoiding the detection of different sub-layers interfaces with GPR. Final physical model thicknesses were of 30.1 cm, 29.3 cm, 30.3 cm and 27.9 cm respectively for the different water contents, 6%, 8%, 10% and 12%.

For verifying the water content at the end of each model construction, measurements were performed by using a nuclear density gauge (Troxler).

Once concluded the GPR tests, for each model, a sand-cone density test was performed for validation of water content values.

Figure 4.9 - Construction phases of soil physical model

4.4.4. Fouled Ballast

The third material was created by mixing the granite ballast and the silt soil referred above.

As reported in Table 4.2, there are five levels of fouling and $R_{b\text{-}f}$ varies in defined ranges. Therefore, for laboratory tests, five $R_{b\text{-}f}$ values were chosen to be simulated during tests, namely the average value of each range, as shown in Table 4.10

Fouled ballast physical model was constructed in a wooden box, characterised by a volume of 0.50x0.75x0.52 m^3. At the bottom of the box, aluminum sheets were placed, similar to the other cases.

For defining the amount of material mixture required (ballast and soil), a fixed ballast weight (180 kg) was considered, calculated for achieving a final thickness of 40 cm, and soil weight was changed for each fouling level.

Table 4.10 - Fouling levels chosen for laboratory tests

Category	$R_{b\text{-}f}$ (%)	Laboratory (%)
Clean ballast	< 2	1
Moderately clean ballast	2 to < 10	6
Moderately fouled ballast	10 to < 20	15
Fouled ballast	20 to < 50	35
Highly fouled ballast	≥ 50	55

The construction of the fouled ballast models was more complex respect the other ones, for several logistic aspects, such as oven-drying the materials, organization of spaces and ovens to use, transportation of materials, etc.

Also in this case, water content values were changed, namely four levels were adopted for the silt soil (6%, 8%, 10% and 12%).

For the first fouling level, the quantity of added soil was very small and a variation of water content would have not affected dielectric properties, for this reason it was decided to consider only the optimum value (8.4%).

For the other four models, fouled ballast was compacted with 6% of water, previously mixed with the fine soil on metal trays and then added to ballast. For saving time, the higher water content values were obtained by adding water to the finished model.

In the case of the last level, 55, fouled ballast was saturated and then air-dried; several GPR tests were performed until it came back to the 12% conditions.

For compaction, four sub-layers of 7.5 cm were compacted, obtaining a final thickness of 30 cm. In the case of index 55, the volume of the mixture was higher than the previous cases due to a higher fine content, so a 35.7 cm final thickness was obtained. The first four models ($R_{b\text{-}f}$ = 1, 6, 15 and 35) were compacted by using a lower energy compactor, and it took about 10 minutes for each sub-layer compaction. The reason was essentially to avoid abrasion and fragmentation of ballast aggregates that would have led to an increase number of fines and to different fouling levels. For index 55, as the quantity of soil was quite high, both

compactors were alternated, taking about 12 minutes for each sub-layer compaction (Figure 4.10).

Figure 4.10 - Highly fouled ballast: phases of construction

After GPR surveys, each fouling ballast sample was taken for sieve distribution analysis. The five curves were put on a graph (Figure 4.11) and compared with the grading envelope obtained for Portuguese fouling ballast materials by Fortunato (2005) (see 4.2.1). As it was expected, there is a certain analogy, i.e. the curve related to index 1 (clean ballast) is not included in the envelope, and so on.

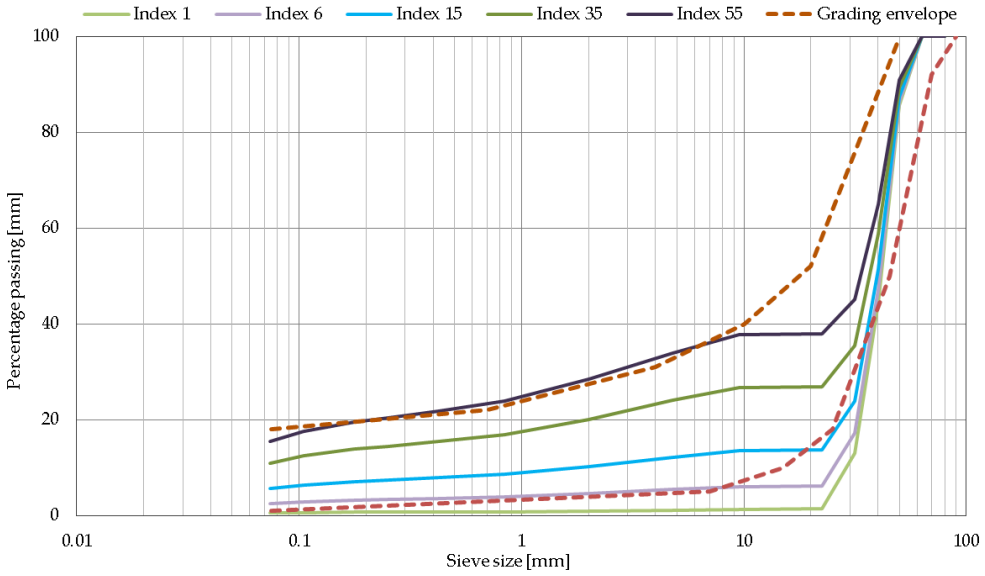

Figure 4.11 - Ballast grading for five levels of fouling

4.5. GPR EQUIPMENT USED

4.5.1. GSSI air-coupled antennas

Three different GPR equipment were used for the present research: two of them were provided by LNEC and they are Geophysical Survey System (GSSI) products (Figure 4.12).

Two pair of GSSI air-coupled antennas, a transmitter and a receiver, with 1 GHz and 1.8 GHz of frequency, were used and a SIR 20 two channel control unit as well.

Antennas were suspended in order to provide the correct configuration, typical for this type, specifically they were mounted 40/50 cm above the tested material surface.

For improving data analysis, a series of filters were applied in both cases:

- for 1 GHz: FIR low pass (3000 MHz), FIR high pass (500 MHz), IIR low pass (1000 MHz) and IIR high pass (100 MHz);
- for 1.8 GHz: FIR low pass (5000 MHz), FIR high pass (500 MHz), IIR low pass (2000 MHz) and IIR high pass (100 MHz).

Time windows were chosen ad hoc, similar to previous experiences: 20 ns for 1 GHz and 12 ns for 1.8 GHz. On the other hand, when the GPR signal was characterised by lower velocities, time window was increased, enabling bottom surface picking.

For each test, three different measurements were performed with the aim to better detect the top and the bottom of the material layer. The first measurement follows air-coupled antenna calibration procedure, in fact it consisted the placement of a quite large metal plate on the material surface for producing a strong metal reflection and therefore picking up a high wave amplitude. In the second, the large metal plate was substituted with a smaller one, for trying to detect both top and bottom of material layer. The third was done with no metal plates, for studying GPR signal without external reflections and therefore to detect the bottom reflection.

Figure 4.12 - GSSI system: 1 GHz (left) and 1.8 GHz (right) air-coupled antennas

4.5.2. GSSI ground-coupled antennas

The second LNEC system was composed by two ground-coupled antennas with 500 MHz and 900 MHz of frequency and a SIR 10H control unit (Figure 4.13).

As already referred in Chapter 2, this type of antennas are directly placed on the surface.

Filters were applied also in these cases:

- for 500 MHz: vertical filters (800 MHz and 100 MHz) and horizontal filters (5 MHz);
- for 900 MHz: vertical filters (1800 MHz and 225 MHz) and horizontal filters (3 MHz).

Measurements were executed in two times: the first by considering the time windows defined before starting tests, namely 40 ns for 500 MHz and 20 ns for 900 MHz. The second, time windows were both reduced for isolating the interest reflections (top and bottom of material layer).

In addition, for the 500 MHz antenna, a time gain application was done, in particular five gain points were chosen before starting surveys (- 4, 0, 8, 17 and 25) for the first measurement and only two points for the second one.

Figure 4.13 - GSSI system: SIR 10H (middle), 500 MHz (left) and 900MHz (right) ground-coupled antennas

4.5.3. IDS antennas

Another GPR system used is an "Ingegneria de Sistemi" (IDS) product, provided by REFER (Figure 4.15).

IDS antenna has a frequency of 400 MHz and it is composed by a dedicated four channel antenna control unit (CU SRS).

It is a shielded antenna and this characteristic is very important moreover in railways studies were catenaries create interference with GPR signal. A shield can be assumed as a container that enhances some features of GPR signal while attenuates others interferences (Figure 4.14).

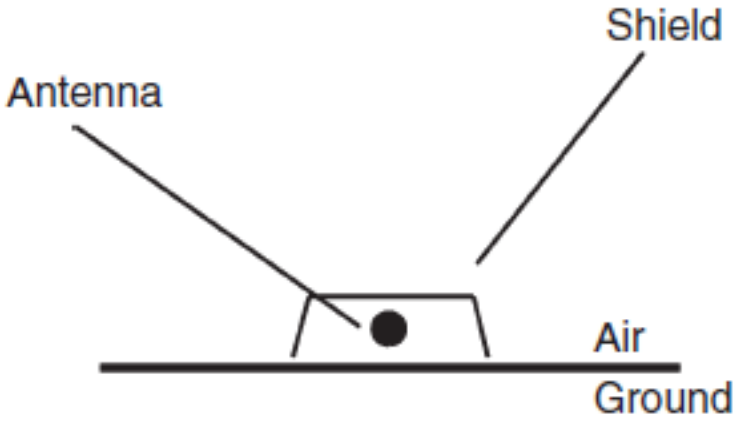

Figure 4.14 - A shielded GPR antenna (Jol, 2008)

The aim of the shield is to improve some signals and remove others, such as maximize the transmitter-target-receiver energy path, minimize the coupling transmitter-receiver, reduce the electromagnetic interferences (EMI) caused by the antenna on other external objects and vice versa. On the other hand, it presents also some disadvantages, for example shielded signals can produce reverberations for long time, the shield itself leads to larger transducer size, greater weight antenna and increase of manufacturing costs (Jol, 2008) .

Some calibration tests were performed before starting the real tests, due to it was the first time of IDS use in laboratory. First, an auto stacking mode was activated on the acquisition software, in order to perform it without distance measurements.

Antenna configuration, in terms of orientation and elevation, was studied. For the orientation on the material surface (x-y), it was evaluated to be indifferent for the used boxes. For the elevation, it was chosen to simulate a ground-coupled position, directly placed on the surface; and an "in situ" position, with antenna above the surface, suspended at about 30 cm.

In the case of the suspended antenna, the two metal plates were placed on the surface for an eventual calibration, in spite of the fact that for this kind of antenna, it is not required.

Time window was established initially at 90 ns and then at 40 ns; no filters or time gains were applied in this case.

Figure 4.15 - IDS system

4.6. GPR SURVEYS

4.6.1. Clean ballast

As already referred, the scopes of the entire tests were to measure the dielectric constant values of three materials and their sensitivity for:

- different antennas frequencies;
- different material conditions (dry, wet and saturated).

For clean ballast, many GPR surveys were performed in serial steps and seven sub-cases can be distinguished:

1) dry clean ballast;
2) wet ballast;
3) saturated ballast;
4) saturated ballast after 48h;
5) saturated for 2/3 of the total ballast thickness;
6) saturated for 1/3 of the total ballast thickness;
7) air-dried ballast.

In particular, after GPR surveys in dry conditions, water was added simulating a rainy event (wet conditions). Then, for the saturated conditions, the box has a hole that was tapped for the event and water was introduced until reaching the surface level GPR surveys were performed for wet and saturated conditions, even after 48h (Figure 4.17). Then, water was removed step by step, as represented in Figure 4.16, and GPR tests were carried out for each phase, until it came back to the initial dry condition.

For each phase, all of antennas were used and installed according to the system. In the seventh phase, GPR tests were carried out every day at about the same hour, until dielectric constant value was equal to the one measured initially, for dry conditions.

As referred, for IDS antenna two cases were studied, in particular in the ballast case the antenna was suspended at about 25 cm.

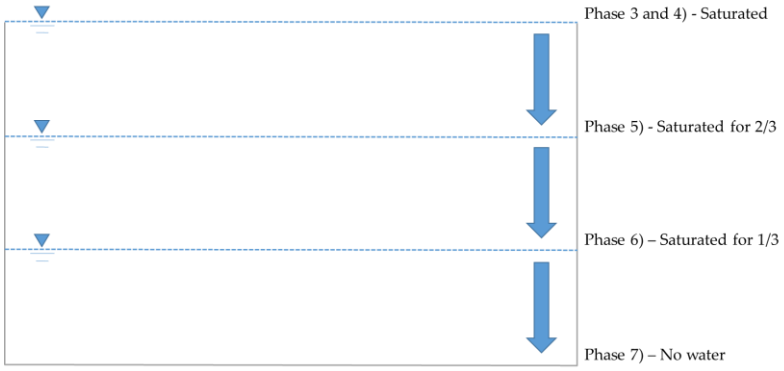

Figure 4.16 - Different saturated phases for ballast GPR surveys

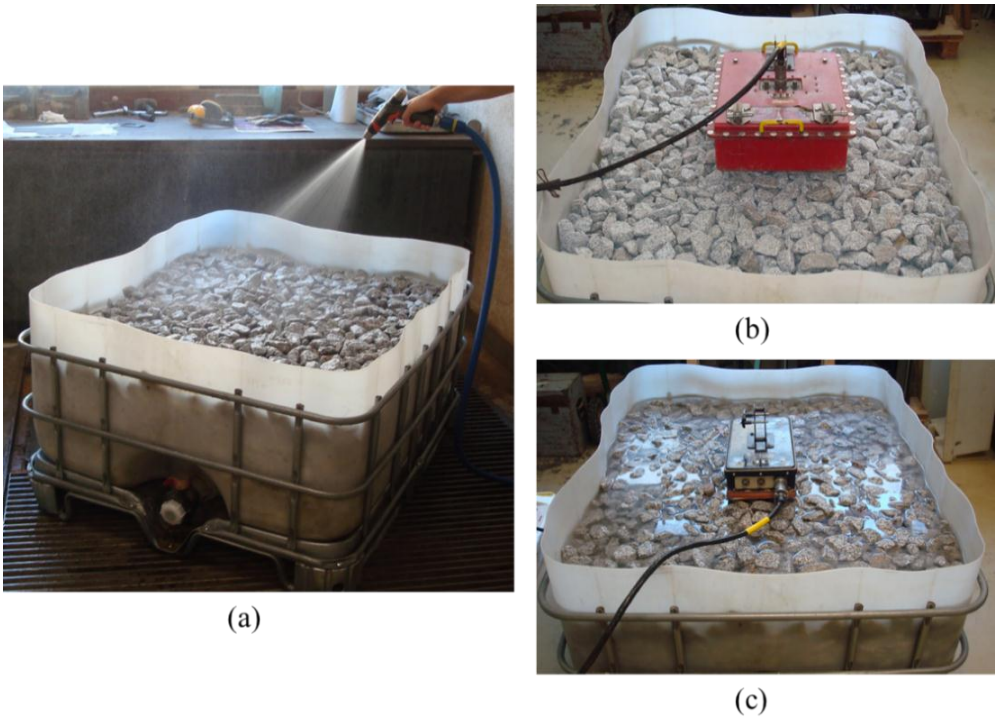

Figure 4.17 - Ballast wetting (a), 500 MHz survey on dry ballast (b) and 900 MHz survey on saturated ballast (c)

From the results (Figure 4.18), generally it can be concluded that dielectric constant values have shown a good relationship with that found in bibliography, and a correct increase of dielectric constant values with water content.

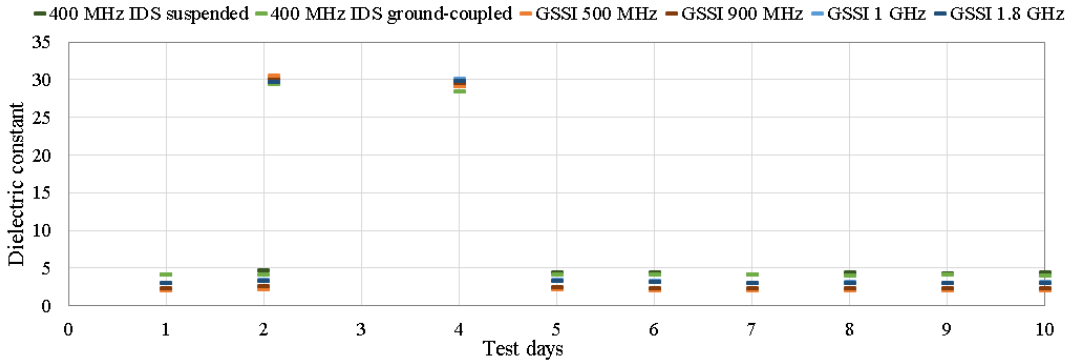

Figure 4.18 - Dielectric constant values of ballast material for different conditions and different antennas

Comparing the five systems, it can be concluded that in general a definite trend among GSSI antennas occurs: the higher the frequency, the higher the dielectric values. In particular, for 1 GHz and 1.8 GHz antennas results are almost similar. On the other hand, IDS antennas show higher values comparing the others, even more when it is suspended.

Some problems occurred for interpreting total saturated and partial saturated cases. In fact, the bottom reflection was quite difficult to detect due to the presence of water and therefore a higher attenuation of GPR energy. Moreover, 500 MHz and 900 MHz antennas have given a diverse response in the case of total saturated ballast.

Results relative to the air-dried ballast phase are represented in Figure 4.19. As expected, a linear and decreasing trend is presented by all the GPR systems.

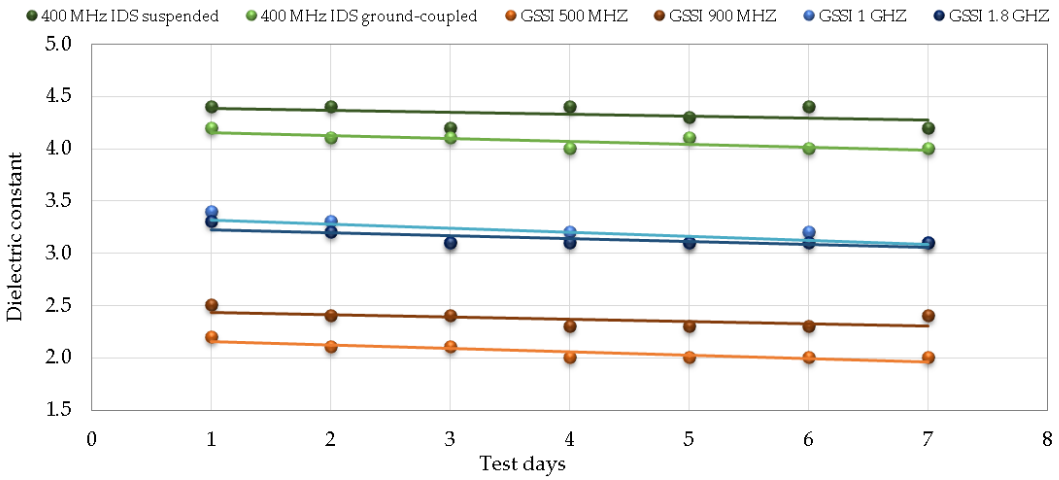

Figure 4.19 - Trend of dielectric constant values during air-dried ballast phase

In order to establish final dielectric constant values for the granite dry clean ballast, average values between initial and final conditions were calculated (Table 4.11). For IDS antenna a value of 4.1 was obtained and can be considered for future in situ tests. While for GSSI antennas, a range between 2 and 3.1 was achieved.

Table 4.11 - Average dielectric constant values for granite dry clean ballast

Category	Dry clean ballast - Average value
IDS suspended	4.15
IDS ground-coupled	4.05
GSSI 500MHZ	2.00
GSSI 900MHZ	2.35
GSSI 1GHZ	3.10
GSSI 1.8GHZ	3.10

4.6.2. Fine soil

For fine soil, four physical models with different water contents were constructed.

Four sub-cases can be underlined:

- soil 6%;

- soil 8%;
- soil 10%;
- soil 12%.

For each sub-case, more than one GPR survey, namely once or twice a day, was performed for obtaining a better reliability of results. Figure 4.20 shows an example of test performed on fine soil with the 1.8 GHz antenna.

Figure 4.20 - 1.8 GHz survey on fine soil

In order to register eventual water content changes, a nuclear density gauge test (Troxler) was performed after each set of GPR tests (five antennas systems). Moreover, before model dismounting, also a sand-cone density test was used for comparing with Troxler test and for obtaining a better precision of measurements (Figure 4.21).

Figure 4.21 - Water content measurements: Troxler (left) and sand-cone density apparatus (right)

Some problems occurred with GSSI low frequencies antennas, due to errors in detecting surface reflection, for this reason results cannot be presented.

A special attention was employed during interpretation of the fine soil than in the case of the clean ballast. This was due to fine soil high conductivity, even higher with the increasing of water content, that causes a faster GPR signal energy dissipation and consequently a lower wave amplitude in correspondence of the metal reflector placed at the bottom of the box.

For this reason, fine soil dielectric constant values are definitely higher than dry clean ballast (Figure 4.22) and comparable with that found in bibliography. It can be confirmed that, for each antenna, dielectric constant value increases with the water content, excepting in a single case (1 GHz - soil 10% - +168h). Also in this case, IDS antennas show values higher than 1 GHz and 1.8 GHz GSSI antennas, which values are very similar, in particular the difference between IDS and GSSI increases with the increase of water content.

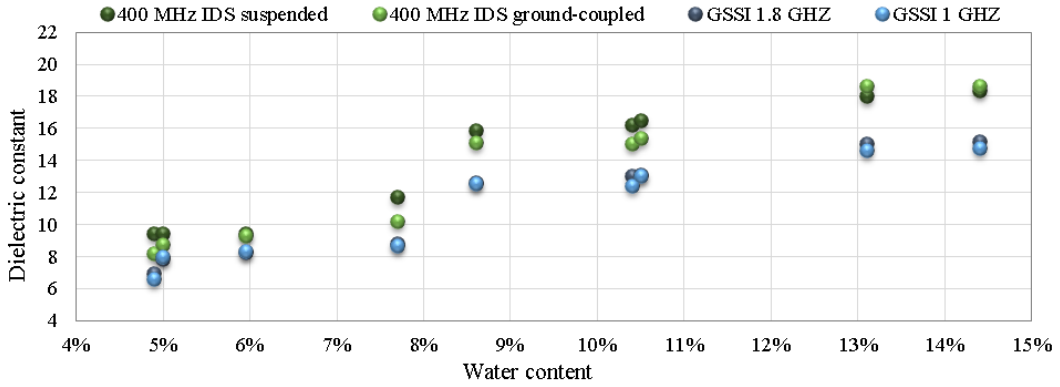

Figure 4.22 - Dielectric constant values of fine soil with water content variation

4.6.3. Fouled ballast

Fouled ballast study can be divided in five main sub-cases:

1) index 1: clean ballast;
2) index 6: moderately clean ballast;
3) index 15: moderately fouled ballast;
4) index 35: fouled ballast;
5) index 55: highly fouled ballast.

For each sub-case, a second classification should be done, based on fine soil water content. Therefore for sub-cases 2), 3), 4) and 5), it is:

- soil 6%;
- soil 8%;
- soil 10%;
- soil 12%.

For index 1, as previously referred, only 8.4% water content was considered. Two GPR set of tests were carried out: the first right after the model construction and the second after 72 hours. Dielectric constant values were calculated as average values of the two measurements and they are reported in Figure 4.23. For 500 MHz and 900 MHz antennas, an error in picking up the surface level during data acquisition impeded data interpretation.

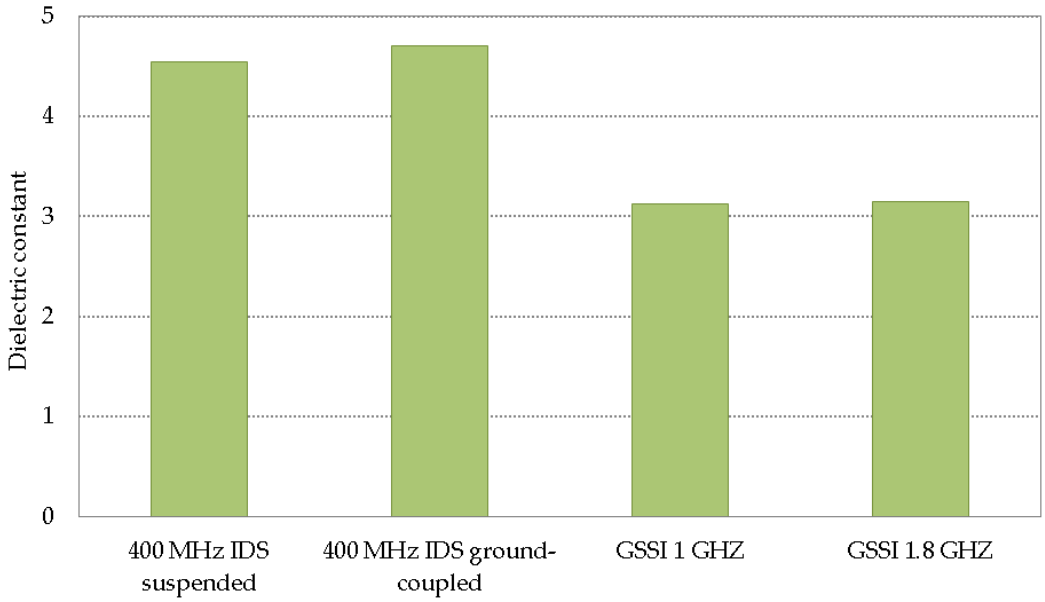

Figure 4.23 - Dielectric constant values for ballast – index 1 and w=8.4%

For the other four indexes, surveys logistic was different, in fact models were constructed with a w=6 % and then water was added in several steps.

For indexes 6, 15 and 35, two GPR tests were performed for each water content, namely one after the construction (6%) or the addition of water (8%, 10%, 12%), and the other after two hours, in order to enable water penetration down the surface and creating a homogenous mixture.

In the case of index 55, only one GPR survey was performed, namely passed two hours from the construction or the addition of water. This was because the high content of fine soil impeded water penetration in short time and it would have not

simulated real conditions. In addition, at the end of the four water content study, more water was added for simulating soaked conditions and then ballast was left to air-dry. For this case, more GPR surveys were performed.

Results were calculated as average of the two measurements (Table 4.12).

Table 4.12 - Dielectric constant values for different fouled ballast and water contents for (a) IDS suspended antenna and (b) ground-coupled IDS antenna

a)	Fouling Index	w = 6%	w= 8%	w = 10%	w = 12%
	6	4.91	5.09	5.10	5.25
	15	5.46	6.05	6.34	6.13
	35	7.09	7.81	8.25	8.56
	55	7.41	7.95	9.10	9.49

b)	Fouling Index	w = 6%	w= 8%	w = 10%	w = 12%
	6	4.99	5.24	5.52	5.91
	15	6.14	6.45	6.955	6.85
	35	6.75	7.32	7.96	8.625
	55	7.24	7.96	8.91	9.52

Figure 4.24 shows an example of test performed with the IDS antenna, in suspended and ground-coupled position.

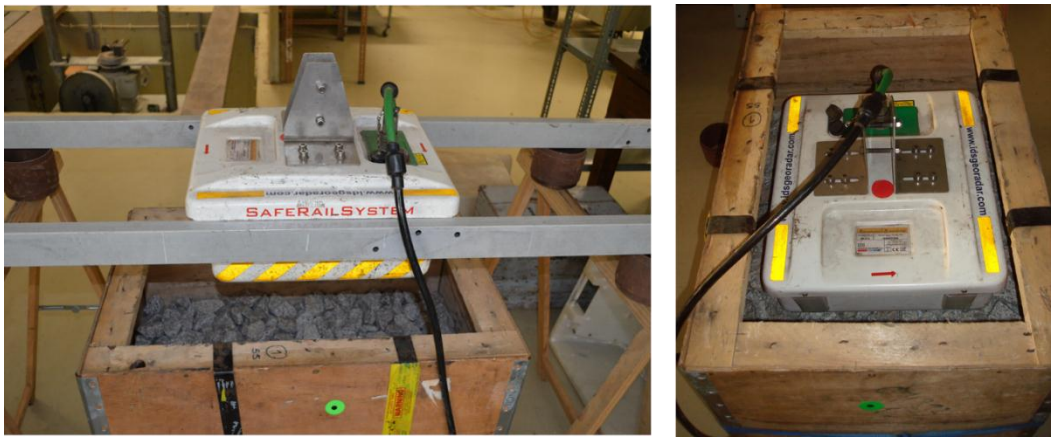

Figure 4.24 - 400 MHz IDS survey on fouled ballast

Figure 4.25 presents briefly the results obtained for all set of antennas: dielectric constant values calculated for index 6, 15, 35 and 55 are plotted against the four water contents. As it was expected, dielectric values increase with the increasing of both fouling conditions and water content, but in different proportions. In fact standard deviation values were calculated for each antenna (Table 4.13), considering two cases: the first by fixing the fouling index and changing the water content, and vice versa. Higher values were found for the second case, meaning that dielectric values are more sensitive to the fouling level rather than with the water content.

Comparing the different GPR systems, IDS suspended antenna has shown higher values for both cases, indicating therefore a major sensibility to ballast conditions changes, reflected in a major dielectric constant values variation. On the other hand, IDS ground-coupled antenna results are similar to 1 GHz and 1.8 GHz GSSI antennas. This difference could be caused by a certain influence of limited dimensions of used boxes. In fact, IDS is characterised by a high beam proportional to its wavelength, and then transmitted signal could be affected by boundary conditions, even more when the antenna was suspended.

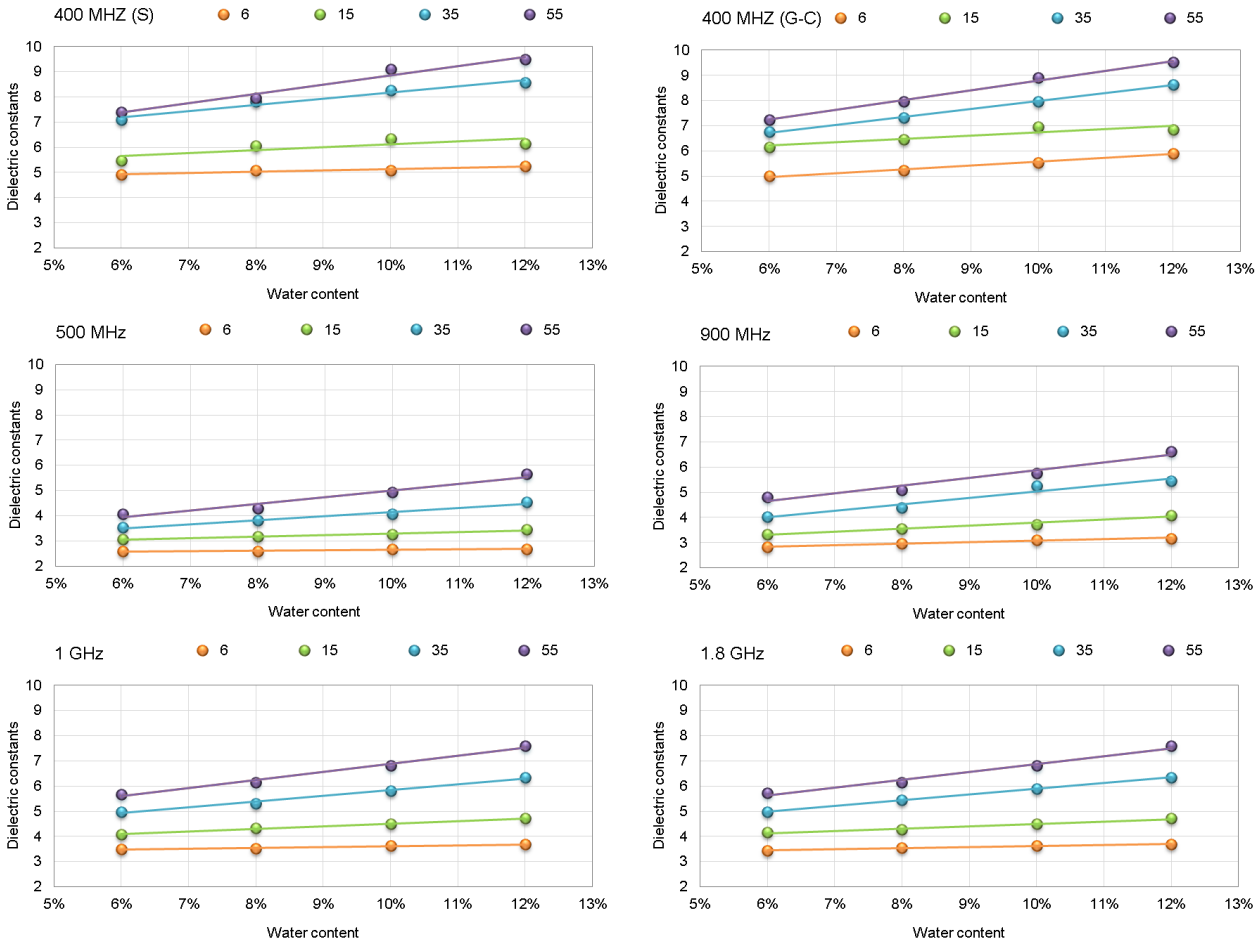

Figure 4.25 - Dielectric constant values variation with water content – four ballast fouling levels

Table 4.13 - Standard deviation of dielectric constant values for fouling conditions

400 MHz (suspended)

Fouling index	Average value	Standard deviation	Water content	Average value	Standard deviation
6	5.09	0.12	6%	6.22	1.06
15	6.00	0.33	8%	6.72	1.20
35	7.93	0.55	10%	7.20	1.57
55	8.49	0.84	12%	7.36	1.73

400 MHz (ground-coupled)

Fouling index	Average value	Standard deviation	Water content	Average value	Standard deviation
6	5.42	0.34	6%	6.28	0.84
15	6.60	0.33	8%	6.74	1.02
35	7.66	0.70	10%	7.34	1.26
55	8.41	0.87	12%	7.73	1.42

500 MHz

Fouling index	Average value	Standard deviation	Water content	Average value	Standard deviation
6	2.63	0.04	6%	3.31	0.56
15	3.23	0.14	8%	3.47	0.64
35	3.99	0.37	10%	3.74	0.85
55	4.74	0.61	12%	4.07	1.13

GSSI 900 MHz

Fouling index	Average value	Standard deviation	Water content	Average value	Standard deviation
6	3.02	0.13	6%	3.75	0.74
15	3.68	0.27	8%	4.00	0.81
35	4.78	0.59	10%	4.46	1.08
55	5.57	0.70	12%	4.84	1.31

1 GHz					
Fouling index	Average value	Standard deviation	Water content	Average value	Standard deviation
6	3.58	0.08	6%	4.56	0.83
15	4.40	0.23	8%	4.82	0.99
35	5.61	0.51	10%	5.18	1.22
55	6.55	0.72	12%	5.58	1.49

1.8 GHz					
Fouling index	Average value	Standard deviation	Water content	Average value	Standard deviation
6	3.57	0.10	6%	4.58	0.86
15	4.41	0.21	8%	4.85	1.01
35	5.67	0.50	10%	5.20	1.23
55	6.57	0.70	12%	5.58	1.49

Figure 4.26 shows the increment (%) of dielectric constant values by passing from moderately clean ballast (index 6) to highly fouled ballast (index 55).

The first feature that can be observed is a quite linear trend for each GPR system.

Second, for w=12 %, dielectric constant values increase of 100 %, except for IDS antenna, for which this value is about 80 %, when it is suspended, and 60 %, when it is in ground-coupled position. While for w=6%, this value is comprised between 50 % and 70 %, except for the IDS placed on the surface.

Comparing the different set of antennas, it can be concluded that the percentages are higher for antennas with higher frequencies (900 MHz, 1 GHz and 2 GHz) respect that of lower frequencies (400 MHz and 500 MHz), except for one case (500 MHz – w=12%).

Also in this case, GSSI air-coupled antennas show very similar results. While IDS antenna confirms dielectric constant values higher than the other antennas, in both of configurations.

These results are very important, indicating a great influence of fines content into the ballast even for lower water contents: dielectric constant values can increase of minimum 50 % by passing from a moderately clean ballast to a highly fouled ballast.

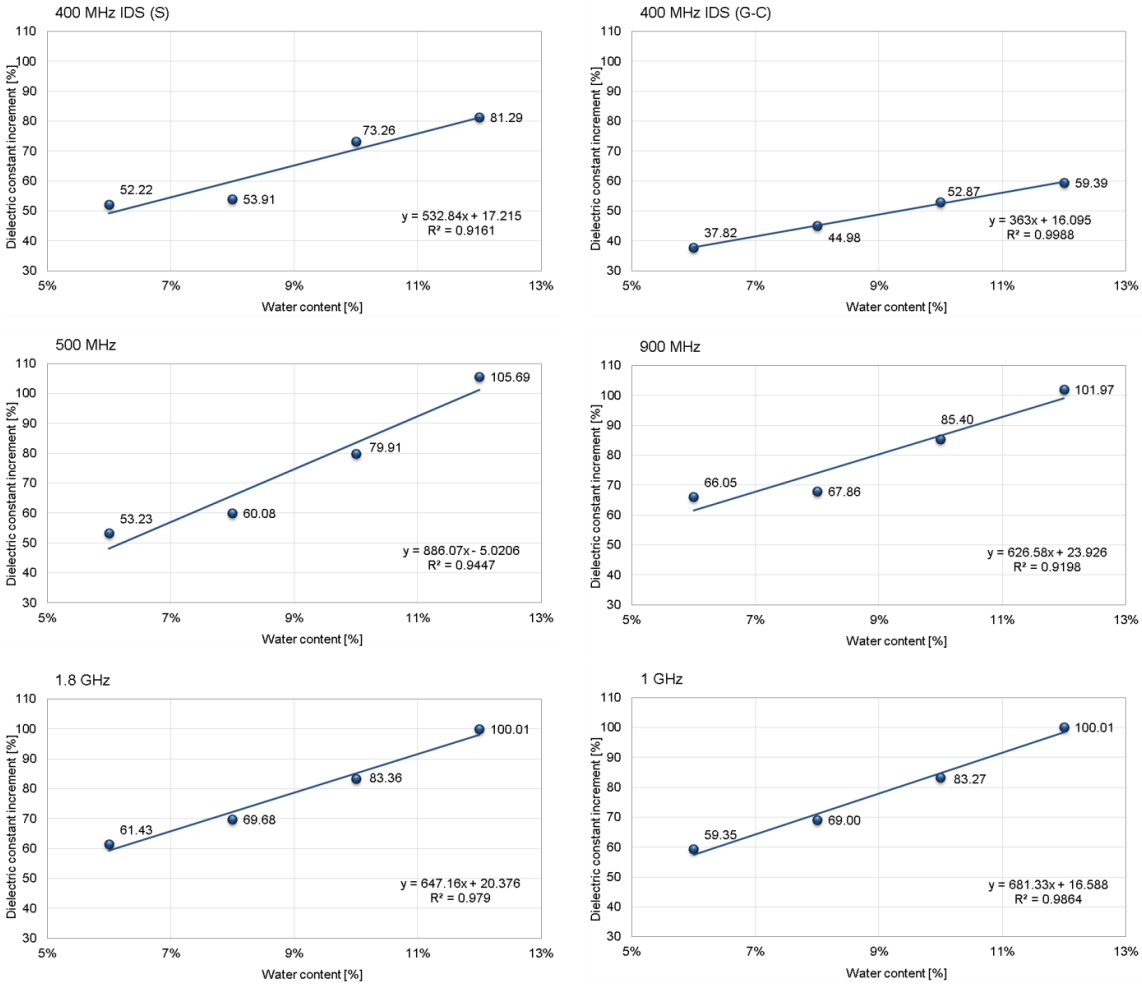

Figure 4.26 - Dielectric constant increment with water content by passing from a moderately fouled ballast to a highly fouled ballast

A second analysis can be made by observing Figure 4.27, in which for each antenna is represented the relationship between the fouling indexes and the dielectric constant values, by passing from w=6% to w=12%.

It can be noticed that the maximum increment of dielectric constant is lower than 50%, that corresponds to the minimum value calculated in the previous analysis, namely they vary between 30% and 40%.

In particular, for lower fouling levels, a significant change in water content does not influence dielectric properties. For index 6, this range varies between 3% (500 MHz) and 13% (900 MHz), excluding IDS antenna in ground-coupled position. For the other antennas, there is a good uniformity of the results.

For index 55, more tests were carried out. Results relatives to soaked and air-dried conditions are reported in Figure 4.28. Dielectric values are represented for each day of survey, for a total of 23 days at the end of which initial conditions (w=12%) were reestablished in terms of dielectric properties.

An almost gradual descendent trend can be observed, moreover for GSSI antennas and in particular for 1 GHz and 1.8 GHz which values are practically equal. This not happens for IDS antennas, also if suspended antenna shows lower values than the other (ground-coupled), on the contrary of earlier surveys.

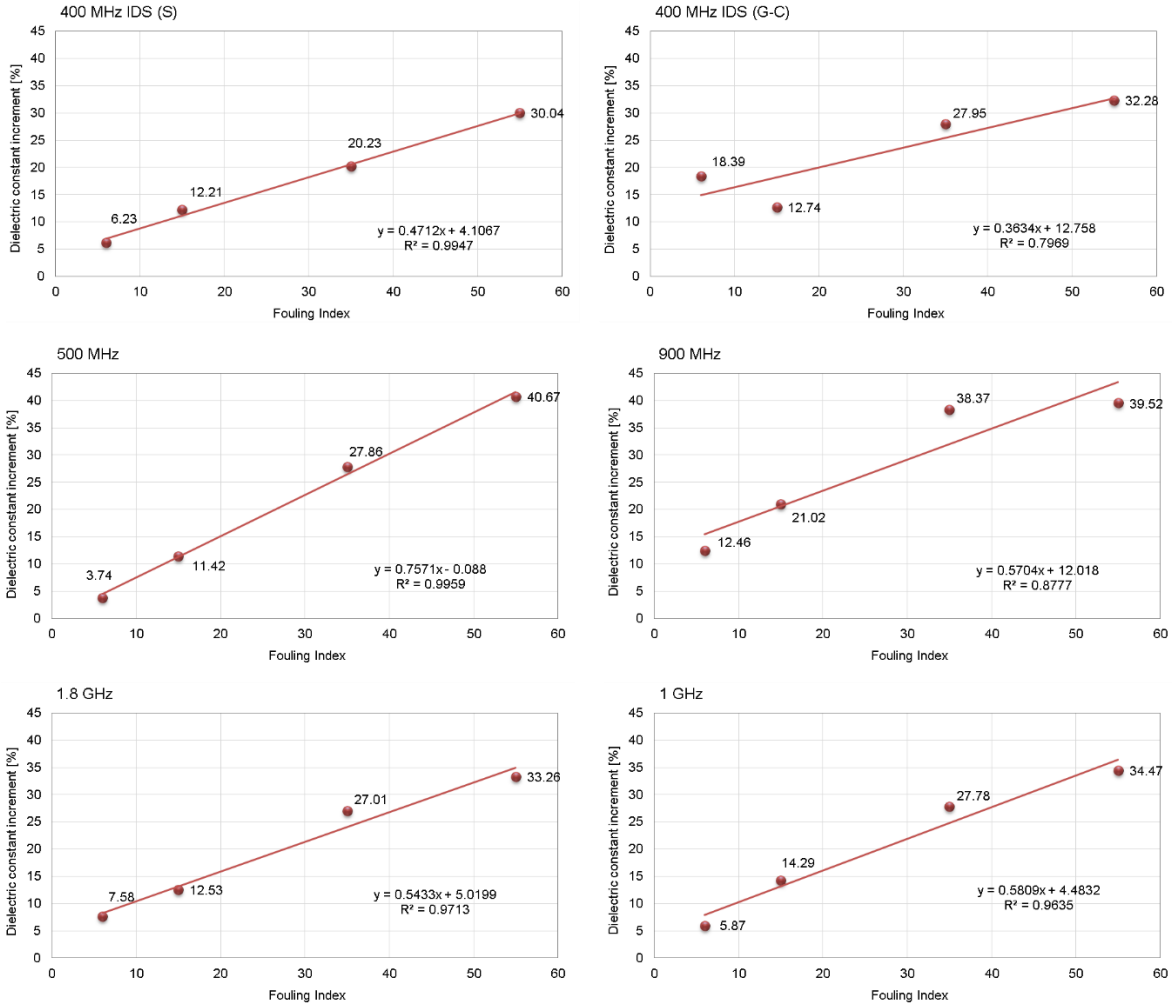

Figure 4.27 - Dielectric constant increment with fouling levels by passing from a w=6% to a w=12%

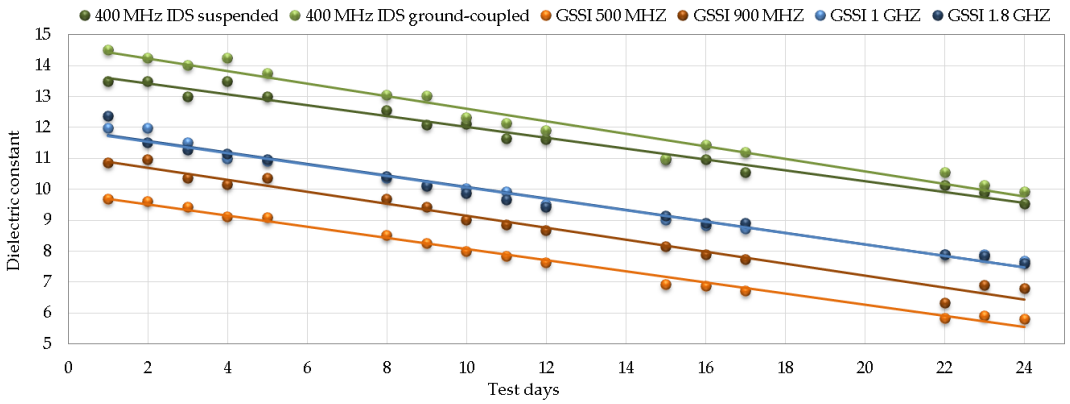

Figure 4.28 - Dielectric constant values for highly fouled ballast, after saturation and in air-dried conditions

In order to catch a definite range for dielectric values for next granite ballast GPR surveys, Table 4.14 reports minimum values (index 6-w=6%) and maximum (index 55-w= 12%). Focusing on IDS antenna, values change between 4.9 and 9.5.

Table 4.14 - Dielectric constant values range – minimum for index 6 - w=6% and maximum for index 55 - w=12%

	ε_{min}	ε_{max}
400 MHz IDS ground-coupled	4.99	9.52
400 MHz IDS suspended	4.91	9.49
GSSI 500 MHZ	2.58	5.65
GSSI 900 MHZ	2.83	6.62
GSSI 1 GHZ	3.50	7.59
GSSI 1.8 GHZ	3.43	7.59

4.7. CONSIDERATIONS FOR INTERPRETATION

Before starting a GPR survey, a good rule is to detect surface reflection in the time window and eventually shift the time scale until its caption.

In fact, in this laboratory study, some data were lost for this reason, namely for 500 MHz and 900 MHz antennas, also because initially there was a certain lack of experience in using them. Therefore, new surveys were performed, specifically for clean ballast study.

Figure 4.29 permits to clarify the problem, on the left is represented the first erroneous data acquisition, in which what it was considered the surface reflection, actually it was the bottom layer reflection, as it can be observed in the second acquisition (right). This was obtained by changing time scale and then choosing a minor initial time window (ns).

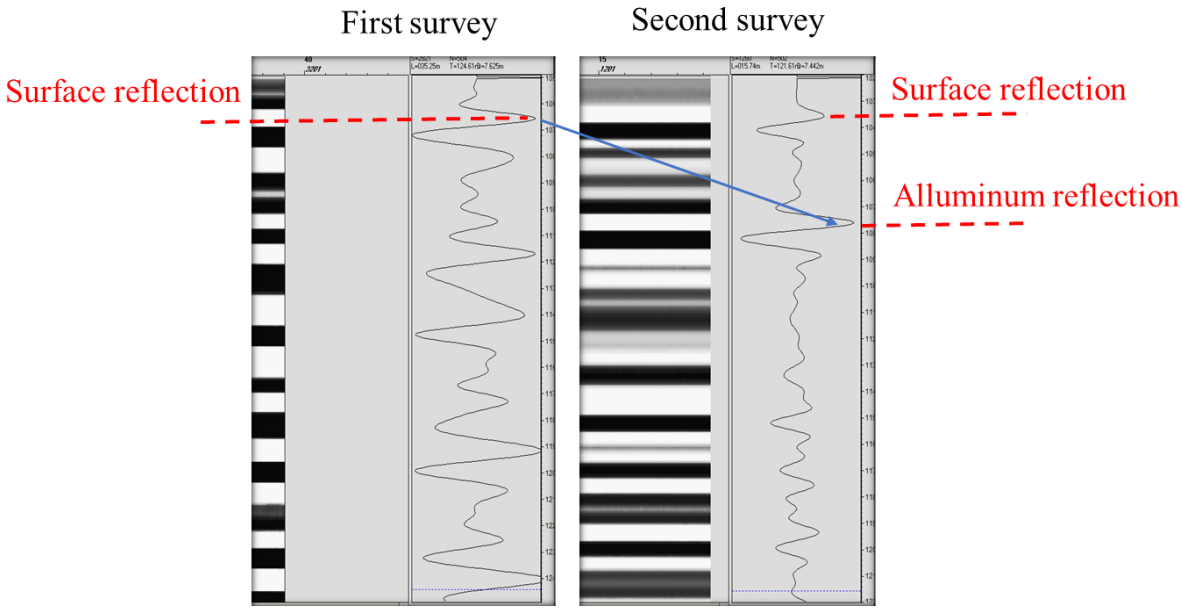

Figure 4.29 - Surface reflection picking: incorrect (left) and correct (right)

For IDS antennas, many difficulties were encountered for defining the zero level, or surface reflection.

As it was suggested from the producers of Railwaydoctor software, zero level can be chosen in automatic or manual mode by picking the top of the sleeper (Figure

4.30), mathematically it can be defined as the successive inflection point after the first maximum positive wave amplitude (right), by increasing time.

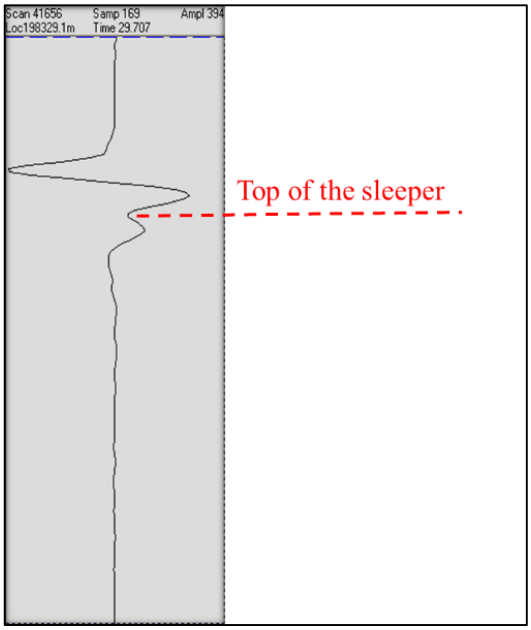

Figure 4.30 - Zero level picking for Railwaydoctor

In laboratory, GPR signal was quite different from that generally visualized for in situ tests and surface level was difficult to detect, probably due to boundary conditions.

In the case of suspended antenna a new methodology was used, according with IDS producers (Figure 4.31):

1) coupling time (T_x-R_x) was measured (t_C);
2) it was considered the antenna elevation from surface and, through the air dielectric constant, the wave travel time in the air was measured (t_A);
3) Zero level (S) was given by the sum of both terms:

$$S = t_C + t_A$$

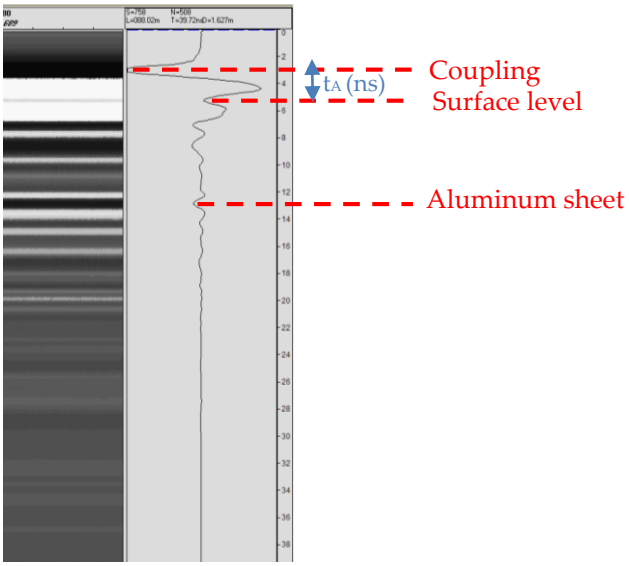

Figure 4.31 - IDS surface level calculation

Also many multiple reflections were noticed, always for the presence of external elements picked by GPR signal, and this fact provided a certain difficulty for detecting bottom reflection. However, this was resolved through to the comparison with data of IDS antenna in ground –coupled mode for which bottom reflection was definitely clearer. On the other hand, for interpreting the antenna in ground-coupled mode, coupling time was considered as zero-level.

4.8. CONCLUSIONS

Chapter 4 has introduced the importance of GPR calibration, as dielectric properties are necessary for GPR data interpretation. Several methods can be used for this purpose, in laboratory or in situ.

GPR laboratory tests performed at the National Laboratory for Civil Engineering (LNEC) were presented.

Five GPR systems were used in order to compare their response: IDS antenna, used for Portuguese railway monitoring together with GSSI ground-coupled and air-

coupled antennas, used by LNEC. For IDS antenna, two configurations were studied, in ground-coupled position and semi ground-coupled, reproducing the in situ conditions.

Three materials were considered: a clean ballast, a fine soil and a mixture of them for simulating fouling conditions; namely, five fouling levels were considered by taking into account the Relative Ballast Fouling Ratio.

Different water content were reproduced: dry, wet, saturated, partially saturated and air-dried conditions for clean ballast; for both fine soil and fouled ballast, four water contents were chosen by taking into account two lower values and two upper values than the optimum value of fine soil.

For clean ballast, results have shown a good relationship with values found in bibliography. IDS antenna has always shown higher values, even more in suspended position, comparing with the GSSI systems. For these latter, it was demonstrated that the higher the frequency the higher dielectric constant values. GSSI air-coupled antennas have confirmed more similar results than other antennas. As expected, a great variation of dielectric constant values was obtained for saturated and partially saturated conditions.

For fine soil, values have shown a linear increment of dielectric constant with the water content, for each GPR system. Some problems occurred for 500 MHz and 900 MHz during data acquisition, anyway a comparison between IDS and air-coupled GSSI was made: also in this case, IDS antenna values resulted higher than 1 GHz and 1.8 GHz GSSI antennas, which values were very similar, in particular the difference between IDS and GSSI increases with the increase of water content.

Fouling ballast case was more complex than the first two. In general water content values were assumed in four levels, as for the fine soil, except for the cleaner ballast where only the soil optimum values was considered. Moreover, for the most fouled ballast, soaked conditions were tested and then also air-dried conditions. Results have shown a linear increment for both fouling levels and water content

variation, in different proportion: dielectric properties are more affected by fouling variation than water content.

Therefore, for railways, the knowledge of dielectric constant values represents a crucial aspect for obtaining good results in terms of ballast thickness and high quality surveys. On the other hand, detection of fouling and water conditions represent still a challenge for GPR railways surveys and new analysis has been developed in the last years for automatize GPR interpretation.

5. IN SITU TRACK CHARACTERISATION WITH GPR

5.1. INTRODUCTION

In the past, cores and test pits were typically used for transport infrastructure evaluation and along the years they have been substituted by non-destructive tests. However they still represent an indispensable method, as for GPR, therefore their performance has been limited but not excluded.

Railways track characterisation with GPR follows the same rules applied for road and airport pavements. For new pavements, GPR can assess layers thicknesses by fixing dielectric constant values. Moreover, in this case, in situ calibration can be limited if considering dielectric constant values obtained in laboratory tests (Chapter 4) or found in bibliography. On the other hand, a certain accuracy in assigning dielectric values is required, even more if tests are performed in wet conditions.

For older pavements, test pits are strongly recommended: they consist in measuring materials layers thicknesses and, through GPR signal response, dielectric constant values can be determined.

The main challenge for railways studies is represented by ballast fouling conditions that can exist in different levels and may be very changeable along the same track, resulting in a high variation of both thicknesses and dielectric constants. Moreover, also thicknesses measurements for calibration results are quite subjective, due to ballast aggregate dimensions and to a gradual passage from clean to fouled conditions and also due to the instability of the ballast layer during test pits performance.

In the last years, new analysis have been developed for improving GPR data analysis at network level: due to ballast distribution, its high number of voids produce a scattering signal which may be representative of its condition (see 1).

For a more user-friendly data analysis, latest GPR interpretation software enables to correlate cores/test pits information with data in the same output window, for facilitating calibration and then interpretation. In addition, new GPR acquisition software enables to mark core location on GPR data record by reducing survey speed in correspondence of location. In both cases, it is important for the operator to mark cores location with precision for obtaining a good relationship.

In this Chapter, the characterisation of a new track with GPR and without test pits is presented. In addition, test pits applications on two tracks for both calibration and results validation are discussed.

5.2. METHODOLOGY

5.2.1. General

Track characterisation at network level with GPR consists in layers thicknesses and respective variation detection (see 3.3), study of ballast quality, subgrade instability, and drainage problems (Hugenschmidt, 2000).

In the last years, many studies were focused on ballast thicknesses measurements and its quality characterisation based on new GPR signals processing and interpretation, anyway they represent still a challenge.

Several studies have been carried out for ballast fouling analysis. Clark et al. (2004), referred by (Al-Qadi et al., 2010), performed tests with 500 MHz, 900 MHz and 1.5 GHz antennas, founding that clean and fouled ballast are characterised by different frequencies, reflected in GPR signal, and can be representing by Fast Fourier Transform (FFT). The characteristic of FFT is enabling to convert time domain GPR data in frequency domain. Silvast et al. (2006), using a 400 MHz antenna, considered the Fourier Transform application by using a new algorithm, developed by Roadscanners, which calculates continuously the area of a GPR signal frequency spectrum in correspondence of a definite ballast depth, obtaining

a frequency sum method that is actually used in Roadscanners products for determining ballast quality.

For ballast fouling detection, also scattering analysis has been widely used together with higher frequency antennas. Frequency is a parameter that depends from electromagnetic wavelength λ and this latter can be correlated with the transmission medium, such as ballast aggregates, and with its scatter objects, such as air voids in clean ballast. This correlation enables three different responses: if the scatterers are of the same size of λ (Mie or resonance response), if they are smaller than the wavelength (Rayleigh response) and, finally, if they are larger than the wavelength (optical response) (Annan, 1992). The last case is not considered as it limits the penetration depth, therefore for GPR inspection antennas are chosen between the first and the second case. If higher frequency antennas are chosen (range of few GHz), a resonance response is expected and a scattering analysis can be developed, while lower frequencies provide Rayleigh response and classical radar detection techniques can be used. In the first case, ballast is considered as a heterogeneous medium and each grain extracts energy as the electromagnetic field passes and scatters it in all directions (Figure 5.1) (Jol, 2008).

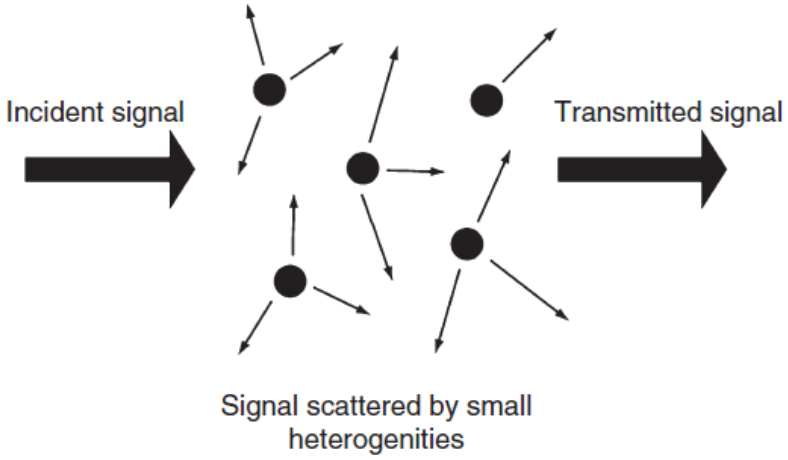

Figure 5.1 - Scattering process (Jol, 2008)

First studies were performed by (Roberts et al., 2006), and confirmed by Al Qadi et al (2008), that used 2 GHz and 1 GHz horn antennas and introduced the scattering amplitude envelope approach. Roberts demonstrated that 2 GHz antenna presented a higher scattering response, than 1 GHz, and respective wavelengths are short enough to detect the presence of air voids and then the presence of clean ballast. On the other hand, a fouled ballast presents a weaker scattering pattern (Figure 5.2).

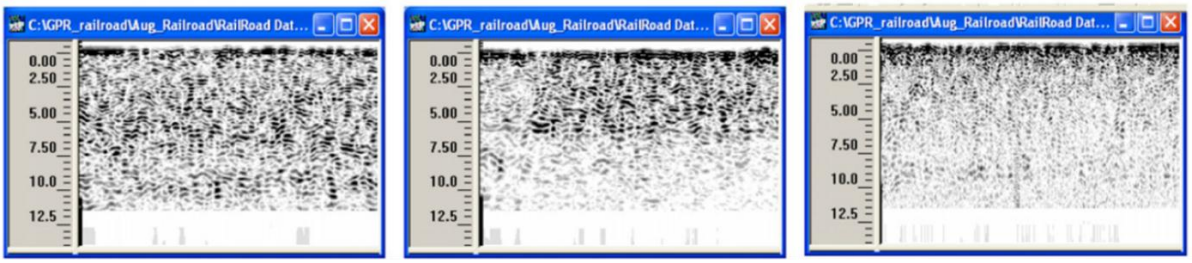

Figure 5.2 - GHz scattering pattern in different ballast cases: (a) clean (b) moderately fouled (c) fouled (Al-Qadi et al., 2008)

As 2 GHz antenna presents a random signal where the energy attenuation is function of frequency and materials, classical techniques, such as Fourier Transform, may be not efficient. For overcoming this aspect, Al Qadi (2010) introduced an innovative GPR data analysis: a time-frequency technique was studied, based on the short-time Fourier Transform (STFT). In situ tests were analysed with STFT. Results (Figure 5.3) have shown different energy attenuations dependent on the number of air voids and therefore on the presence of fouling. In particular, for clean ballast, the energy attenuation rate with time is quite slow (from red to blue). When the ballast becomes moderately fouled and then a certain water content is present, the energy attenuates gradually. Finally, when ballast becomes seriously fouled with presence of water traps, the passage from red to blue is quickly.

More recent is the application of another technique: the Wavelet transform (Shangguan et al., 2012). The improvement consisted in resolution. In fact in the

STFT window, after that is chosen, resolution does not vary, while the Wavelet is a multiresolution technique that can be adjusted depending on frequencies and times changes. Comparing with other techniques, wavelet transform enables to estimate fouling conditions also when a clear interface between clean and fouled ballast does not exist and also it permits to process all GPR scans automatically, while with STFT is possible to process one scan at a time.

If higher frequency antennas are useful for evaluating ballast conditions, lower frequency antennas are necessary for overcoming higher antenna frequency depth limitations, even more when wet soils are tested and dielectric permittivity can largely reduce GPR signal penetration. Multi-frequency systems have shown to be more efficient (Su et al., 2011). Roberts et al. (2008) presents a multi-frequency application, namely 2 GHz and 500 MHz antennas, concluding that the latter antenna enables detecting stronger reflections between the cleanest ballast and sub-ballast, and, in some cases, between sub-ballast and subgrade. Reflections were also visible in presence of fouling, but for higher percentages this is a rare event, as the difference between the dielectric constant of fouled ballast and sub-ballast is lower.

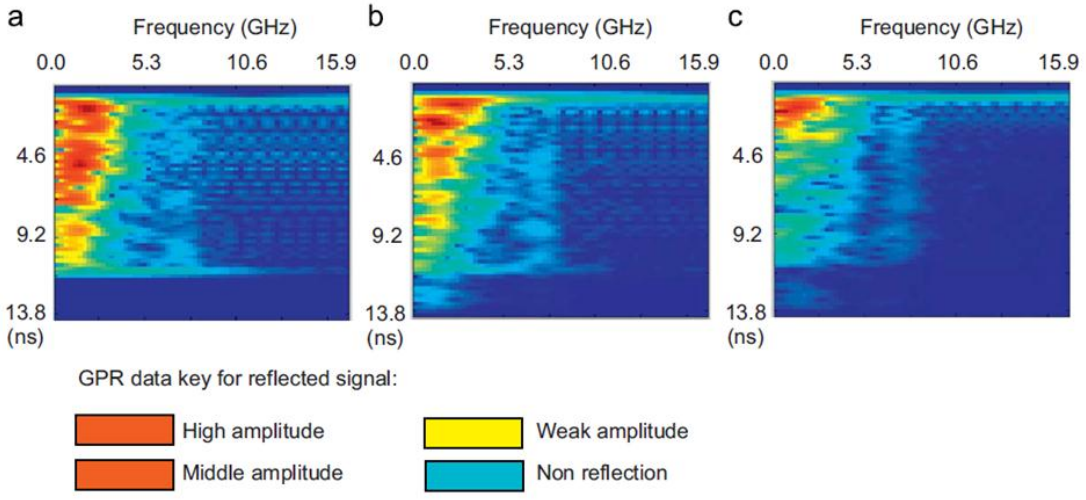

Figure 5.3 - STFT results (Al-Qadi et al., 2010): a) clean ballast, b) moderately fouled ballast, c) fouled ballast

Further studies based on scattering analysis were developed by Forde et al. (2010), Zhang et al. (2011) and Manacorda and Simi (2012). The last one for distinguishing zones with compliant ballast from that with undersized ballast. They demonstrated that even if both materials were characterised by the same dielectric constant values, their scattering attenuation was different. In this manner, materials can be characterised: for a compliant ballast, a stronger scattering attenuation and therefore a clear reflection is expected, and vice versa for an undersized ballast.

A different methodology, based on the magnitude spectrum was developed by University of Wollongong (Shao et al. 2011). Comparing three different types of ballast, namely clean, 50 % coal fouled and 50% clay fouled, it was observed that the respective traces had different magnitude spectra, determined with the Discrete Fourier Transform. In addition, the methodology includes a support vector machine for ballast fouling classification.

Other older non-destructive tests can be used for fouling detection, for example Anbazhagan et al. (2011) presents a comparison study between GPR and seismic surveys. Multi-frequency GPR has shown to be faster and efficient for determining fouling depth, giving a quality response. On the other hand the spectral analysis of surface waves enables characterise fouling in a quantitative manner.

About subsoil conditions, studies focused on track stability problems were developed (Olhoeft and Selig, 2002; Sussmann et al., 2003), also combining GPR with other destructive and non-destructive tests (Gunn et al., 2007; Donohue, 2011).

5.2.2. Track evaluation: a Portuguese case study

For the study of a renewed track in Portugal (Fortunato et al., 2010), a different procedure was developed. Layers thicknesses were used as input data and dielectric constant values were determined. Thicknesses were considered reliable as topographic measurements were performed during construction phase. The

track presented different structure solutions, namely it was composed by ballast, sub-ballast, capping layer and embankments or cuttings, all of them variable in thicknesses and materials. A 10 km long track was selected and two structure solutions were studied (Figure 5.4): one, named "traditional" that is constitute by 35 cm of granite ballast, 15 cm of granite sub-ballast, 35 cm of limestone capping layer and a variable subsoil (fine and coarse sands, clays, heterogeneous materials, etc.). The second solution presented the same characteristics of the first one for ballast, sub-ballast and subsoil, but the capping layer thickness was 20 cm and, in addition, a rockfill layer was included with a thickness variable among 35, 40 and 44 cm.

The aim of the study was to detect, along the track, changes of the layers in terms of both thicknesses and materials characteristics, namely dielectric properties.

Data processing and calibration were executed. First, zero level was chosen by considering antenna elevation (see 4.7). Filters were applied, namely background removal, horizontal high pass filter for removing rails noise, horizontal low pass filter for removing sleepers noise and arithmetic operation for changing signal sign. Then, a correction of the coordinates was performed in order to guarantee the right location. The simplest procedure consists in checking a metal bridge in the event file (see 3.2.2), if it exists, as it always presents a high level of noise in the GPR files, and then in moving the GPR coordinates conforming the GPS coordinates (Figure 5.5).

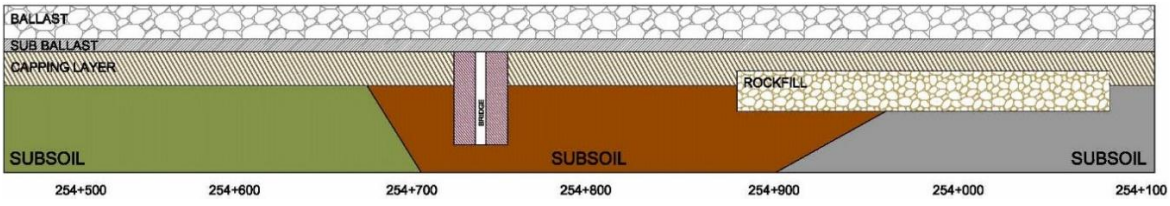

Figure 5.4 - Part of the studied track - Different structures: Traditional solution (left) and Solution with rockfill (right)

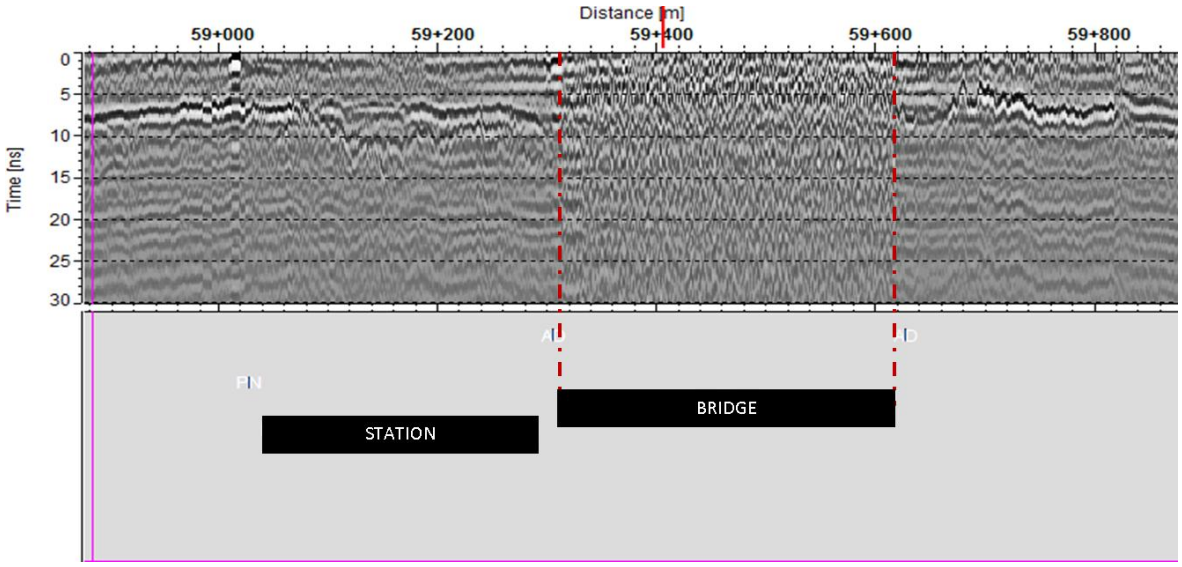

Figure 5.5 - Calibration of GPR data

Then GPR data interpretation started. Changes in the structure were detected, for example, a variation of the subsoil, in particular from sand to heterogeneous material. Also, a bridge can be distinguished (Figure 5.6).

Different layers interfaces were detected. Comparing two solutions, interfaces were clearly better in the traditional one. Moreover, some problems occurred for the solution with rockfill, characterised by a high level of noise in correspondence of deeper layers. In addition, others parts of the track showed a clear transition between the two structural solutions, where it could be observed the change in capping layer thickness from 20 to 35 cm (Figure 5.7).

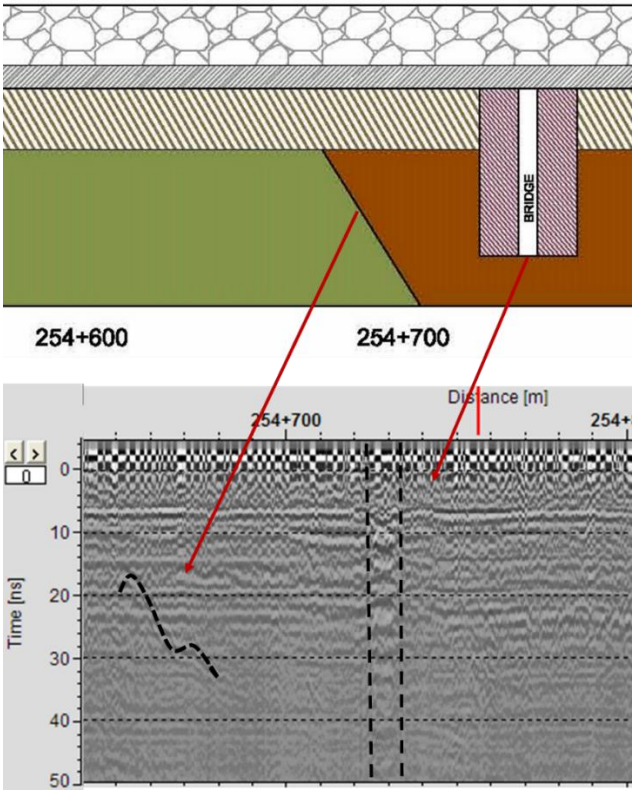

Figure 5.6 - Structural changes detected by GPR

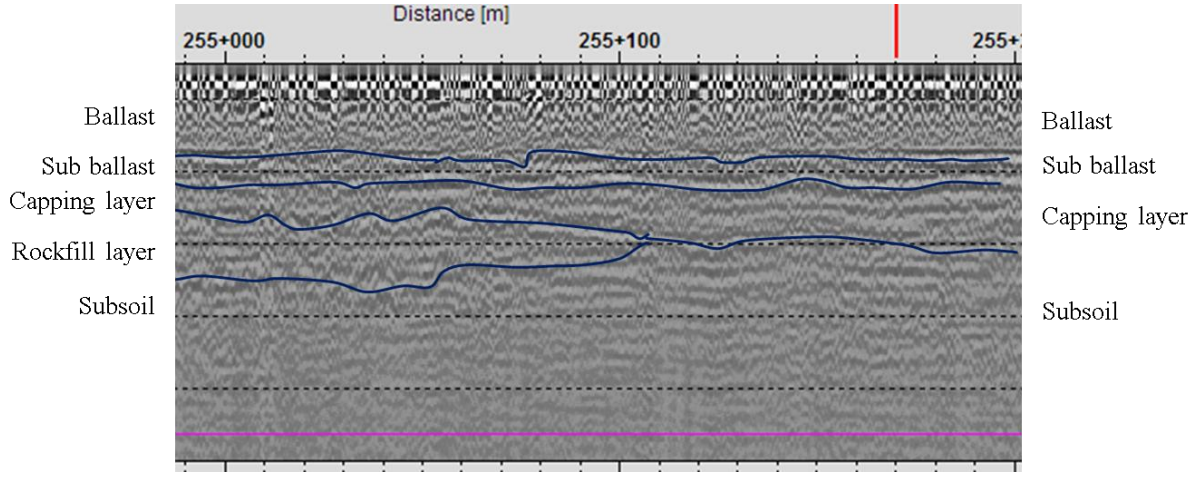

Figure 5.7 - Layers interfaces detected with GPR – two solutions

The second scope of the study was determining and comparing different materials dielectric constants and studying their variation with water content. Three different periods of measurements were taken into account (September 2011, January 2012 and March 2012). Precipitations trend, namely the average per month values, is represented in Figure 5.8.

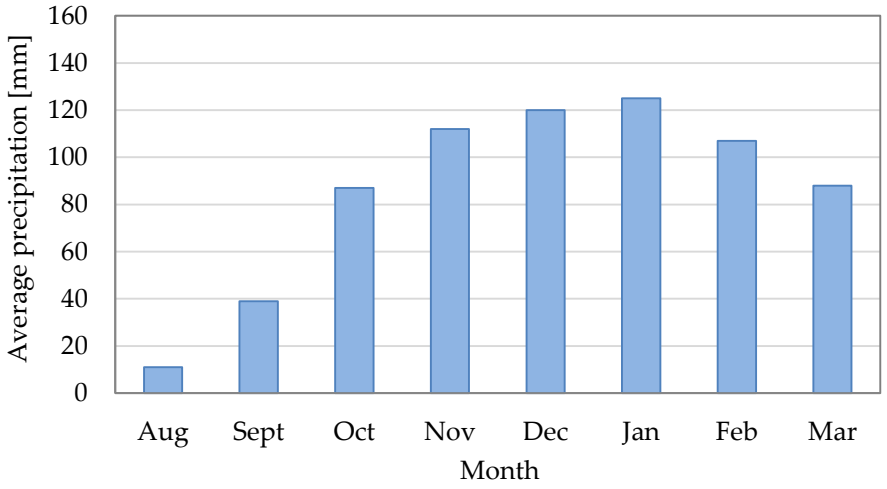

Figure 5.8 - Monthly average precipitations

As already referred, some parts of the track were clearer than others and for this reason just a certain number of points were selected for interpretation: solution with rockfill from 1 to 15 and traditional solution from 16 to 21.

Therefore, through layers thicknesses and the wave travel time (see Eq. 2.24), the dielectric constants of the different materials were determined for each testing campaign (Table 5.1).

Figure 5.9 represents the values for ballast material obtained in each point. In general, the values obtained in September are lower than that found for January and March that are quite similar. Table 5.1 shows the average values obtained for each month. It can be noticed a little increment with water content and that they are in agreement with values obtained through test pits (see 5.3).

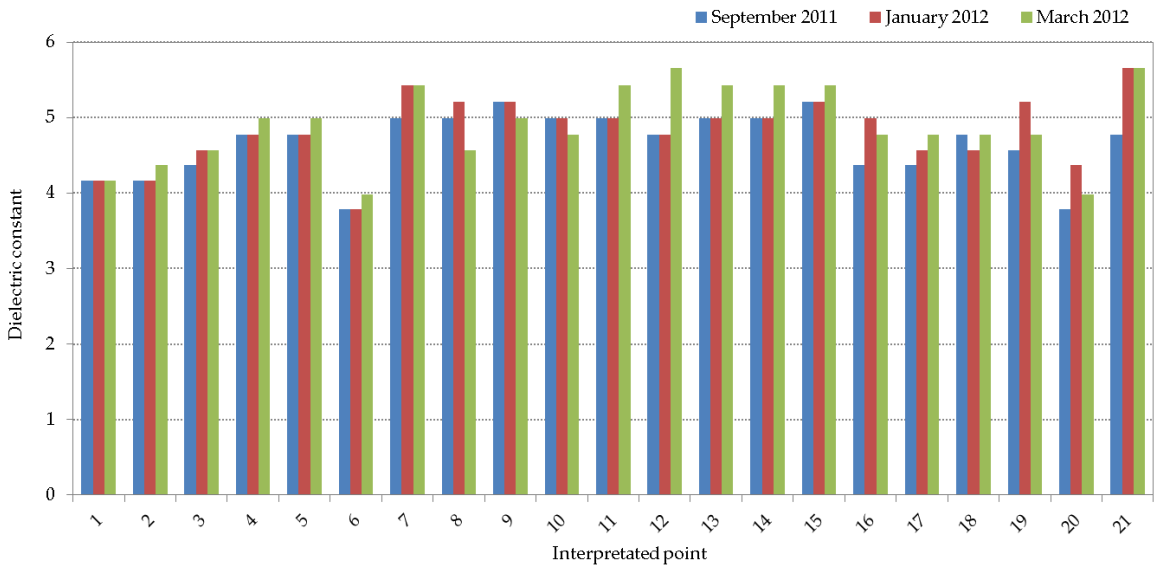

Figure 5.9 - Dielectric constant values for ballast material

Table 5.1 - Average values for ballast dielectric constant

	ε
September 2011	4.66
January 2012	4.83
March 2012	4.90

For sub-ballast (Figure 5.10), interface detection presented some difficulties mainly in the solution with rockfill, while in the traditional one, a clear interface could be observed. Anyway, values have shown some differences. Comparing the three campaigns, water content influence is not evident like in the case of ballast. However, a certain increment is appreciated in March, probably due to the fact that water was not well drained. About the average values (Table 5.2), they can be considered suitable.

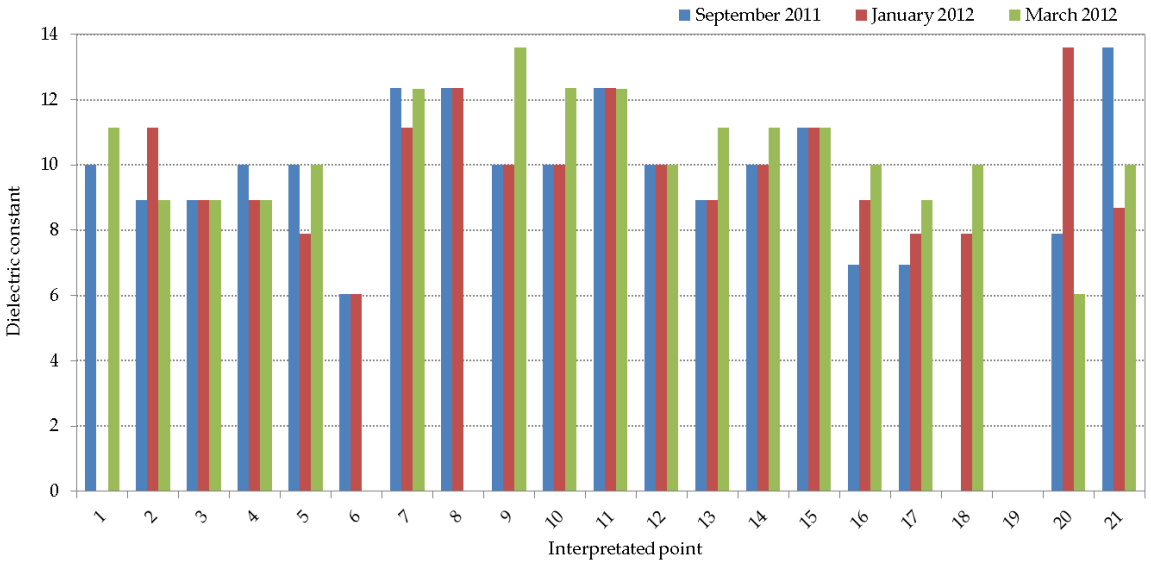

Figure 5.10 - Dielectric constant values for sub-ballast material

Table 5.2 - Average values for sub-ballast dielectric constant

	ε
September 2011	9.81
January 2012	9.78
March 2012	10.38

For capping layer material, there is no a clear trend (Figure 5.11). Also in this case it is probably due to a great difficulty in detecting deeper layers, moreover in the solution with rockfill. The average values are satisfactory and they present the opposite situation of sub-ballast: values are lower in March than in September and January, that are similar (Table 5.3).

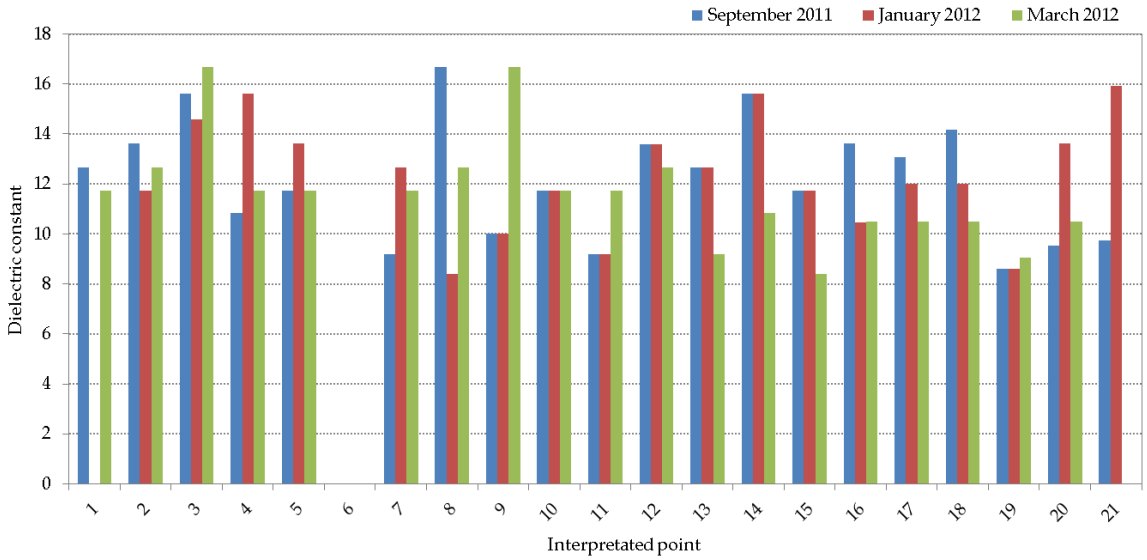

Figure 5.11 - Dielectric constant values for capping layer material

Table 5.3 - Average values for capping layer material dielectric constant

	ε
September 2011	12.18
January 2012	12.30
March 2012	11.64

For the rockfill layer (Figure 5.12), the interpretation was even more difficult due to its deeper position. However, average values are rather similar (Table 5.4).

Finally, it can be concluded that results have shown a good reliability with that found in bibliography and in past laboratory tests (see 4.3 and 4.6).

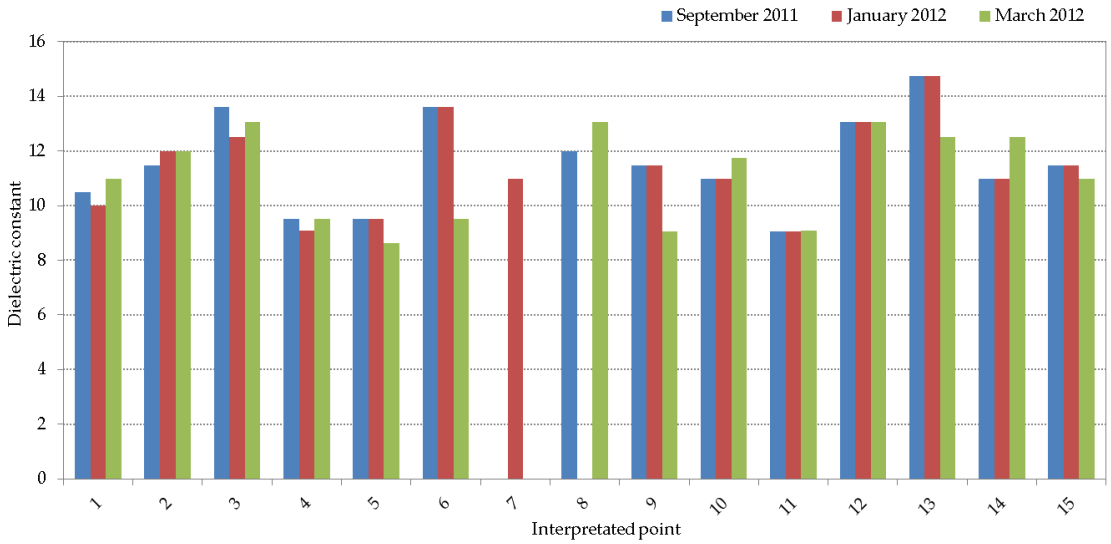

Figure 5.12 - Dielectric constant values for rockfill material

Table 5.4 - Average values for rockfill material dielectric constant

	ε
September 2011	11.57
January 2012	11.39
March 2012	11.12

5.3. TEST PITS

5.3.1. Overview

As introduced in Chapter 4, GPR data calibration is a necessary step for obtaining accuracy of results. The traditional method is represented by the execution of cores and/or test pits. This method is time consuming and limits traffic but, on the other hand, it may be more efficient, as real track conditions can be observed.

Several studies have been developed by comparing GPR and core efficiency in road pavements studies. Wenzlick et al. (1999) present several applications, finding for GPR good results in terms of accuracy with and without core calibration. Morcous and Erdogmus (2009) have shown that in GPR surveys, the number of cores can be reduced from 10 to 2 and that the average difference in concrete thickness measurements using GPR (with calibration cores) and drilled cores was found to be about 0.3 cm for a total thickness of about 25-33 cm, which represents an average measurement accuracy of 98.5%, that is relatively high.

In general, cores and test pits are more required for older pavements studies, where layer properties can be different from the initial ones. For example, the dielectric constant of concrete is highly dependent on its age, which significantly affects the measured thickness: Morcous and Erdogmus (2009) present laboratory tests which results have demonstrated that using an assumed value for concrete dielectric constant lead to a significant reduction in the measured thickness of 0.03 cm per day as the concrete gets older. On the other hand, for example, asphalt pavements may have rutting on surface and/or stripping or intrusion in base materials that can lead to some concern about the accuracy and precision of thickness measurement. Therefore, Uddin (2006) suggests to make 3-5 thickness measurements of a core and calculate the average value, as well as to take an average of three measurements inside the core hole if possible.

Cores locations should be selected ad hoc, depending on the aim of the survey. For network level tests, constant sections in terms of layers thicknesses and materials should be chosen, as a certain error in GPR data or core location should be admitted. For rehabilitation works, points with problems should be selected for studying the type of problem and its severity.

Materials conditions evaluation represent a key factor for data calibration, then more reliable results can be obtained if representative materials samples are collected and studied in laboratory for characterisation. In particular for railway studies, water content and ballast fouling index determination are both very important. As expected, this process is very difficult to actuate and therefore it is

usually done separately from GPR tests but often loosing reliable conditions information.

In railways, tests pits are performed, as the impossibility of extracting undamaged cores. Uncertainties can occur for ballast thickness detection due to aggregate dimensions and, in case of fouling conditions, a certain difficulty may emerge for defining thickness of both clean and fouled ballast. Firstly because the passage from clean to fouled ballast happens in a gradual way, secondly due to the fact that fouling can vary in the same cross section, namely it increases under sleepers where loads actions are higher.

For this reasons, in recent studies, test pits have been used, for fouling detection through analytical models, i.e. using Fourier Transform (Silvast et al., 2010).

For the present research, two sets of test pits were performed in Portugal and the selection of the tracks studied was made for various purposes, namely some for GPR calibration and others for validation of the results.

5.3.2. Calibration procedure

The first track studied is part of the Portuguese North Line and, in particular, two old stretches of it were considered. The structures consists of a ballast layer, on the top of the soil, and it presents twin block sleepers. It was recently subjected to a tamping action but some geometric parameters, i.e. alignment (Figure 5.13), still present higher standard deviation values compared with the requested values. In addition, this track section was used to study the determination of dielectric constant values of different materials.

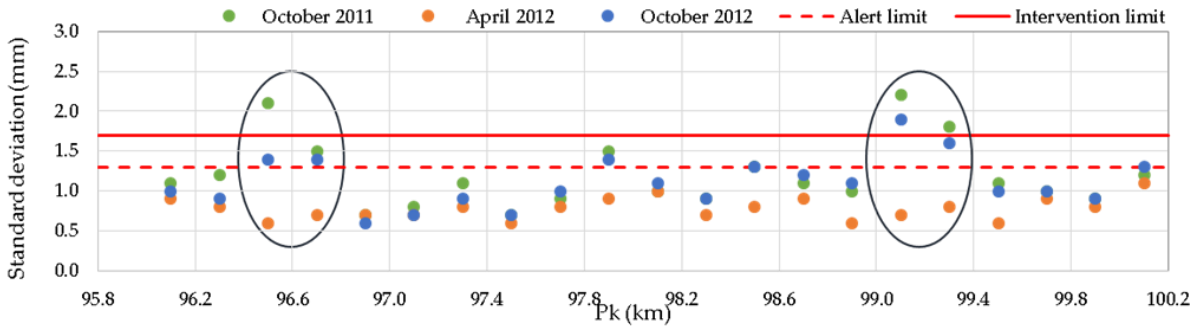

Figure 5.13 – Alignment trend - Portuguese North Line

Test pits locations were selected ad hoc. The common rule was to choose points where GPR signal presents uniform and consistent reflection, as a certain location error should be admitted. In this case, the scope was to obtain different examples to analyse and characterise, namely where GPR signal showed different and variable interfaces. Then, twelve test pits location were selected.

The determination of the thicknesses was performed. Two measurements for each test pits were done: one in correspondence of the end of the sleeper and the other between rails, where GPR antenna measures. In the two sites, differences between clean and fouled ballast conditions were assessed, due to specific track behaviours under sleepers for dynamic traffic loads (see Chapter 6). However, only measurements between rails were taken into account for calibration, due to the fact that lateral antennas were not mounted during monitoring as, after the first tests, it was observed that rails reflections made interferences with the signal, turning the interpretation very difficult.

As already referred, the separation of the different conditions, such as clean ballast and fouled ballast, or moderately fouled ballast from highly ballast, represented a crucial aspect for both in situ measurements and GPR analysis, mainly because the passage from clean to fouled occurs in a gradually way. In situ, it was observed that, in some cases, the same layer presented more than one thickness (between rails) in the same test pit, therefore thicknesses average values were calculated for data calibration (Figure 5.14).

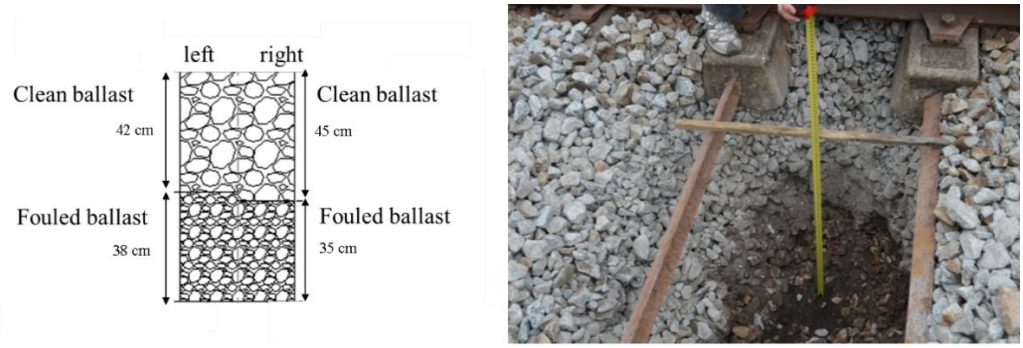

Figure 5.14 - Different thickness measurements for the same test pit

Dielectric constant values were calculated for clean ballast (Figure 5.15). It can be observed that values are quite similar with that obtained in 5.2.2.

On the other hand, for fouled ballast, calculation was quite difficult, as already referred, and results are not presented.

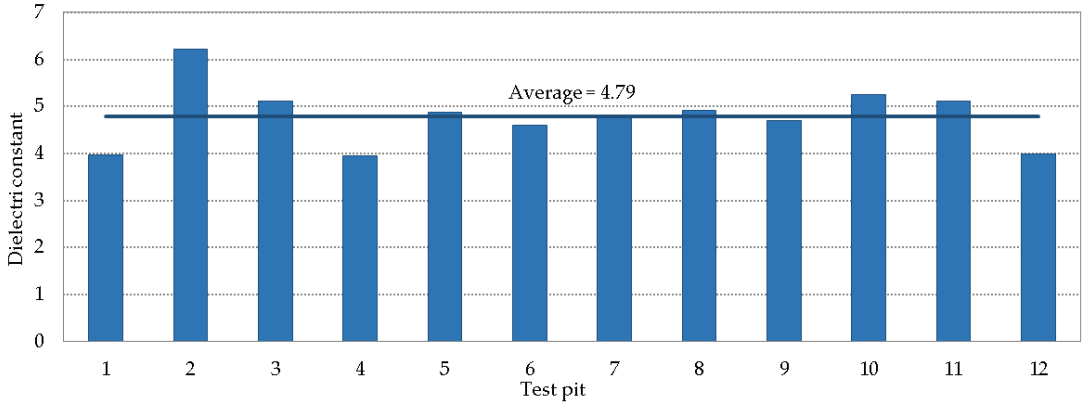

Figure 5.15 - Dielectric constant values for granite clean ballast – track 1

The test pits were performed also for studying the different GPR records for different track materials, trying to find patterns for developing a future procedure at network levels. Then, for each test pit different situations in terms of thicknesses and materials were encountered, namely:

- clean granite ballast;

- fouled granite ballast, with different levels of fouling;
- limestone ballast;
- fouled limestone ballast, with different levels of fouling;
- sub-ballast.

As expected, where there were significantly different layers or changes in structural condition, higher wave amplitudes and clearer interfaces were detected, namely between clean ballast and subsoil (Figure 5.16), granite ballast and limestone ballast (Figure 5.17), ballast and sub-ballast, and sub-ballast and subsoil (Figure 5.18). On the other hand, gradual conditions changes have showed minor waves amplitudes, i.e. between clean ballast and fouled ballast (Figure 5.19).

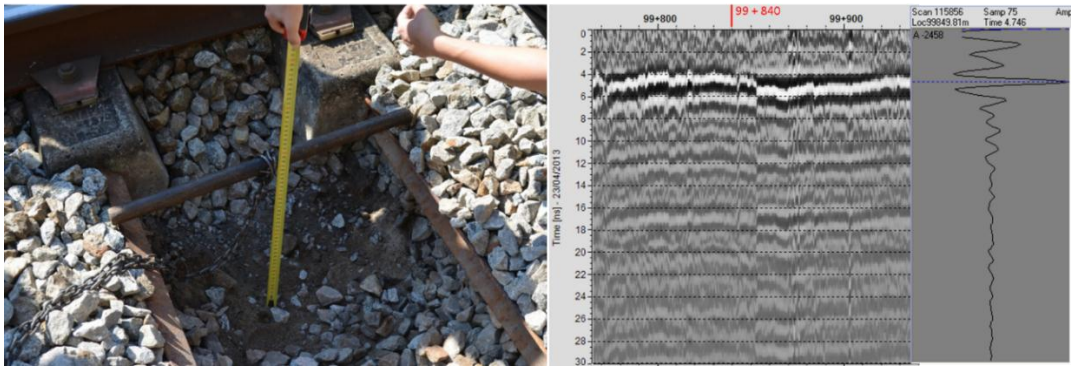

Figure 5.16 - Test pit characterised by clean ballast and subsoil: test pit (left) and GPR signal (right)

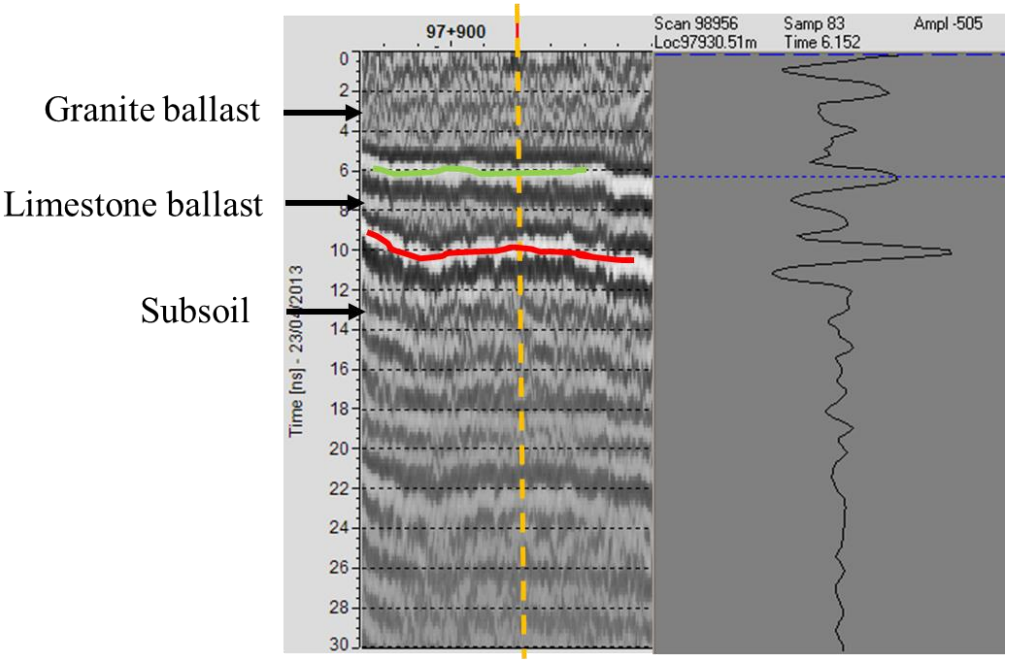

Figure 5.17 - Clean limestone ballast

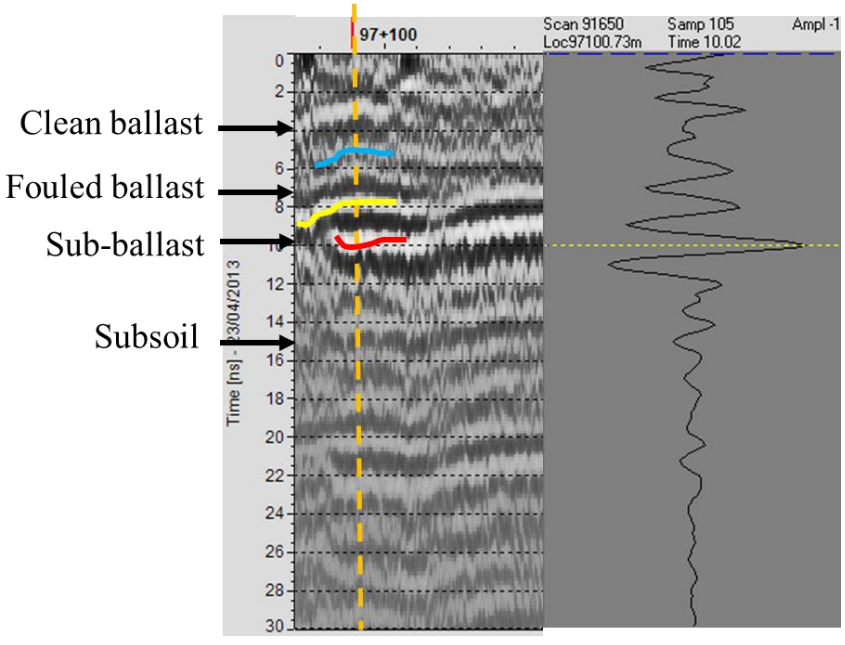

Figure 5.18 – Sub-ballast detection

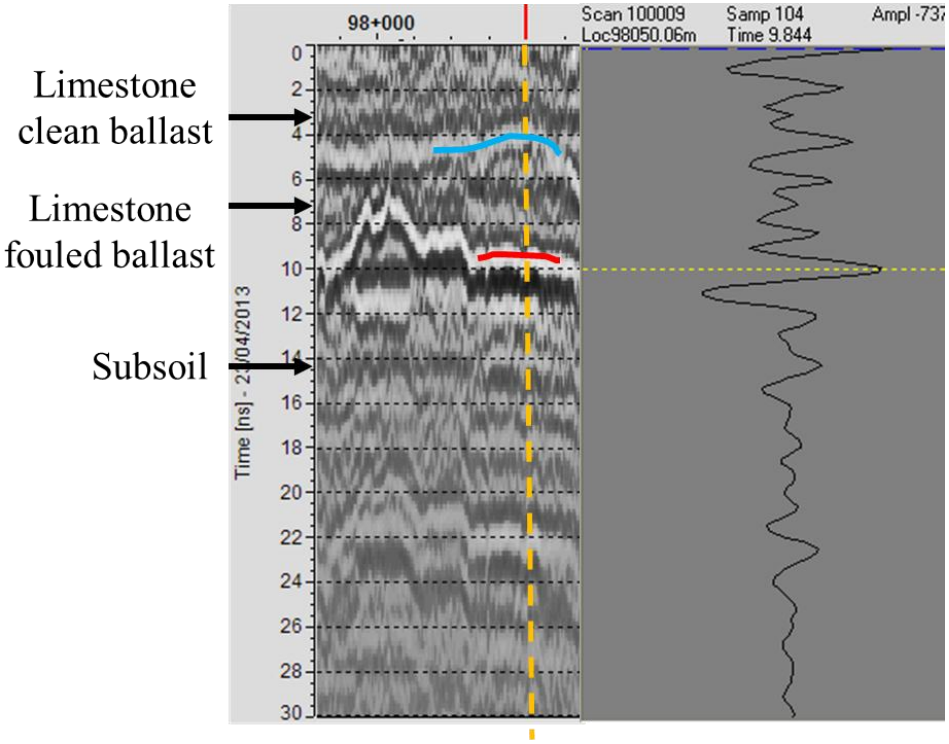

Figure 5.19 - Clean and fouled limestone ballast

5.3.3. Verification

The second track studied in this research is a section of a main freight railway, situated in the centre of Portugal. It consists on ballast overlaying the soil, no sub-ballast layer, and it has monoblock sleepers. As recently limestone ballast was replaced with granite ballast, it was chosen exclusively for verifying the dielectric constant value of granite clean ballast.

Eleven test pits were performed on track shoulders, and not between sleepers, for facilitating the work and to guarantee the safety of the personnel that could have been more difficult.

Some pits presented a certain fouling level, due probably to the fact that during ballast renewal, this was not completely removed from the track, as it can be observed in Figure 5.20. Anyway, only measurements of clean ballast were done in order to validate the dielectric constants evaluated in the laboratory tests, already presented in Chapter 4. In addition, limestone fouled ballast was encountered as well.

Figure 5.20 - Test pit with granite and limestone fouled ballast

Analysing GPR signal, the interface between clean ballast and the lower layers was not always clear in terms of wave amplitude, excepting where a definitely difference in dielectric constant properties existed with the adjacent layer.

For verifying the acceptability of the dielectric constant value at 4.79, that correspond to the average value obtained in the first set of test pits (see 5.3.2), clean ballast thicknesses were calculated (Figure 5.21). As can be noticed, values are quite similar indicating that for future surveys 4.79 represents a good value to be adopted for automatic interpretation in order to determine the thickness of clean

ballast and also that GPR can be considered as an efficient tool for confident thickness evaluation.

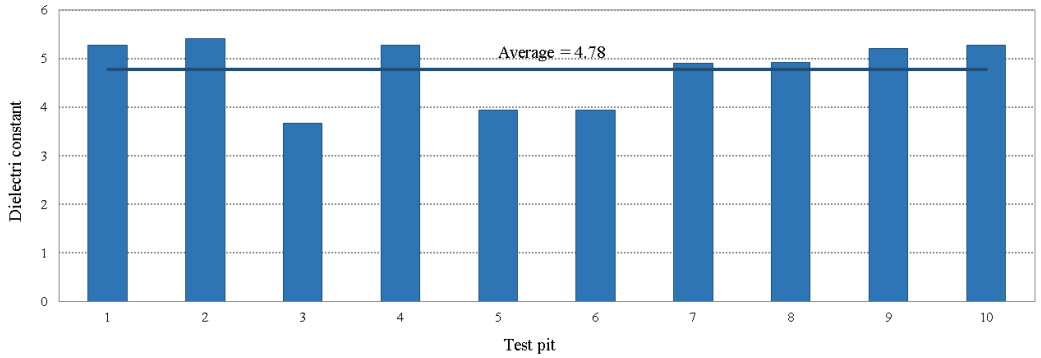

Figure 5.21 - Dielectric constant values for granite clean ballast – track 2

A second verification analysis was performed by using dielectric constant value obtained in laboratory. Also in this case, the difference for each test pits can be demonstrated to be insignificant. First, it should be taken into account that there is always a certain error in measuring layer thickness, even more when there are fouling conditions. Second, if fixed the dielectric constant value at 4.10 (see Table 4.11), layers thicknesses can be recalculated and also the differences with that measured in situ (Figure 5.22). As can be noticed, the line represents the maximum aggregate dimension for ballast material (63 mm) and the differences are in general minor than this value. Therefore, this explains as considering or not even only one ballast aggregate in thickness measurement can lead to a certain difference in dielectric constant value, that therefore can be accepted.

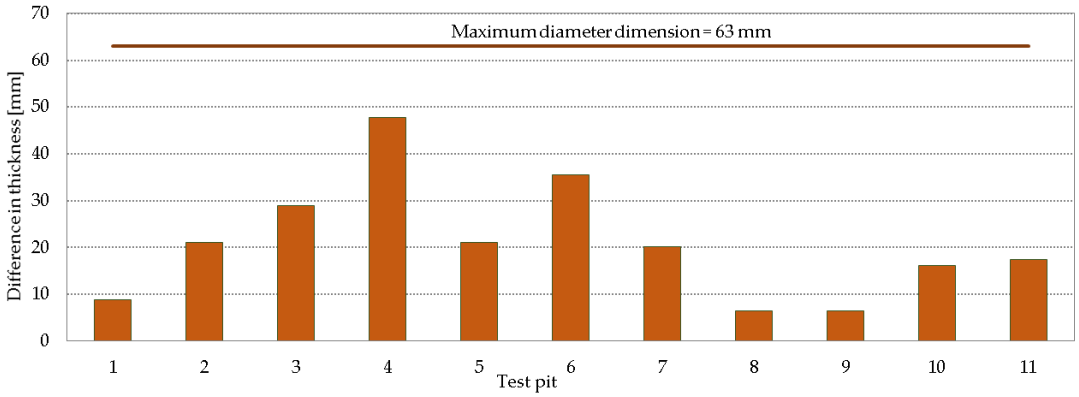

Figure 5.22 - Differences between ballast thickness (measured and calculated with $\varepsilon = 4.10$) for each test pit

On the other hand, it should be observed that this difference in dielectric constant values is also located within the range between dry and wet conditions, both in laboratory and in 5.2.2. Therefore, an increased care is required. If default dielectric values are considered as input data for new or renewal track, it should be also taken into account when tests were performed, namely in winter or summer campaigns, and also the precipitations trend should be studied, together with water content measurement, that has to be performed whenever possible. For older tracks, test pits for layer thickness measurements should be performed with accuracy and materials should be taken in laboratory for both water content and ballast fouling classification.

5.4. CONCLUSIONS

GPR represents an efficient tool but for improving the accuracy, an efficient calibration procedure is required. It consists in determining materials dielectric constant values in laboratory (Chapter 4) or by measuring layers thicknesses through core/test pits performed in situ, discussed in Chapter 5.

For railways studies tests pits are strongly recommended. On the other hand, for new pavements GPR data interpretation can be done by considering default dielectric constant values found in bibliography or determined with laboratory tests.

A monitoring procedure, based on GPR data collection, is presented using as case study a renewed track in Portugal. As layers thicknesses were known, they were used as input data and dielectric constant values were determined. Two structural solutions were taken into account. GPR has enabled a confident detection of changes in the structure in terms of thicknesses and materials, and particular events, such as bridges and switches, have been easily identified. Three test campaigns were considered for comparing dielectric constant values and it was found a consistent sensibility of the dielectric properties of railway materials with the water content variation. For sub-ballast layer, the dielectric values presented a certain increment in March, that might indicate an incomplete drainage. For the interpretation of both capping layer and rockfill material, some difficulties were encountered. Anyway some points could have been interpreted and in general results have shown a great reliability with values encountered in bibliography and also in past laboratory tests.

A second analysis focused on test pits that have been performed on two tracks. For the first track several situations in terms of materials were found and one of the scope consisted in characterise track layers through GPR, namely different responses in terms of reflection were found. Then thicknesses measurements of clean and fouled ballast were performed and dielectric constant values were calculated. Values calculated for clean ballast were quite similar with those obtained in the previous case study (renewal track). On the other hand, for fouled ballast, GPR wave reflection and the dielectric constant calculation was more complex, requiring more data about the materials condition, so future research is needed for a better definition of the evaluation procedure for this railway material.

In the second track, a verification analysis was performed. Considering the average dielectric constant value obtained for the first track, layers thicknesses

were calculated in correspondence of test pits points and then compared with values measured in situ. An insignificant difference was found, indicating therefore a good relationship between GPR and test pits. In addition, a second study was performed by taking into account the average value obtained in the laboratory tests, and also in this case the difference was acceptable. This indicates that a certain difference in dielectric constant value can be acceptable, as it could be caused by a small difference in ballast layer thicknesses measurements.

Concluding, this study has led to dielectric constant calibration for clean ballast layer but present challenges and uncertainties for the others layers. The main problem for fouling layers was the real thicknesses measurement, confirmed by the fact that the calculated dielectric constant values were not within the expected range. In addition, in some cases, problems for detecting layers interfaces in GPR signal occurred.

Calibration resulted difficult also because materials were not studied in laboratory, where it could have been possible classified ballast with a fouling index (Chapter 4).

Anyway, it was a tentative to improve the methodology by relating different track conditions with GPR signals in a systematic way.

For overcoming these problems, new advanced methodologies have been developed but they are still at prototype level, in order to quantify fouling level conditions and to determine dielectric constant values, for network applications. Neverthless, they have to be calibrated for the materials existing in each country, due to the diversity of railways structures and to the materials used along the time.

6. TRACK MAINTENANCE

6.1. INTRODUCTION

In railways, the increment of higher speed lines and dynamic axle loads requires a better infrastructure, able to satisfy the new project requirements, developed in the latest years. This in order to guarantee the execution of operations with comfort and safety but also limiting traffic interruptions due to maintenance interventions and optimising life cycle costs.

The entire process starts with geometric and functioning deterioration of the infrastructure elements. These deteriorations involve a series of maintenance costs with the aim of restabilising the initial quality level, or almost an acceptable level, for in service phase. Maintenance costs are divided into different infrastructure sections and it was observed that track costs are fundamental as they represent about 50% of the total costs (Lopez-Pita et al., 2008). For this reason, track plays an important role for life cycle and its degradation should be limited.

Track maintenance can be divided into: rail geometry, track geometry, track substructures, ballast bed, level crossings and miscellaneous (Esveld, 2001).

A wide presentation of track maintenance and different measurements can be found in Selig and Waters (1994) and Esveld (2001).

Track geometry has a key role since the construction phase (Esveld, 2001), as a track with good inherent quality provides good rides, needing few maintenance, and vice versa (Selig and Waters, 1994). For determining track conditions, monitoring inspections are executed. This can be done by performing track geometry inspections in two manners: an automatic way through recording cars and through visual inspections. For saving time and costs, the first method is currently used (Sadeghi, 2010). Recording cars (see Chapter 3) permit geometric parameters measurements and also they are suitable for distinguishing sections of

track with different performance levels. On the other hand, causes of track geometry degradation may not be investigated.

With particular reference to track substructure, its degradation provide an irregular track geometry, track stiffness variation and premature deterioration of track components. In general, layers deformation is caused by progressive settlements that are exacerbated by poor drainage and ballast fouling levels conditions (Hyslip, 2007). In order to find the causes of track substructure degradation, in the last years, a great development has been performed by using different tools and analysis, such as GPR (see Chapter 2), rolling track stiffness (Smekal et al., 2006; Norman et al., 2006; Berggren, 2009), track geometry data analysis and improved database software applications. Track geometry data analysis consists in finding track patterns by studying historical data for the same parameter or linking more than one parameter that can be indicators of future behaviours. In this context, fractal analysis studies were carried out by Hyslip (2002).

Several deterministic and stochastic approaches for predicting railways conditions have been proposed in the last 30 years (Audley and Andrews, 2013), in Europe and in North America, such as ORE (Esveld, 2001), Shenton model, Sato model and that developed by the Technical University in Munich (Vale and Calçada, 2013).

In order to describe the quality of the track, indexes have been widely developed for years and they have been used in different railways administrations, such as:

- track roughness index developed in USA (Ebersohn, 1998) referred by (Van der Westhuizen, 2009);
- J and W5 synthetic indexes used in Poland (Madejski and Grabczyk, 2002);
- TQI indexes by Federal Road Administration (Zhang et al., 2004);
- TGI index based on standard deviation and developed by Indian railways by (Mundrey, 2010);
- Q-number developed by Sweden railways (Andersson, 2002) cited by (Stenström, 2012);

- OTGI index (Sadeghi, 2010);
- SRPM-TQI index, based on TQI index, has been proposed by Xu et al. (2011).

Regarding vertical profile patterns, they are influenced by track substructure condition. INNOTRACK project (European Research Project) dedicated a part for developing new methodologies for improving condition assessment of the track substructure (Anders Ekberg, 2010). For example a combination of geometric parameters, namely longitudinal profile, dynamic stiffness and GPR was considered and good results were found moreover for solving soil and embankment problems (Berggren, 2010). Also in USA, a similar methodology has been developed by Amtrak (Hyslip et al., 2012), focused on researching the root cause of bad track performance, combining several information: background information, geometric parameters, topographic and asset mapping (FliMap® LiDAR), GPR, geotechnical testing and instrumentation, innovative databases and visualization tools.

During years, software and deterioration models for future maintenance decisions have been developed. They consist in joining and analysing different types of data (Jovanovic, 2004; Silvast et al., 2006; Smekal et al., 2006; Van der Westhuizen, 2009) in order to predict future problems. Costs can be also included for a complete maintenance management system, such as ECOTRACK software, developed by ERRI's D 187 Committee and 24 European railways between 1991 and 1998 (Jovanovic and Pearce, 2000; Esveld, 2001).

Most of European railways are old tracks where design has not been optimized and subgrade has been ignored for years. A better knowledge of these tracks through their investigation is required, with the aim to establish an acceptable level of quality and capacity (Anders Ekberg, 2010). For this purpose, GPR may help to detect track characteristics, such as layer thicknesses and layers variation, track defects, such as a soft subsoil layer due to, for example, a high water content, ballast fouling conditions, ballast pockets and trapped water (Hyslip et al., 2003).

In this thesis, particular attention was dedicated to track degradation and its possible causes, trying to identify track patterns for a better maintenance policy. The aim is developing a methodology by combining a widely used track inspection vehicle (EM 120) and GPR. Some cases are studied and compared, for demonstrating that GPR, jointly with track geometry measurement, are efficient tools for maintenance interventions decisions.

6.2. TRACK DEGRADATION

6.2.1. General

Given the contact wheel-rail, the heavy axle loads can lead to rail defects. On the other hand, the track reacts to the dynamic loads and it may result in loosening of fastenings, erosion of the bottom of the sleepers, ballast fouling conditions. In addition, lack of drainage and an insufficient ballast thickness may provide variations of both lateral and longitudinal level and this can lead to a poor track bearing capacity. These faults can be solved by using special track machines during maintenance.

The original tests for studying the deterioration rate of track geometry were carried out by ORE (Esveld, 2001). The main deterioration causes were identified, such as random ballast settlements, due to the ballast itself or from stiffness variation, rails deformations and variation of dynamic loads (Esveld, 2001).

The deterioration process starts with an initial exponential growth of track irregularities (presented in Figure 6.1), in which both particles abrasion and high compaction are settled. Then, track follows a linear deterioration trend until that standard deviation limit, established conforming the comfort level required, is reached. Therefore tamping is performed and quality is restored. Even if the objective of the intervention consists in leading the track to initial quality conditions, this is very difficult moreover for tamping. After a certain series of

tamping cycles, and depending on both traffic loads and construction quality, linear trend may change in an exponential trend. It may happens for example when ballast cleaning intervention is carried out too late or when formation problems occur. In fact, ballast becomes fouled and it loses its capacity of load distribution, leading to a high level of pressure under the sleepers and on the subgrade layer. In this way, tamping results inefficient and desired quality levels cannot be restored (Lichtberger, 2007).

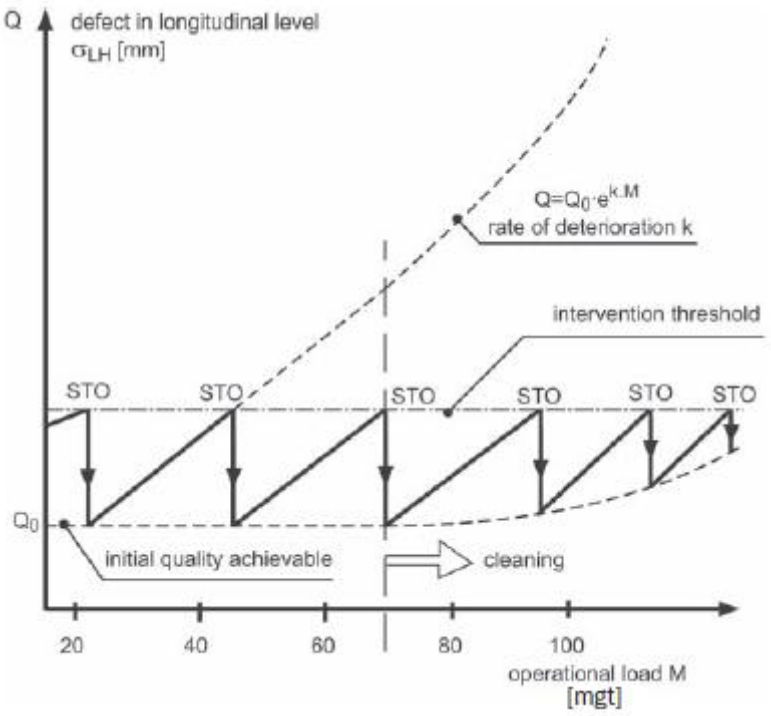

Figure 6.1 - Track deterioration process (Lichtberger, 2007)

Track deterioration can be caused by any of the several layers that form the track, namely ballast, sub-ballast, subsoil and also by drainage problems. In particular, in the ballast layer, fouling conditions represent the most important cause of instability and consequently they lead to poor drainage conditions. In addition a wet fouled ballast reduces shearing strength and it may deform excessively, also supporting vegetation growth that reduces drainage capability even more. About

sub-ballast layer, if it is placed beneath a fouling ballast layer, it can lose its strength and becoming an unstable layer. Formation can be subjected to instability for several reason, depending on the type of soil, if there are rapid changes of loads conditions and environment conditions.

For overcoming track instability problems several techniques can be adopted. Removal and replacement of poor formation soil ensures a sufficient ballast thickness with good quality material. An adequate sub-ballast layer (of granular material or bituminous mixture) may be constructed for reducing stress level on subsoil and ensure a satisfactory drainage. Also, geogrids, ballast undercutting and shoulder cleaning for improving ballast drainage, short piling or lime-cement pillars for improving bearing capacity can be considered.

6.2.2. Ballast fouling

Along the time, due to climatic changes and traffic loads, ballast layer is the most affected track layer (Selig and Waters, 1994). Aggregates modify their asset due to traffic loads, and this factor modifies its characteristics: flakiness increases, corners become smoothers, and granulometric distribution decreases. Therefore, fouling conditions occur and they represent the main cause of ballast problems (Selig et al., 2001).

Ballast fouling consists in filling ballast voids with fine particles. Selig and Waters (1994) identify this phenomenon when fine aggregates pass the 4.75 mm sieve (see Chapter 4) and they presented a study developed by University of Massachusetts in 1988 for determining the causes of ballast fouling. It consisted in considering different track conditions and the results have shown that the first cause of fouling is ballast degradation, namely breakage and abrasion of particles, then infiltration from ballast surface, sleepers degradation, infiltration from underlying granular layer and subsoil material migration.

Namely ballast degradation is due to:

- traffic loads, such as dynamic loads and vibrations, that produce particles abrasion;
- tamping and compaction damage;
- climatic changes, such as freeze thaw cycles;
- chemical weathering.

Surface infiltration may be come from the ballast itself, or dropped from car trains, or due to wind blown or by particles transported by water.

Degradation of rail sleepers can be caused by different aspects, such as slurry mobilization that comes from ballast degradation, and sub layers fine particles (pumping). These factors can cause damage to the ballast particles placed around sleepers, and to both wood and concrete sleepers.

Infiltration from ballast sub layers, like sub-ballast and subsoil, may come from traffic pumping actions that can produce migration of fine particles into the ballast layer, that is favourite by saturated conditions and depends on track structure. A first case happens if old fouled ballast has not been removed during a ballast cleaning intervention, for example, and then fine particles exist. The second case occurs if the track is old and ballast layer is directly placed on subsoil. The third case verifies if the track is new or renewal and then a sub-ballast layer exists, in this case migration can be due to an inadequate particles distribution. As result, migration can produce muds of silt or clay (Figure 6.2) (Bailey et al., 2011), that can lead to poor drainage, being the primary cause of ballast degradation (Maal and Carr, 2011).

Figure 6.2 - Example of silt/clay muds (Bailey et al., 2011)

Also in Great Britain, the British Railways authorities studied the same problem (Selig and Waters, 1994). In this case, results have demonstrated that the main cause of fouling was leakage due to the passage of car trains and external factors. Same conclusions were defined by Tutumluer et al. (2008) that confirms that coal dust from cargo trains may represent the main source of ballast voids filling in North America.

Obviously, the presence of fouled ballast represents a poor condition for railway performance, where the main effects can be associated with the formation of settlements in the substructure. Then, ballast is unable to fulfil its functions, and in particular supporting loads, enabling stiffness and drainage characteristics. An advertisement of fouling conditions is represented by the rapid loss of track quality, in terms of geometric parameters, after a maintenance intervention as ballast is overloaded. A study developed by ERRI has demonstrated that a critical level of fouling, with poor drainage conditions, is reached when 30 % of the total consists of fine material (Esveld, 2001).

In order to prevent and control fouling aspects, saving time and costs, different solutions can be adopted. The best choice should be the most cost-effective,

considering traffic, environmental conditions and cost of material and its transportation (Selig et al., 2001). For example in Portugal and in the rest of Europe, a substitution of limestone ballast was performed in the latest years, namely preferring a granite one, as it presents higher performance.

For ensure the separation from fine soil, geotextiles between ballast and subsoil are frequently placed, even if they do not represent an optimum solution (Selig et al., 2001). For this reason, a good alternative is placing an additional layer between them that is known as sub-ballast layer.

Ballast fouling conditions can be assessed through different methods, among them the vertical track deflection and GPR. Track deflection measurement has been developed by several groups in North America (Sussmann et al., 2012) and it is useful for detecting risks associated with large track deflections and with their variations along the track, that can be caused by the presence of a fouled ballast. Anyway, this procedure does not permit to distinguish more ballast conditions, namely dry and wet, from which deflections are highly dependent. For this reason, GPR has become a necessary tool for a better analysis (see 6.4 and 6.5). New software have been developed with the aim of correlating both track geometric parameters and GPR, together with ballast fouling information, i.e. fouling index, and moisture content conditions (Silvast et al., 2006; Li et al., 2010).

6.2.3. Sub-ballast and subsoil defects

Sub-ballast is in general a good quality layer and it has been placed in new and renewal tracks. One of its function is to prevent the contamination of the ballast layer with subsoil, in order to protect the second one from freeze-thaw actions, to limit fine soils and muds migration upward and to promote proper surface drainage, etc. (Fortunato, 2005). In addition, sub-ballast layer should respect other series of functions such as reducing transmitted loads to subsoil layer. In some cases, its performance can be low, namely when a not sufficient quality of construction is reached. A latest improvement has been constituted in replacing granular sub-ballast with bituminous sub-ballast, on the other hand this solution

is quite expensive and therefore it is used especially in high speed lines, such as in Italy and Japan (De Chiara et al., 2011).

Regarding subgrade, degradations are provided by traffic loads and by weather effects such as precipitations, erosions and wind. These result in irregular settlements under sleepers and they can be manifested under different forms. The most common are: progressive shear failure (Figure 6.3) and excessive plastic deformation (Figure 6.4) (Li and Selig, 1998). The first occurs principally to formations with soils characterised by a high clay content, while the second takes place for all types of fine-graded soils and causes ballast pockets formation. Other effects can be manifested on (Selig and Waters, 1994; Lichtberger, 2007):

- sandy formations, where fine soil migrates up to the entire ballast layer, reaching ballast surface and causing ground movements;
- unbound formations, i.e. not well compacted during construction, where loads can cause loosening, leading to cracking and shattering creations;
- cohesive formations in wet conditions, in this case saturation can take place quickly;
- cohesive formations, that may be also subjected to pumping actions under dynamic loads manifesting in holes formation beneath sleepers;
- clay and silt formations with frost susceptibility that may lead to degradation, especially in correspondence of the edge of the track;
- attrition, or known as local subgrade failure, that may result in slurry formation in presence of water.

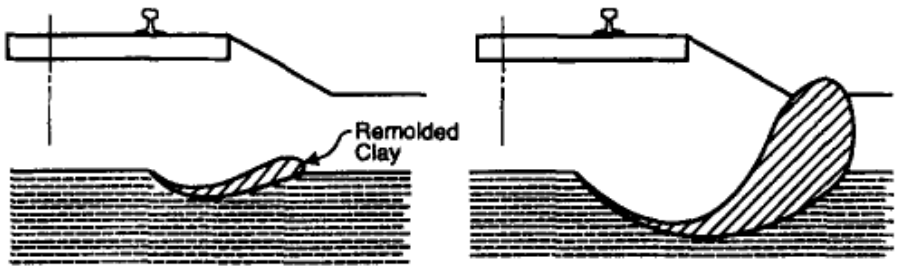

Figure 6.3 - Subgrade progressive shear failure (Li and Selig, 1998)

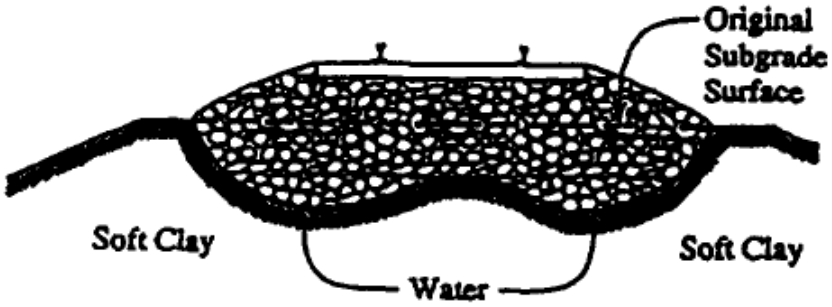

Figure 6.4 - Excessive subgrade ballast deformation (Li and Selig, 1998)

6.2.4. Interventions

Track geometry is affected by ballast, sub-ballast and subgrade movements. Anyway, in general, the adjustment of geometry is performed by rearranging the ballast.

In particular, ballast changes along time cause a worse behaviour respect loads, vibration attenuation and drainage capacity. As consequence, when ballast does not respect initial characteristics, track loses stiffness and uniformity. In particular, vertical defects with a wavelength higher than 3 m are due to ballast degradation.

In order to repair ballast deterioration, a series of maintenance interventions are required, such as tamping and cleaning.

In general, maintenance of track geometry can be divided into systematic maintenance, carried out with heavy machines, and incidental maintenance, that consists in repairing local irregularities (Esveld, 2001). Systematic maintenance is performed by:

- Tamping machines, for correcting level, cant and alignment;
- Ballast regulators, for establishing correct ballast profile;
- Stabilizers, for ballast compaction;
- Ballast cleaners, for cleaning ballast bed.

Local defects can be repaired manually or with small machines.

The most important work consists in levelling and tamping using vibrating compactors or tamping tines. Also the use of jacks for raising the track and filling the space with ballast material rectifies track level defects and this can be done by using manual compactors, vibrating compactors or impact tampers (Esveld, 2001).

The most common maintenance intervention is tamping and in general its performance is decided by observing poor geometric qualities in terms of vertical (longitudinal) and/or horizontal (alignment) profile. It consists is rearranging ballast particles in order to restore the track to the desired geometrical position rails position. It can be performed manually or automatically, with specific machines. The operation consists in two actions, namely the down-feed action and the squeezing action (Figure 6.5). Machines can work in a cyclic way or in continuous way (Wenty, 2011). Machines that work in cycles stop and accelerate sleeper after sleeper. In comparison, continuous machines present some advantages, i.e. a higher work rate, lower energy costs, noise and vibrations, the possibility of integrating other interventions as sleeper regulation and track stabilization.

It is necessary to take into account that machines can also modify the ballast characteristic by generating heavy stresses in stones. In fact, due to fatigue, only a limited number of this kind of maintenance sessions can be applied during the entire life cycle of the ballast.

In addition, tamping should be done in selected track sections, where geometry is poor but commonly it is performed also on adjacent sections that do not require intervention and, even more, it aggravates ballast conditions, as tamping causes damage to ballast particles. Even if it is the a cheap intervention, tamping does not correct the origin cause of the irregularity (Selig et al., 2001) and it is not efficient at long term. Therefore, finding the root cause of track degradation is a priority.

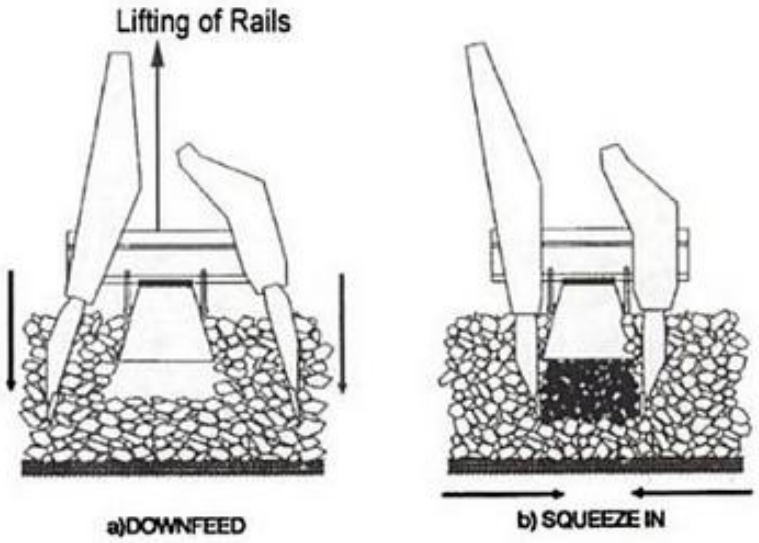

Figure 6.5 - Tamping actions (Selig and Waters, 1994)

Ballast cleaning and renewal represent fundamental interventions for avoiding ballast fouling and assuring a good drainage of surface water. During cleaning, the ballast is excavated and a part of it can be re-used by separating it from the spoil through tools of screening, and then placed it back into the track together with the new material. After, geometry is restored with tamping tools and track is stabilised. Depending on the quantity of new material, this last operation can be done by compacting several sub-layers (Schilling, 2005). Anyway, ballast and renewal interventions are expensive and they also cause high traffic interruptions. They should be performed with a certain accuracy, avoiding the risk of removing or damaging the existing sub-ballast layer and also taking into account the width and inclination of the cut surface for ensuring an efficient drainage into the clean ballast (Selig et al., 2001).

Two bad situations could take place and are presented by Lichtberger (2007). It can be demonstrated (Figure 6.6) that if cleaning is performed on track shoulders, this provides good drainage from the right-hand side of the track (see Figure 6.6 a), but not under the sleepers, and the critical rainfall rates that can still be drained successfully are between 0.5 and 30 mm/h, according to the degree of ballast

fouling. A second case occurs if ballast cleaning is performed also under the sleepers but inefficiently (see Figure 6.6 b), therefore fouled ballast remains in the shoulder area and this causes lack of drainage and the critical rainfall rates are between 1 and 10 mm/h. The correct case happens when fouled ballast is totally removed from track and water is able to flow immediately (see Figure 6.6 c) and rainfall rates are up to 150 mm/h.

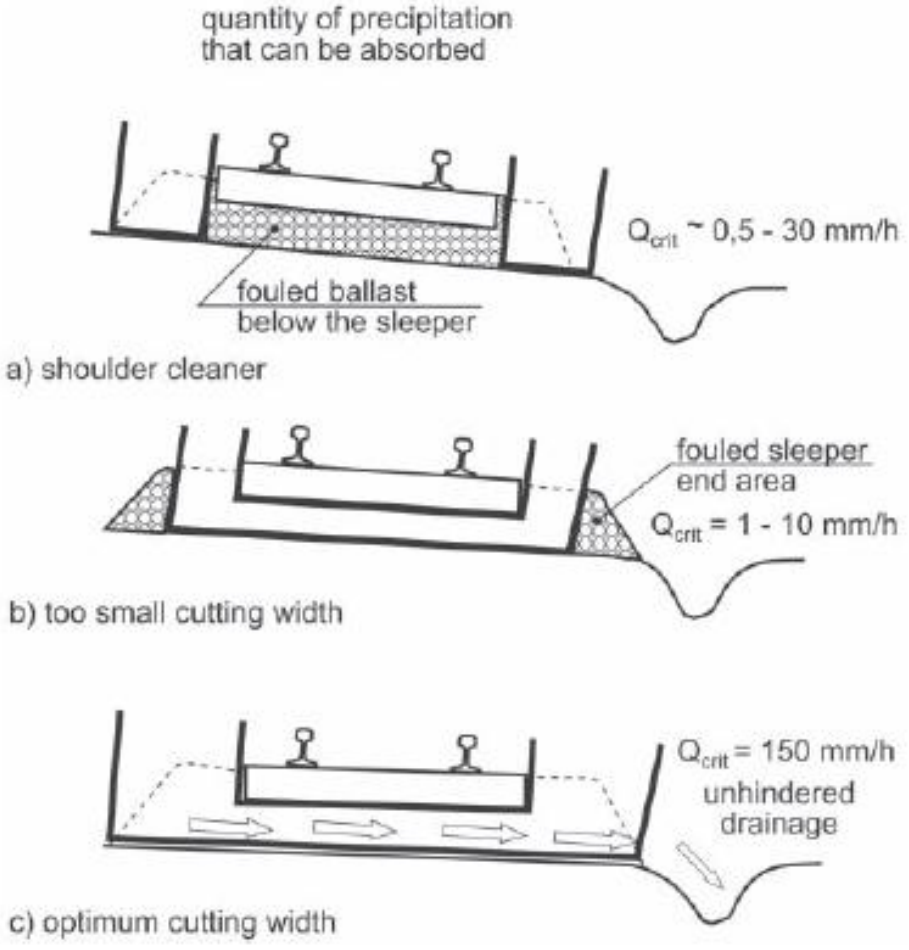

Figure 6.6 - Ballast cleaning intervention (Lichtberger, 2007)

6.3. TRACK MAINTENANCE POLICY

6.3.1. European Standards

European Standards (EN 13848-5:2008, 2008) define the admissible values for the most important geometric parameters with the aim of describing track quality. In particular, these parameters are: the longitudinal level (left and right), the alignment (left and right), the cross level, the gauge and the twist.

Standards indicate three reference values for admissible values:

- extreme values of isolated defects;
- standard deviations over a defined length, typically 200m;
- mean values.

For each admissible value, three main levels have to be considered:

- Immediate Action Limit (IAL): it is a safety limit which value, if exceeded, could lead to derailment risk. In this case operations are limited, by reducing traffic speed or closing the line, and maintenance interventions are required immediately by correcting track geometry and re-establishing an acceptable ride level;
- Intervention Limit (IL): it is a corrective maintenance limit. It refers to the value which, if exceeded, enables the execution of normal ride operations but it requires maintenance interventions in order not to reach the immediate action limit before the next inspection;
- Alert Limit (AL): it is a preventive maintenance limit. It corresponds to the value which, if exceeded, enables the correct execution of ride operations. Anyway an analysis of track geometry conditions is required and it should be considered in the regular maintenance plans.

These values are given for a loaded track and in function of speed, that is an important factor for the evaluation of track geometry quality.

In particular, longitudinal and alignment values, during their acquisition, are filtered and then classified based on three wavelength (λ):

- D1: 3 m < λ < 25 m;
- D2: 25 m < λ < 70 m;
- D3: 70 m < λ < 150 m for longitudinal level and 70 m < λ < 200 m for alignment.

Where D_3 is mostly related with vehicle ride quality (for high speed lines) and it is not directly linked with safety.

Unlike immediate action limits, which take into account the track/vehicle interaction, the other two quality levels are mainly linked with maintenance policy.

The normative part of European Standards defines immediate action limits, namely the EN 13848-5:2008 gives values for isolated defects and mean track gauge. As example, Table 6.1 shows limits values for the isolated defects of longitudinal profile.

Table 6.1 - Limits for longitudinal level – isolated defects – mean to peak values (EN 13848-5:2008, 2008)

	IAL		IL		AL	
Speed (km/h)	D_1	D_2	D_1	D_2	D_1	D_2
V ≤ 80	29	-	16 - 20	-	12 - 18	-
80 < V ≤ 120	26	-	12 - 18	-	10 - 16	-
120 < V ≤ 160	24	-	10 - 17	-	8 - 15	-
160 < V ≤ 220	20	33	9 - 14	18 - 23	7 - 12	14 - 20
220 < V ≤ 300	17	28	8 - 12	16 - 20	6 - 10	12 - 18

In addition, the EN 13848-5:2008 gives alert and intervention limits for isolated defects and mean track gauge and alert limits for standard deviations in an informative way. In fact, Standards define that these values have to be set by the European infrastructure managers. Their definition has to ensure safety, achieve a

good or a given level of ride quality, and limit life cycle costs. Also, conforming the intervention and alert limits, European managers should choose the frequency of inspections.

In this thesis, particular attention was dedicated to track substructure degradation. The parameters that usually defines a track geometry maintenance intervention are the short wavelength (D_1) of longitudinal and/or alignment level measurements.

6.3.2. Maintenance policy

Maintenance tasks can be divided into the following three main categories (Budai-Balke, 2009):

- corrective maintenance, or known as breakdown maintenance, that is performed for restoring a failed or malfunctioning system. It is usually an expensive action mainly due to the urgency in repairing a defined damage and moreover it is not always completely efficient as it can cause damage also to other systems;
- preventive maintenance, that is performed for limiting disadvantages produced by corrective maintenance actions, therefore damages and failures are prevented and discovered, if hidden, by pre-planning and systematic adjusting intervention actions, i.e. renewals and/or replacements. Another advantage consists in the fact that some operations can be performed without traffic interruptions and actions can be planned and managed when it is more convenient for infrastructure managers;
- predictive maintenance, or conditional, is performed when direct monitoring methods are used to determine the exact status of track systems with the aim of predicting possible degradations and detecting sections that required maintenance. Therefore, the objective consists in predicting the time of degradation and, based on it, planning future actions.

Nowadays, predictive maintenance has been widely used due to safety requirements and costs savings, as maximize the life of a certain component may cause degradation of others.

Railway system is complex and is very difficult monitoring the single components and managing them. For this reason, predictive maintenance is not useful for complex systems. Then, a systematic preventive maintenance may be convenient even if maintenance actions could be performed also to not complete damaged systems, enabling higher costs.

6.3.3. Portuguese Standards and actual methodology

Portuguese maintenance policy follows the previous classification, in particular for correcting track irregularities predictive maintenance plans are performed.

Portuguese standards (REFER, 2009) defines two geometric parameters for maintenance decisions, namely the short wavelength (D_1) of longitudinal and alignment level measurements, and respective Standard Deviation (σ) values calculated every 200 m.

Lines are divided in six classes, based on ride speed. Table 6.2 presents alert limit values for the standard deviation of longitudinal value and alignment, conforming the class of the line.

Table 6.2 - Alert limits for longitudinal level and alignment – Standard deviation values

Speed		Standard Deviation [mm]	
Class	[km/h]	Longitudinal Level	Alignment
VI	$V \leq 40$	3.3	2.1
V	$40 \leq V \leq 80$	3	1.8
IV	$80 \leq V \leq 120$	2.7	1.5
III	$120 \leq V \leq 160$	2.4	1.3
III	$160 \leq V \leq 230$	1.9	1.1
I	$V \geq 230$	1.5	1

For track maintenance decisions, in Portugal, two indexes are calculated:

- Tamping index (AMP);
- Quality Index.

AMP is considered as the maximum standard deviation value between longitudinal level and alignment. For the longitudinal level, it is calculated as the maximum between right and left rail, while for the alignment it corresponds to the minimum value between right and left rail.

Quality index is calculated as the maximum standard deviation value between longitudinal level and alignment, and they are both calculated as the average value between right and left rail.

AMP is a key parameter for establishing interventions, in particular tamping, while Quality index is used for statistical scopes with the aim of characterise track quality in a global way.

For both indexes, σ value is compared with limits imposed by Portuguese Standards that define three conditions for deciding maintenance programs (Table 6.3).

Table 6.3 - Limits for Portuguese railways maintenance plans (REFER, 2009)

Track geometry analysis for 200 m lenght sections	
QN_1	≤ Alert Limit
QN_2	> Alert limit and ≤ 1.3 x Alert Limit
QN_3	> 1.3 x Alert Limit

Namely if σ is included in QN_1, it means that the 200 m section is in good condition. If it is include in QN_2, it means that section needs of maintenance intervention in a medium term. While if it is in QN_3, maintenance interventions are required in short term. Relating to Europeans Standards, it can be affirmed that in Portuguese Standards Intervention Limit are calculated as 1.3 times the Alert Limit.

The general rule is that a single QN_3 value (200 m) or two consecutive QN_2 values (200 m plus 200 m) in the September campaign means including an intervention into the tamping plan (AMP plan) of the following year (Figure 6.7). Anyway, some alterations should be considered and included in the AMP plan, for example if consecutive campaigns present twist values near the Alert limit, or a defined section needs geometry correction in terms of cross level, etc.

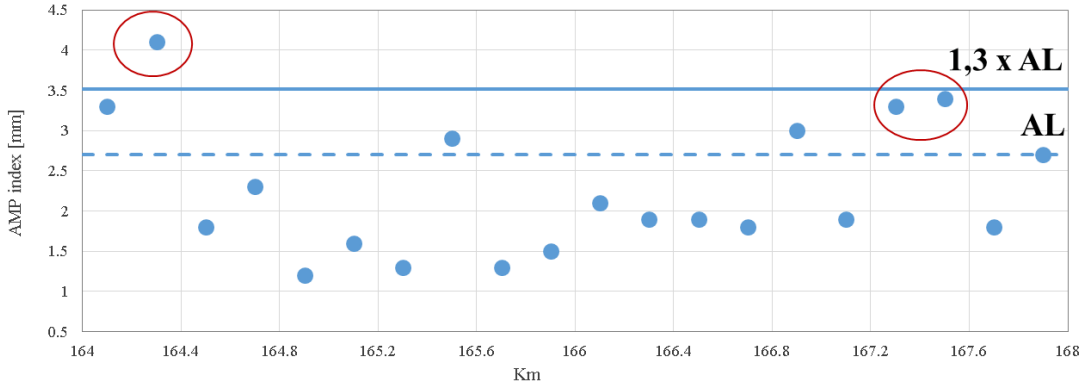

Figure 6.7 - Example of AMP index and tamping interventions requirement

As already referred, tamping may be performed manually or mechanically. The first option in general occur when sections have a maximum length of about 20 m. For defining the right length of the section to be corrected, standard deviation values are compared with the graphics of geometric values, measured by EM120. This also for checking if section is in straight or in curve line, as tamping cannot start or finish in a track transition curve.

None of these considerations takes into account other maintenance interventions, such as ballast cleaning. In fact, actually, for economic reasons, cleaning is performed in extreme situations, namely during visual inspections where the presence of fouling conditions on ballast surface can be noted.

The actual procedure presents some disadvantages, first it consists in treating only the effect and not the causes of the problem (Figure 6.8). This may lead not to solve

the real problem and tamping intervention may result not always suitable. Therefore, the procedure may result not efficient nor economics.

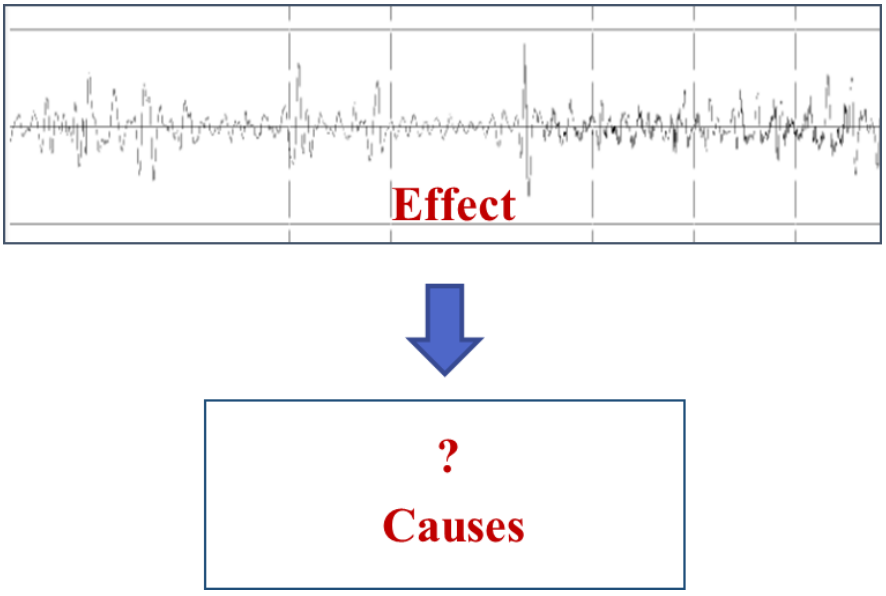

Figure 6.8 - Actual methodology scheme

For this reasons, a new methodology has been developed in the present research thesis, aiming to find the real causes of track degradation.

6.4. IMPROVED DIAGNOSIS CRITERIA: COMBINATION OF GPR DATA WITH RAIL GEOMETRIC PARAMETERS

6.4.1. Introduction

The new methodology aims to combine geometric parameters, measured by EM120, with GPR data. The scope is identifying track patterns and obtaining information about the causes of defects for then treating them, and not the effects, with right interventions (Figure 6.9). In addition, a better precision for the localisation of the defects, not only longitudinally but also in depth, can be

obtained. All this factors may lead to time and costs savings and to a better maintenance with a higher track life cycle.

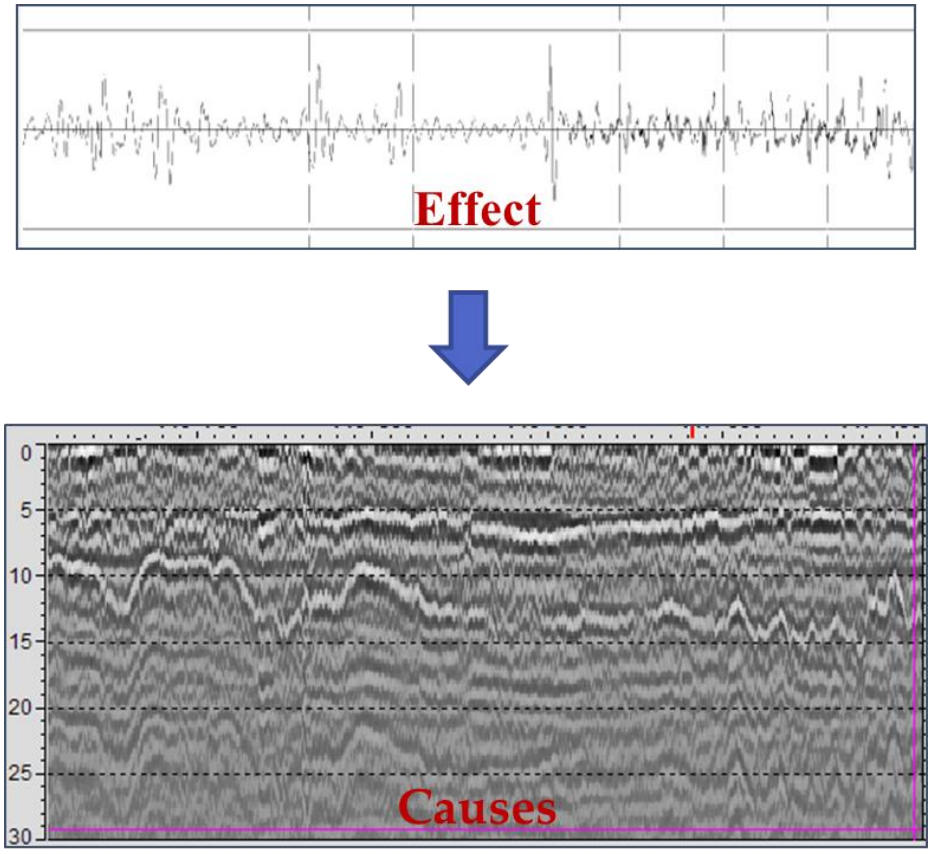

Figure 6.9 - New methodology scheme

As described in the previous chapter, some of GPR advantages are that:

- it is a quick and effective technique;
- it can be used during construction and monitoring phase;
- it limits the number of test pits;
- it evaluates layers thicknesses;
- it assesses materials properties;
- it detects defects.

On the other hand, some of these are not completely true, as GPR use in railways is quite recent, namely:

- data interpretation is still difficult;
- a certain number of test pits is required for calibration;
- assessment of layers material properties is still very difficult, as they are very sensitive to water;
- detection of defects is still very difficult.

Anyway, from Chapter 4 and 5, it can be concluded that the present research has helped in improving some of still difficult features. In fact, test pits execution has enabled not only dielectric properties evaluation but also location of zones with different materials and ballast fouling conditions. Laboratory tests have permitted to obtain a wide range of dielectric constant values, namely simulating various levels of fouling and wet conditions, for three materials generally used in Portuguese lines. Finally, a different procedure for detecting surface level has been proposed, improving and simplifying data interpretation.

In this paragraph, the new methodology is described and several case studies are analysed, with the aim of comparing the actual and the new methodology.

6.4.2. Proposed methodology

The new methodology proposed in this research can be divided into three main steps:

- detection of critical areas;
- GPR analysis;
- maintenance intervention decision.

The detection of critical areas can be subdivided into three parts:

(1) continuous standard deviation;
(2) data analysis from different campaigns;
(3) critical zones detection.

The first consists in calculating standard deviation values (200 m) in a mobile window, every 0.25 m (that corresponds to the EM120 measurement step), in order to have a continuous trend and not punctual, as for the actual methodology (Figure 6.10). For a correct visualization of graphs, it should be taken into account that points are positioned in the middle of the 200 m long interval, i.e. the representative point related to interval 164+200-164+400 km is located at 164+300 km. Through the continuous trend, a better localisation of the problem can be quickly achieved, avoiding the risk of loss of information and limiting, in some cases, the interventions to a restricted area and then saving time and costs. A clear example is represented in Figure 6.11 where, for the actual methodology, 400 m of an existing line need tamping intervention, namely from 167+200 to 167+600 km, while, with the new methodology, it can be observed that about 300 m require tamping correction, namely from about 167+240 to 167+540 km. In addition, an example of loss of information is represented in Figure 6.12, where it can be observed that for the actual methodology tamping is needed from 164+200 to 164+400 km. On the other hand, with the new methodology this is not exact as IL limit is overcame before, namely at 164+072 km, that is included in the previous Standard deviation interval (from 164+000 to 164+200 km) that would not require intervention in a first analysis. In fact, as already referred, the length of section that need tamping intervention depends also on other geometric parameters. For this reason, the proposed procedure is not definitive but always requires more studies. Namely more geometric parameters graphs observations have to be considered, as indicated by the actual procedure.

In addition, the new methodology includes GPR analysis that can give more information about the length of the section. Also, it can help in defining if tamping is the more efficient intervention or not. Then, another research scope consists in identifying which intervention may be more suitable. In particular, with the instruments and data available in this research, it can be established if cleaning or ballast renewal or a deeper intervention (if the defect is detected in at formation level) are better than tamping. Therefore, GPR can be useful not only for defining

the length of section but also for indicating at which depth it requires intervention (see 6.5).

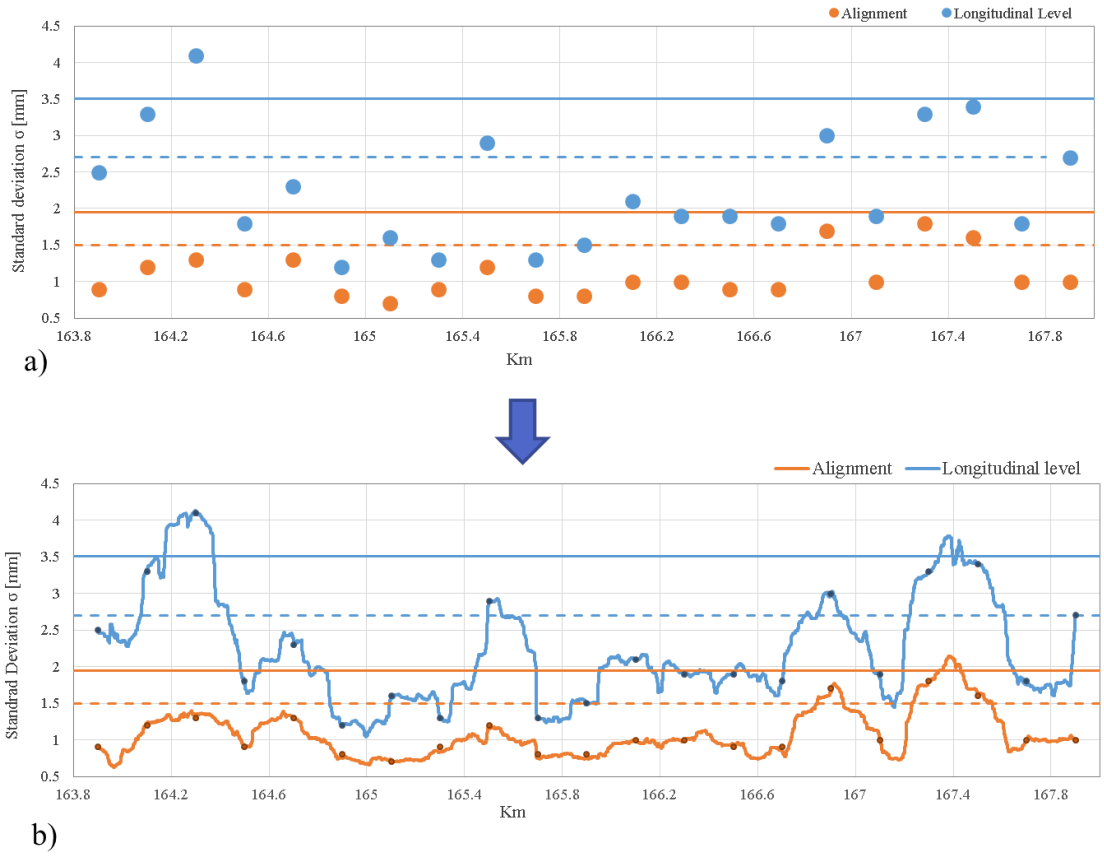

Figure 6.10 - Punctual (a) and continuous standard deviation (b)

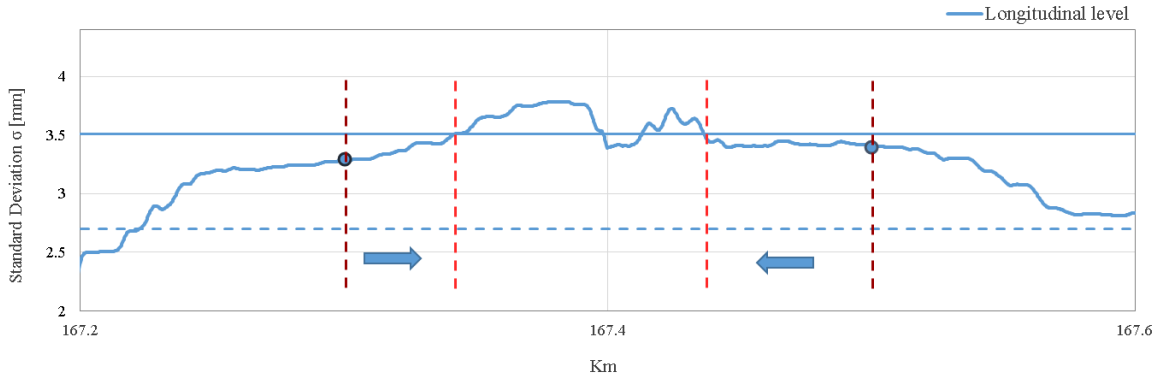

Figure 6.11 - Different section lengths determined for intervention with actual (dark red) and new methodology (clear red)

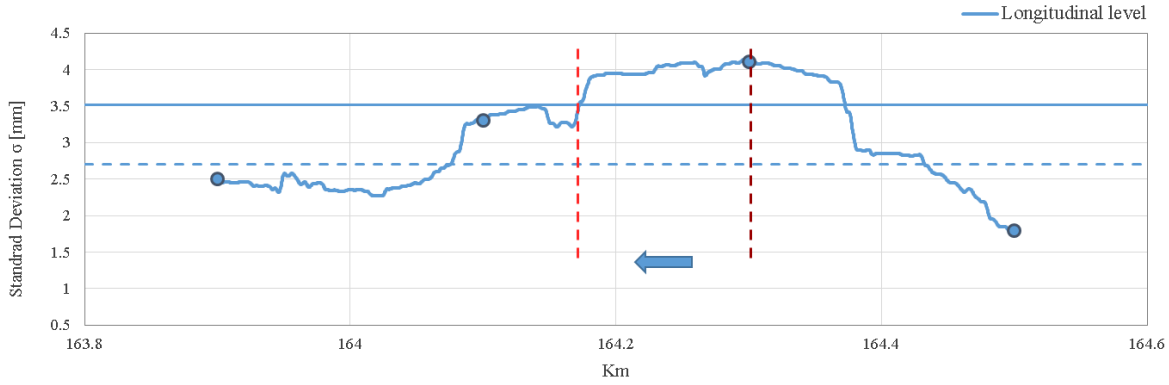

Figure 6.12 - Example of limited loss of information with new methodology

An important part that is included in the new methodology is the analysis of several EM120 campaigns and the identification of locations with systematic degradation. In particular, special attention should be paid to zones with standard deviation values minor than the IL and AL limits and that do not still require interventions (Figure 6.13). In fact, if values rise campaign after campaign, this means that degradation is increasing and generally it is due to deeper layers, i.e. subgrade. Therefore, this procedure is useful for checking critical zones and predicting future failures with the aim of performing a better management of costs and interventions.

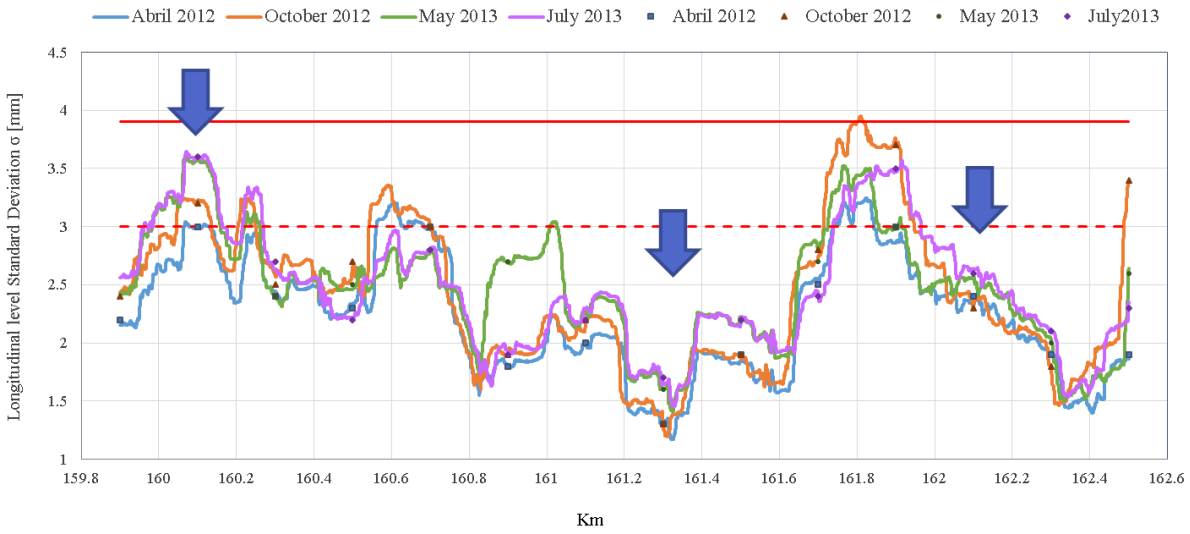

Figure 6.13 - Standard deviation values of different campaigns and localisation of zones with problems

6.5. COMPARISON BETWEEN ACTUAL AND NEW METHODOLOGY

6.5.1. Case study 1

A first case study is focused on analysing a section in which standard deviation of alignment or longitudinal level overcomes the IL limit. As example, that represented in Figure 6.12 can be studied, that is referred to an existing line in which ballast is directly placed on subsoil layer.

Actual methodology considers the interval between 164+200 and 164+400 km in a first phase and then additional studies of others geometric parameters, i.e. cross level and twist are considered, in order to define the correct interval for tamping intervention.

For the new proposed methodology, interval starts from about 164+072 to about 164+473 km and, as the actual methodology, more geometric parameters should be considered. Ignoring them in this context, the following step is GPR analysis. The aim consists in evaluating GPR response in the considered interval, and in the adjacent zones, for identifying possible problems to track layers level.

After GPR data processing (see Chapter 3), a global (Figure 6.14) and then a particular interpretation, at single trace level, was performed.

From Figure 6.14 different situations can be observed. A variation of ballast layer is clearly identified and also different reflection amplitudes (contrast white/black). It should be considered that the variation of ballast layer can be caused: or by different thicknesses, if dielectric constant value is quite constant along the studied section, or by different dielectric properties, namely if more than one ballast condition is found in the section, i.e. clean and fouled ballast. Anyway, from the experience acquired in this research, clean and fouling conditions can be distinguished quite well, from refection amplitudes and for this reason a first evaluation can be developed, even without test pits performance.

The studied stretch can be divided in three sections (A, B and C) and then analysed case-by-case. Of course, for better understanding GPR response, in particular in correspondence of the initial and final parts, a greater interval should be considered.

Section A is characterised by a great variation of ballast layer and a high reflection amplitude, indicating a high difference in terms of dielectric properties between ballast and subsoil material (Figure 6.15 (a)). This is confirmed also by the single trace picture (Figure 6.15 (b)), where a definite great wave amplitude can be distinguished. It can be concluded that section A presents a clean or moderately clean ballast with a high variation in terms of thicknesses, as dielectric properties can be assumed quite constant.

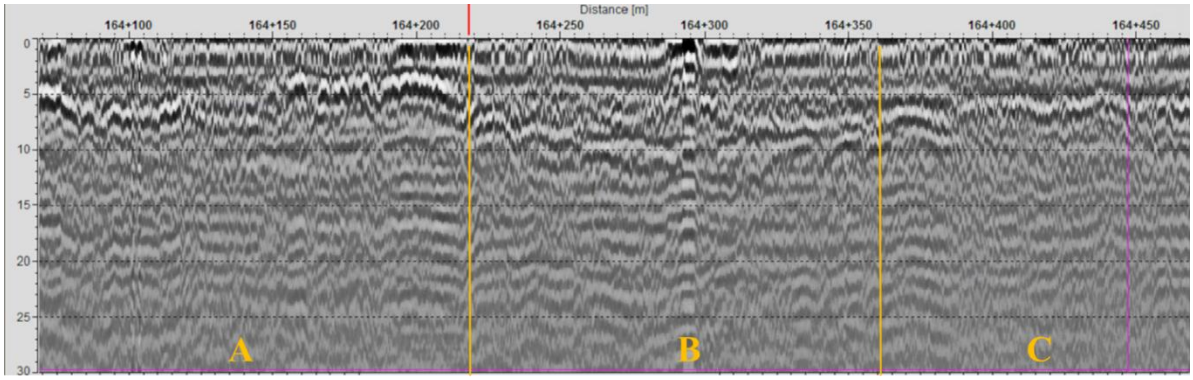

Figure 6.14 - GPR trace – track section with longitudinal level defects – case study 1

Section B interpretation was more complicate. Comparing to section A, trace is more confused. In fact, a certain difficulty was encountered for defining ballast layer interface, in particular from 164+300 to 164+350 km, where a less clear interface was observed (Figure 6.16 (a)). From bibliography, this situation can be symptom of fouling conditions. For a better analysis, single traces were studied. It should be affirmed that the single trace interpretation was not obvious, on contrary several traces were picked and analysed, as the majority had showed irregular waves, impossible to interpret. Anyway, a good example is presented in Figure 6.16 (b). It can be observed that two waves with higher amplitudes are identified and the first one separates two different ballast conditions. In this case, due to the structure of the track, fouling conditions are probably caused by soil pumping from subsoil and it should be considered that also a certain settlement is caused. It is impossible to quantify fouling conditions, moreover because a low frequency antenna was used, but only a comparison between them can be performed. Therefore, it can be affirmed that the deeper interface separates subsoil from a more fouled ballast and the shallower one, the more fouled ballast from a more clean ballast. Anyway, interpretation can be supported by past test pits as these situations were encountered (see Chapter 5) for similar lines. On the other hand, new tests pits are always needed for verification, even if in a small number.

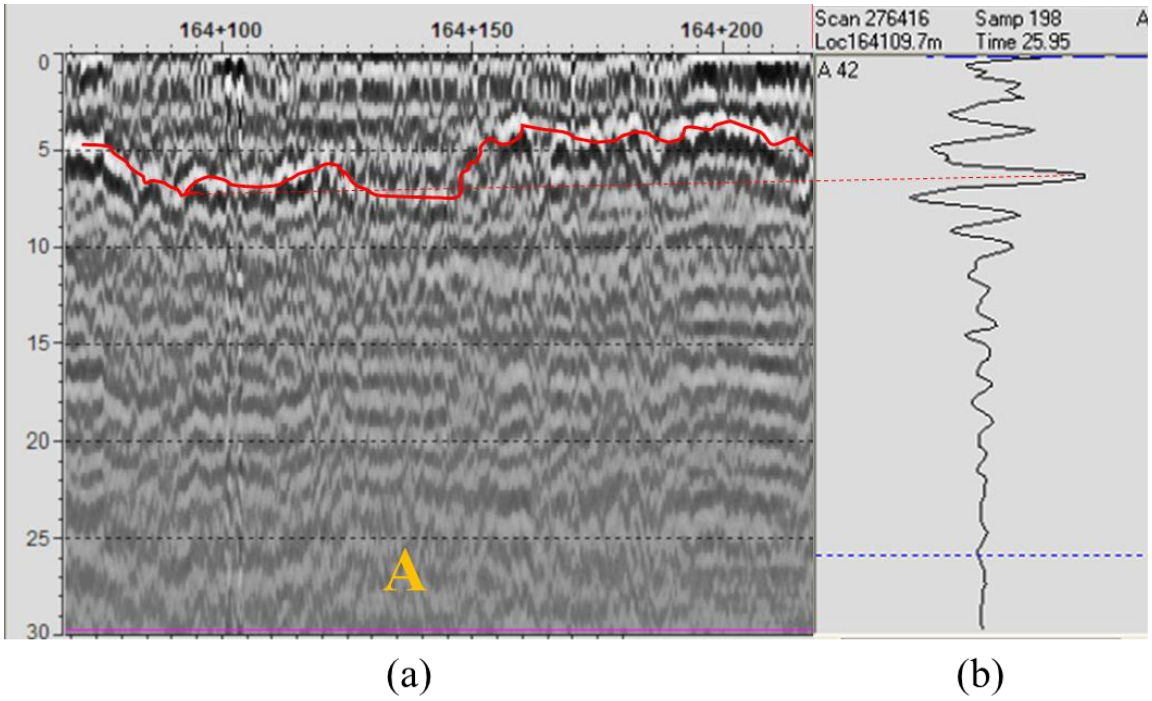

Figure 6.15 - Interpretation of track stretch with longitudinal level defects: a) section A; b) 2D trace; c) single trace

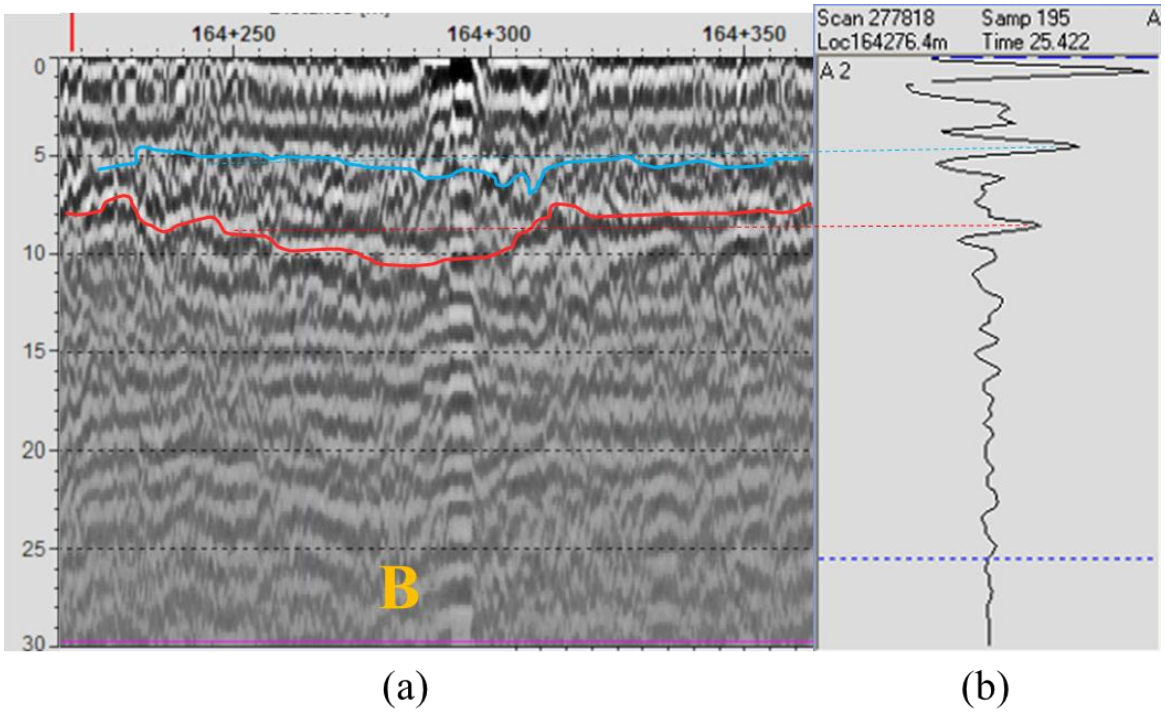

Figure 6.16 - Interpretation of track stretch with longitudinal level defects – section B
(a) 2D trace (b) single trace

Section C is similar to section A and, comparing with it, it presents a more regular trend and a high reflection amplitudes, that confirms the presence of clean or moderately clean ballast (Figure 6.17).

Finally, in the studied stretch, actual methodology indicates a tamping intervention for geometry correction. Through the new procedure, and then with the GPR analysis, it can be concluded that different patterns have been detected and tamping may not always solve the problems. Namely section A and C are quite similar and tamping may be sufficient. On the other hand, section B, with a length of about 150 m, was demonstrated to be in fouling conditions and then tamping may be not the most appropriate intervention.

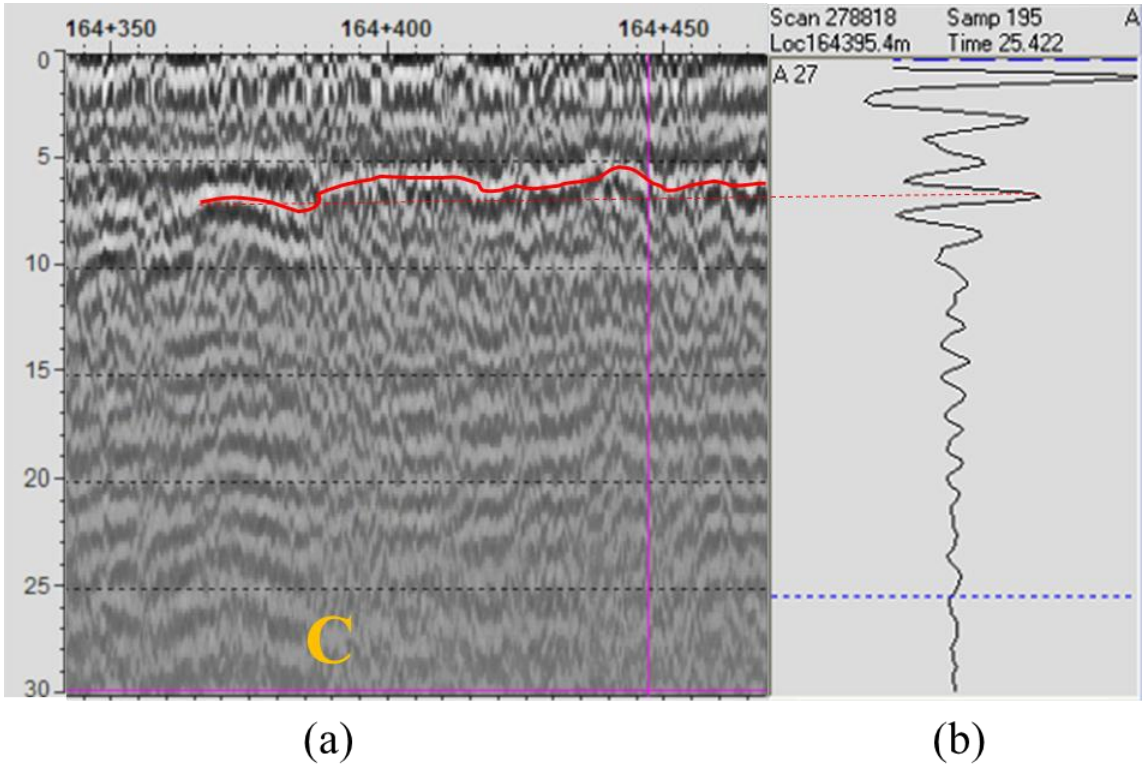

Figure 6.17 - Interpretation of track stretch with longitudinal level defects: a) section C; b) 2D trace; c) single trace

6.5.2. Case study 2

A second study aims to represent an example of not efficient tamping intervention. The same line of case study 1 was considered and namely a stretch of 200 m. In April 2011, AMP index overcame the IL limit and for this reason, tamping was performed. After two campaigns, standard deviation value overcame AL limit for two consecutive campaigns (Figure 6.18). This indicates that at the end of the second year after the intervention, another tamping is required. The new methodology was applied. First, continuous standard deviation values were determined and represented in Figure 6.19.

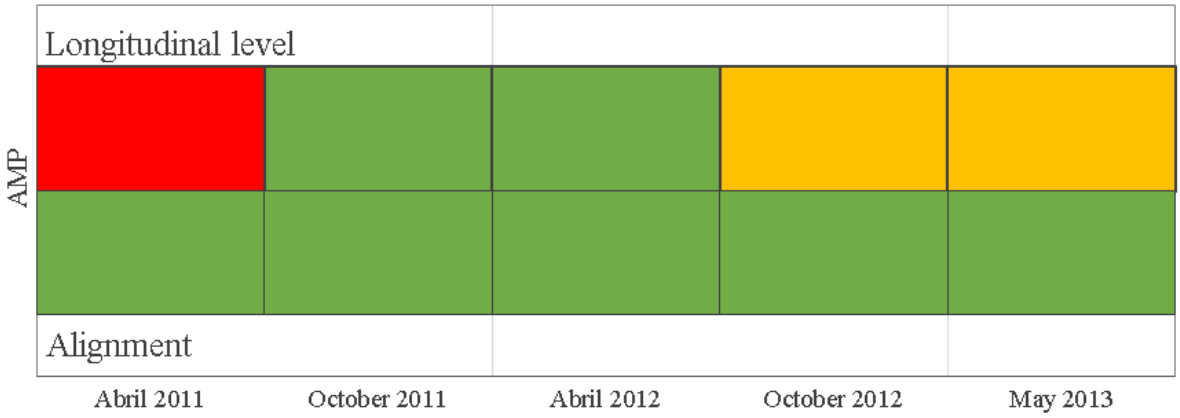

Figure 6.18 - AMP index trend

In this case, the choice of the interval to study is more difficult, as trends above AL limit are quite dissimilar. For safety reasons, the larger between them will be considered for GPR analysis, namely that related to May 2013 campaign, from 158+130 to km 158+530 km (Figure 6.20).

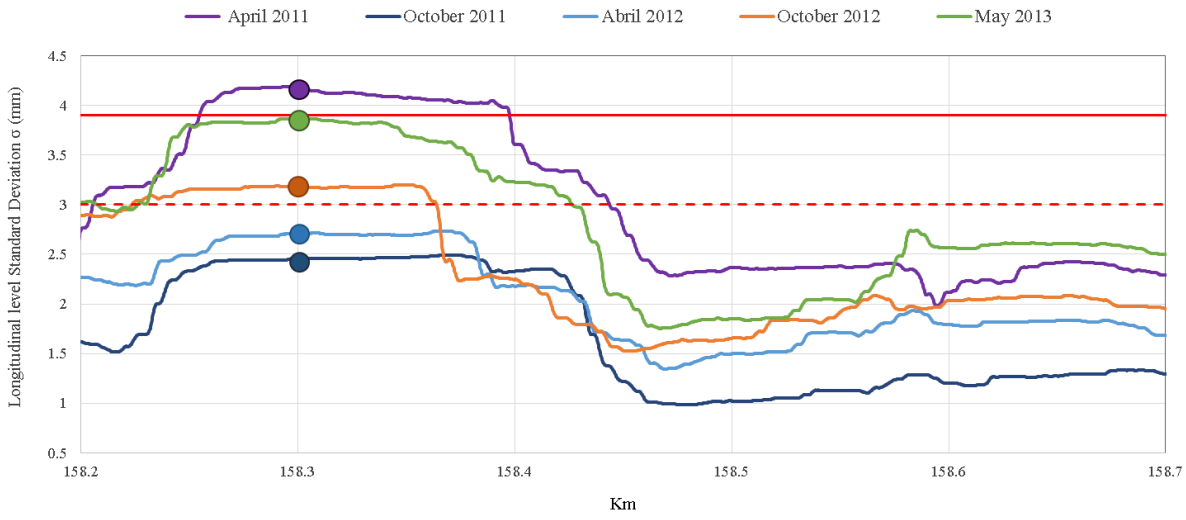

Figure 6.19 - Continuous standard deviation trend of longitudinal level

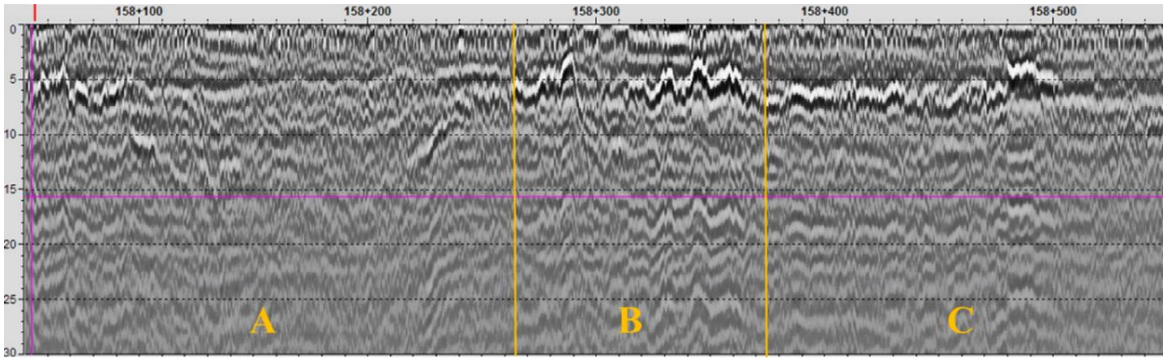

Figure 6.20 - GPR trace – track stretch with longitudinal level defects – case study 2

In a first analysis, as case study 1, three different situations can be observed.

As referred, section A was interpreted by observing GPR also before the defined interval, where one interface was detected. From 158+100 km (Figure 6.21) it can be observed that two interfaces exist and they divide three layers, namely starting from the top: clean ballast, fouled ballast and highly fouled ballast. In addition, the second interface becomes indistinguishable until 158+200 km, that indicates more serious highly fouling conditions, where dielectric properties are practically similar to subsoil. Also this interface shows a clear descendent trend that signifies problem at subsoil level. Therefore, in this section it can be concluded that tamping has been not efficient, and a deeper intervention, i.e. ballast and a partial subsoil renewal, should have been performed. Test pits should be performed in a minimum number for a better localisation of the defects, anyway performed laboratory tests (Chapter 4) can help to estimate at which depth is necessary to intervene. By giving indicative dielectric values to each layer, taking also into account if tested campaign may present wet conditions or not, thicknesses can be evaluated with a certain margin of error.

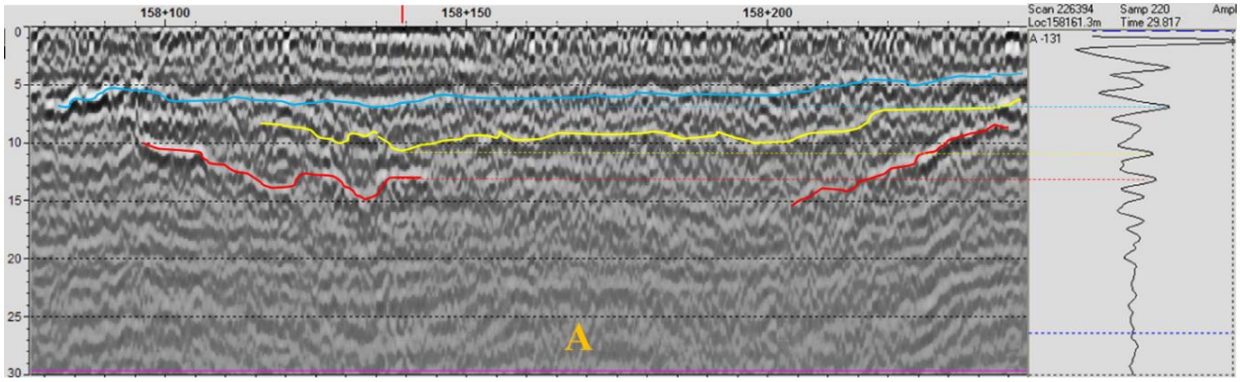

Figure 6.21 - GPR analysis – section A – case study 2

Section B, contrary to section A, shows merely one interface, that divides a clean or moderately clean ballast layer from subsoil (Figure 6.22). In fact the high amplitude wave reflection, and therefore the high black and white contrast, is symptom of a clear difference in the two materials dielectric properties. About trend, a certain variation exists.

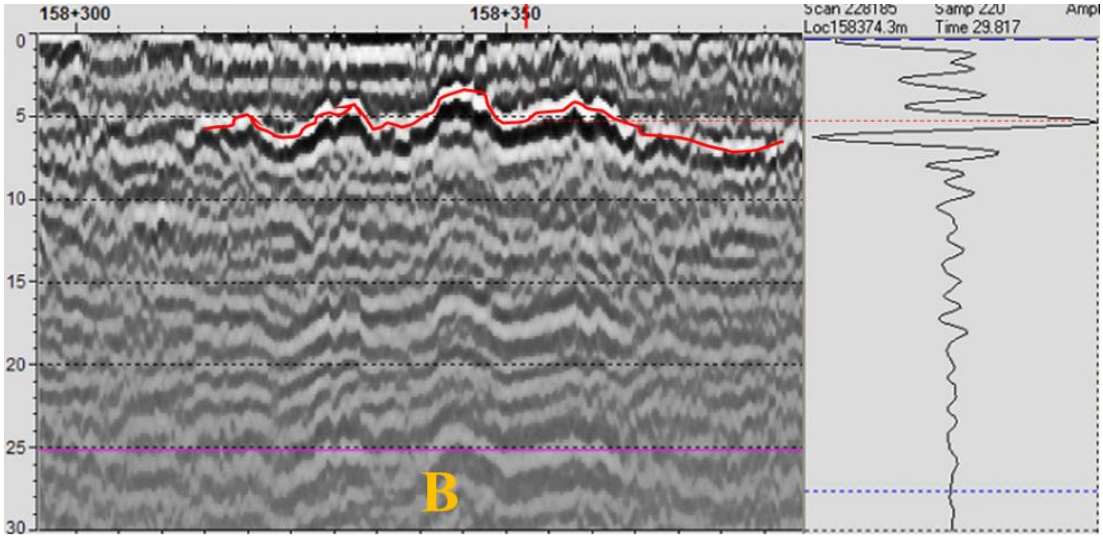

Figure 6.22 - GPR analysis – section B – case study 2

Finally, section C presents a good situation, where a clear interface without variations is detected (Figure 6.23).

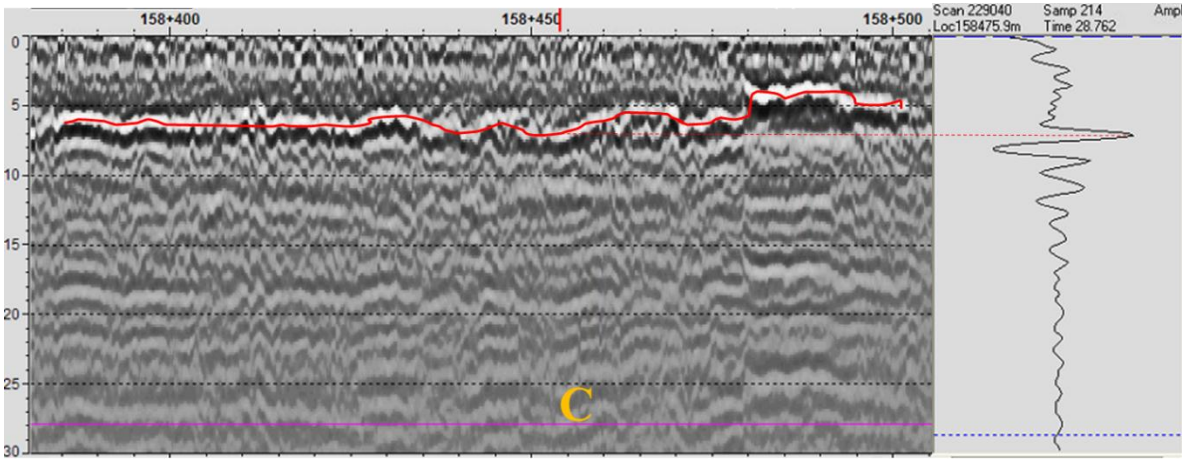

Figure 6.23 - GPR analysis – section C – case study 2

It can be concluded that the studied stretch presents different conditions and therefore they require different interventions. In particular, it can be divided in two patterns: section A should be intervened at subsoil level, while for section B, and eventually C, tamping is sufficient. As already referred, start and final points indicated for interventions should be defined also after a study of raw data of others geometric parameters.

6.5.3. Case study 3

The third study was focused on the analysis of EM120 geometric parameters related to several campaigns. The aim was to detect stretches of the track with systematic degradation, which values do not overcome the IL limit or they overcome merely the AL limit for a short distance.

The same line of previous case studies was considered and an example is shown in Figure 6.24, where longitudinal level standard deviation values of consecutive campaigns are represented.

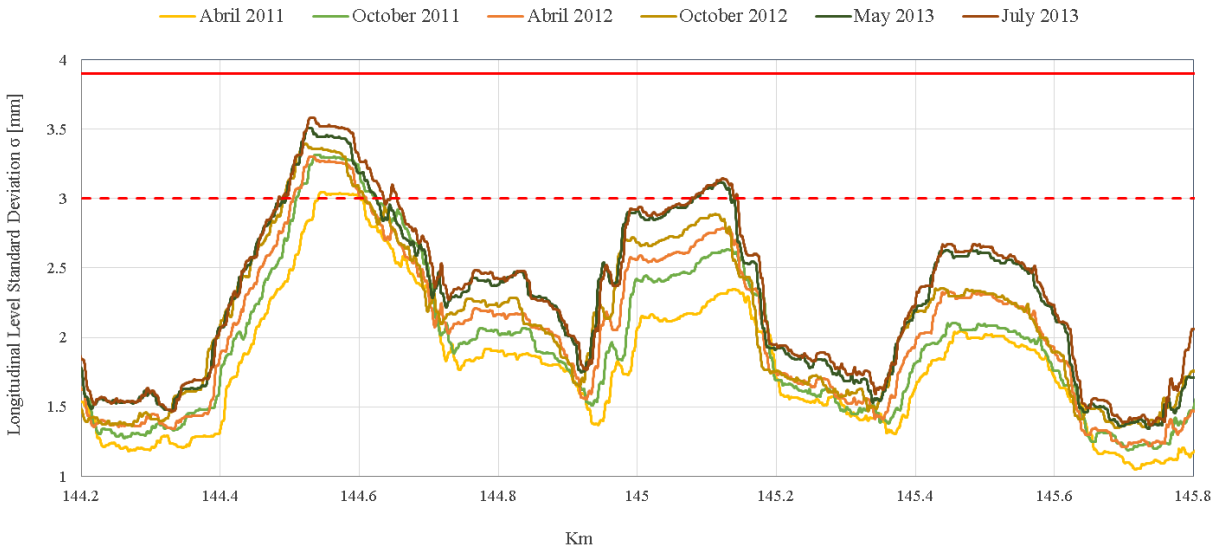

Figure 6.24 - Longitudinal level standard deviation trend – case study 3

For the actual methodology, this section would have not been studied, as values are minor than requisites for tamping intervention. Anyway it can be observed that a definite increment of values occur and this aspect is symptom of degradation.

The new methodology aims to find the real causes by using GPR (Figure 6.25). In this case, two interfaces can be detected and therefore three layers are distinguished: clean ballast, fouled ballast and subsoil. In particular, upper interface is quite constant, no variations are noticeable and a high reflection is visible. From previous studies, it can be affirmed that a difference in term of dielectric properties between adjacent layers, namely clean and fouled ballast, exist. The deeper interface also shows a high reflection, then the fouling level for ballast is not so high as that found in case study 2, where interface was not visible.

On the other hand, a great variation of interface occurs and this indicates an obvious problem at subsoil level, probably not only due to soil pumping, as also found for case study 2.

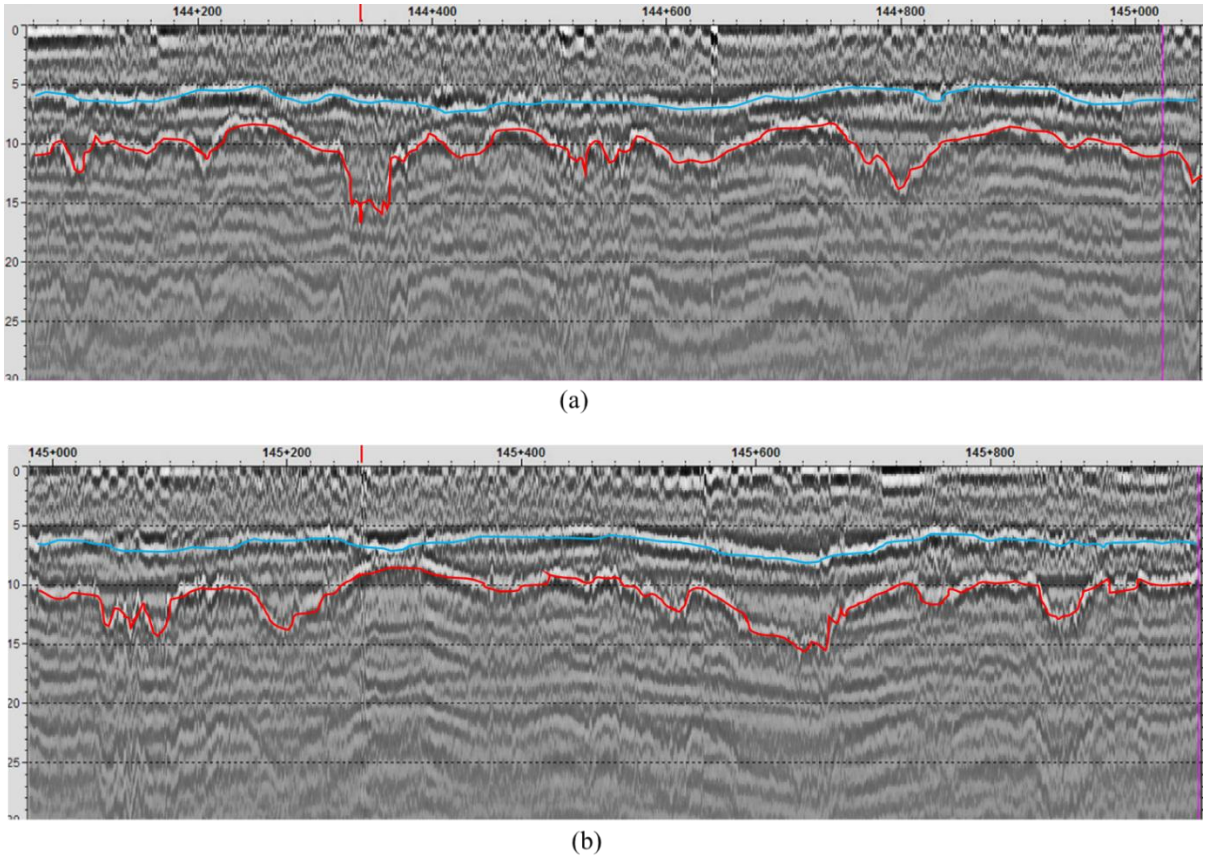

Figure 6.25 - GPR trace – case study 3

Of course, for economic reasons, also the new methodology suggests not to intervene before that limits are overcome. In particular, in this case, the most appropriate intervention would be the renewal of the entire stretch. Anyway, this procedure can be useful for making a prevision of degradation, controlling its evolution and performing a correct management of maintenance interventions, with the aim of saving time and costs.

6.5.4. Interventions comparison

In case of fouled ballast, settlements and substructure problems, an intervention between tamping and ballast cleaning/renewal has to be chosen. In addition, a complete track renewal is sporadic intervention but necessary after a longer period.

Comparing the tamping intervention and ballast cleaning or renewal, it can be concluded that tamping is an efficient intervention at short term depending on the cause of the degradation. Namely:

- it is faster and cheaper;
- it permits an easy restoration of track geometry, but along the time not until the initial level;
- its mechanical operations causes degradation of ballast aggregates (fouling);
- after a certain number of tamping cycles, degradation increases faster;
- it may provide a higher number of interventions (2/3 for year);
- it causes speed restriction.

On the other hand, ballast cleaning/renewal:

- both restores track geometry at initial level;
- the time between intervention increases;
- life-cycles increases;
- they enable material savings.

For this reasons, it is important knowing the causes of track degradation in order to choose the best suitable solution for intervention.

6.6. CONCLUSIONS

In Chapter 6 have been discussed several aspects concerning track maintenance. Track degradations and possible interventions have been presented. European and

Portuguese Standards adopted for maintenance policy were referred, and in particular the actual methodology used in Portugal for maintenance interventions decision process.

The central theme of this chapter was to develop an improved methodology to support the maintenance intervention decisions. The proposed procedure is different from the generally used one in several aspects. Firstly, the selection of stretches with problems is performed differently. Namely, actual procedure calculates a tamping index (AMP) by using "punctual" standard deviation values of both longitudinal level and alignment, every 200 m. Then this value is compared with the alert and the intervention limits, which change in function of the studied speed line, and if two consecutives values overcome the alert limit or only one the intervention limit, tamping is planned. With this methodology, it may occur that tamping is performed also on sections that do not require intervention, enabling waste of money and aggravating ballast conditions, as tamping causes damage to ballast particles. On contrary, the new procedure considers a continuous standard deviation trend of both longitudinal and alignment, in this manner a better localisation of defects can be achieved. In addition, the new procedure aims to study better the consecutive test campaigns that present a systematic increment of standard deviation values, even if the specified limits are not overcome.

The most important innovation presented in the new methodology is the use of Ground Penetrating Radar. It was used as an additional tool in correlation with the traditional measurement of track layout, performed in Portugal with the track inspection vehicle, EM120. The choice of using GPR was due to find the causes of geometric defects that are not discovered in actual maintenance methodologies. In particular, while the actual methodology used by Portuguese railway administration solves the effects of degradation, the new proposed procedure aims to also identify the causes of the deterioration. Also, actual procedure promotes tamping interventions, and only when fouling conditions are detectable at ballast surface level by visual inspections, ballast cleaning or renewal intervention can be performed. On the other hand, the procedure developed in this research gives the

possibility to choose the most appropriate intervention, by eventually dividing the studied stretch in patterns, and indicating for each one an intervention, depending on the identified defect. Laboratory tests (Chapter 4) and test pits results may be helpful in these situations for giving dielectric constant values to interpreted layers, even if with a certain margin of error, in order to localise the problem also in depth and knowing the thickness that requires intervention. The precise definition of the thickness of the ballast to be cleaned is crucial for the maintenance planning and costs.

For better understating, the two methodologies have been compared in three case studies that demonstrate how the proposed procedure can be more useful and it may provide time and costs savings. Case study 1 has shown how continuous standard deviation permits to select defects with more precision. Then GPR analysis has been performed and it has been shown how it was possible to identify two separate patterns. One in better conditions where tamping was considered sufficient, and a second one, that consists in fouled ballast and then that needed a more accurate intervention, i.e. ballast cleaning. Case study 2 has presented an example of not efficient past tamping intervention. It was verified with GPR that the intervened stretch was characterised in part by high fouling conditions and that an intervention, at a higher depth, would have been performed. Case study 3 has highlighted the importance of detecting and analyzing that zones with improved degradation during years, even if values were not necessary to investigate. In fact, it was demonstrated with GPR that problems at substructure level might occur and therefore this kind of analysis results useful for predicting degradation and for managing future intervention works and costs in a better way.

It is necessary to remember that other geometric parameters should be taken into account for a better definition of the stretch interval to be maintained and also that more test pits are fundamental for verifying track conditions.

Also, the GPR antenna of 400 MHz frequency was used, that permits reaching high depths with less resolution. For this reason, the scope was to identify eventual different ballast conditions, namely clean, fouled and, if possible, highly fouled,

but not a precise quantification of fouling level, that can be achieved with higher frequency antennas and new developed model (see Chapter 5). Then this was a first approach for deciding track conditions and deciding the best intervention between tamping and ballast cleaning/renewal.

7 CONCLUSIONS AND FUTURE DEVELOPMENTS

7.1. CONCLUSIONS

The research was focused on the improvement of railways monitoring procedures. The methodology developed herein aims at determining the real causes of track defects, it is based on non-destructive continuous tests and it combines two measurements: the generally applied one, namely the track geometry measurement performed with track inspection vehicles, and a recent prospection methodology, more and more used for railway evaluation, but still as a prototype test, namely the Ground Penetrating Radar (GPR). This latter enables the assessment of the subsurface layers almost continuously, and therefore it is finally possible to evaluate the condition of the infrastructure layers, such as ballast, sub-ballast and foundation in a non-destructive way and consequently to adopt maintenance measures according to the real track condition. It should be highlighted that test pits have to be performed but in a significantly reduced number.

This research addresses the case of Portuguese National Railway in terms of inspection and maintenance policy, as it was possible to access the different data needed for the approach development in this research.

Track inspection vehicles measure, simultaneously, several geometric parameters for determining the track layout and rail wearing condition. For track degradation, longitudinal level and alignments are the main parameters taken into account. European Standards define limits for them in order to plan maintenance interventions. Generally, during maintenance the track layout is restored by tamping, aiming only to correct the geometric defects but neglecting the track layers' condition. With the recent application of the GPR to railway inspection, it becomes possible to evaluate the track condition and to adopt maintenance solutions suitable to the track condition.

GPR is considered, as reflected in the state-of-the-art, an efficient device for road infrastructures studies, as it enables to collect data in a continuous way. It is not time-consuming, neither requires traffic interruptions, and, at the same time, the results obtained are helpful for determining pavement layers thickness, construction quality and pavement defects, such as moisture content and cracks.

GPR application in railways is more complex than in roads. The particular conditions for the antennas installation and of the track itself, like the significant amount of metal present, imply special attention for test preparing and interpretation. First, the antenna frequency should be chosen in accordance with the purpose of the monitoring. As known, the higher the frequency the higher the resolution but the lower the depth of GPR survey penetration. For railways, the combination of higher and lower frequencies represent the ideal equipment configuration, in order to detect ballast fouling, and also deeper subgrade problems, at the same time. Antennas configuration should be studied for guaranteeing a better performance along the tracks. Also, they should be positioned in order to limit the GPR signal noise caused by the reflections of rails, sleepers, catenaries and rolling stock. Then, antenna orientation should be defined in order to irradiate more energy parallel to the direction of the rails and less energy to the sides. Finally, also the antenna elevation has to be considered, as they can be damaged during tests by hitting the sleepers, the ballast between the sleepers or the switches. Also, other parameters must be defined before survey starting, such as the sampling density, the time window and the sample/scan density. During data processing, specific filters have to be applied for reducing the noise in the signal. For data interpretation, the detection of surface is more complex than in the case of roads, due to the presence of sleepers, therefore the surface velocity wave cannot be used as additional calibration for the automatic evaluation of the wave velocity in the top layer, like in case of pavement measurements. In this thesis, a new process for surface detection was adopted, by overcoming problems due to high metal reflections. Nowadays, interpretation is facilitated by the new advanced software but it is always required to correct the row data collected, namely the GPR coordinates have to be adjusted to the EM120

coordinates, measured by a GPS system mounted on it. Finally, the interpretation can be done by assigning dielectric constant values to the different layers interfaces detected and determining their thicknesses.

A second aspect, not yet solved for railways studies, is GPR data calibration. It consists in determining materials dielectric constant values in laboratory or by measuring layers thicknesses through cores/test pits performed in situ.

During the research, laboratory tests were carried out at a Portuguese research centre, National Laboratory for Civil Engineering (LNEC), in order to recreate, in physical models constructed under controlled conditions, the in situ conditions for railway materials. Different materials were studied: clean ballast, fine soil and various mixtures of them, for simulating the fouling conditions. In the latter case, a recent developed fouling index, more practical to be applied and more realistic, namely the "Relative Ballast Fouling Ratio" was considered. For each material, different conditions were simulated in terms of water content and fouling levels. Moreover, different GPR systems and antennas frequencies were used: IDS antennas (400 MHz), used for Portuguese track railways monitoring, and LNEC's GSSI antennas, two ground-coupled (500 MHz and 900 MHz) and two air-coupled antennas (1 GHz and 1.8 GHz). In addition, in the case of IDS antennas, two configurations were adopted during tests, one position in contact with the material surface, ground-coupled, and another position suspended, air-coupled. Laboratory tests results have shown values within the same range variation mentioned in the existing literature and obtained in past tests for all materials. Consequently, the reference value recommended to be adopted in future studies for the clean granite ballast, used in Portugal, is of 4.1 for tests performed with IDS 400 MHz antenna. Nevertheless, the values obtained for clean ballast in situ are insignificantly higher due to the presence of some fines, normal for the ballast in service condition.

Differences were obtained when comparing the different antenna systems, mainly between different antenna producers IDS and GSSI. For all materials, as expected, a high sensitivity of dielectric constant values with water content was obtained

during tests. In the case of fouled ballast, this aspect was even more significant with the increase in fouling level.

GPR presents the advantage of limiting the number of test pits in situ, anyway they are still strongly recommended in railways applications. For the validation of the results obtained in laboratory, a series of test pits were performed along two Portuguese tracks. For the first track, thicknesses measurements of clean and fouled ballast were performed and dielectric constant values were calculated. For clean ballast, results have shown good agreement with the values obtained in laboratory and an average dielectric constant value of 4.79 was determined. On the other hand, for the other layers, this study presents challenges and uncertainties. The main problem for fouling layers was the real thicknesses measurement, due to a gradual passage from clean to fouled conditions. It was confirmed by the fact that the calculated dielectric constant values were not within the expected range and also because interpretation was more complex due to a major difficulty in detecting GPR wave reflections.

In addition, several conditions in terms of materials were found: one of the scope of this study consisted in characterise track layers through GPR by identifying different responses in terms of reflections. After that, the test pits of the second track were taken into account and a validation analysis was developed. It demonstrated that 4.79 can be assumed during GPR interpretation at network level. In addition, another study was performed comparing in situ and laboratory results for clean ballast material. It was observed that a certain difference in dielectric constant values can be accepted as it could be caused by the presence of small amount of fine particles and results in a insignificant difference in ballast layer thicknesses measurements.

For new railways pavements, GPR data interpretation can be done by considering default dielectric constant values determined during the laboratory tests. In this thesis, a monitoring procedure, based on GPR data collection, is presented using as case study a renewed track in Portugal. Layers thicknesses were known and used as input data and then dielectric constant values were determined, showing

reliable results with values encountered in the technical documents, in past laboratory tests and in the tests performed in this research, namely in laboratory and in situ. Three test campaigns were considered for comparing dielectric constant values and it was found a consistent sensibility of the dielectric properties of railway materials with the moisture variation. In addition, it was demonstrated that GPR enables a confident detection of changes in the structure in terms of thicknesses and type of materials. Also, it is easy to locate the measurements for later references, as GPR identifies with precision special events, such as bridges and switches.

After GPR calibration, interpretation of GPR data collected on the entire Portuguese railway network can be performed. An improved procedure was developed and is presented in this study. An optimised methodology, to support the maintenance intervention decisions at network level, was proposed. Then, several other features of the general monitoring and data processing procedure, used in Portugal, were also improved. Some aspects were considered to be inadequate and not efficient for track railway monitoring. First, the actual maintenance methodologies, including the Portuguese one, take into account merely the track geometric parameters, in particular the longitudinal level and the alignment. In this way, the effects and not the causes of track degradations are treated. Also, the actual Portuguese procedure considers tamping as the main maintenance intervention and ballast cleaning or renewal intervention are performed exceptionally, namely only when fouling conditions are detectable at ballast surface level by visual inspections. All these aspects lead to expensive maintenance campaigns and to an accelerated deterioration of the track condition, in case of weak foundation, and also lead to ballast wearing, due to tamping action itself. For improving the methodology, track study with GPR was analysed in this study and it was demonstrated to be an efficient tool. An improved procedure for railway monitoring and maintenance was proposed herein. It was shown that it enables a better location of defects longitudinally and in depth. Also, with GPR tests it is possible to identify and to study better the track stretches with problems, for example by taking into account consecutive test campaigns that present a

systematic increment of geometric parameters values, even if it is not yet recommended by Portuguese and European Standards, as it is a quite recent test. The proposed procedure was demonstrated to be a helpful tool for choosing the most appropriate intervention, by eventually dividing the studied stretch in patterns, and indicating for each one an intervention, depending on the identified defect. Also, a prevision of track degradation and the identification of the problems in depth has demonstrated to be an useful analysis for predicting degradation and for managing future intervention works, resulting in cost and time savings.

Laboratory tests and test pits results may be useful in these situations for providing dielectric constant values for the interpreted layers, even if with a certain margin of error, in order to localise the problem also in depth and knowing the thickness that requires intervention. The precise definition of the thickness of the ballast to be cleaned is crucial for the maintenance planning and costs. Also, the GPR antenna of 400 MHz frequency was used, that permits reaching high depths with less resolution. For this reason, the scope was to identify different ballast conditions, namely clean, fouled and, if possible, highly fouled, but not a precise quantification of fouling level that can be achieved with higher frequency antennas and new developed models. Then this was a first approach for deciding track conditions and deciding the best intervention between tamping and ballast cleaning/renewal.

7.2. FUTURE DEVELOPMENTS

In general, GPR represents still some challenges, as its application for railway evaluation is quite recent. For this reason, several developments have been carrying out, as for example for data interpretation that presents still some difficulties.

A second aspect not yet solved with GPR is the calibration of the measurements. Even if one of GPR characteristics is limiting the number of test pits, in railways studies they are still required and they are crucial. Therefore, during the research,

the evaluation of the railway materials on laboratory, for different conditions in terms of fouling and water content, was a necessary step.

A limitation of GPR tests is represented by the evaluation of material properties. In fact the presence of water, even in small quantities, changes in a significant way the dielectric constant of the material. The same considerations can be made for ballast layer when it is fouled. In this context, detection of fouling and moisture conditions represent still a challenge for GPR railways surveys and new analysis has been developed recently to optimize a semi-automatic GPR interpretation.

During this research, test pits analysis presented some problems for the evaluation of the layers thicknesses, being very difficult to distinguish the interfaces between the clean ballast and the fouled ballast and even more difficult when more layers of fouled ballast, with different fouling levels, were detected. In addition, for fouled ballast, GPR wave reflection and the dielectric constant calculation was more complex, requiring more information about the materials condition. Therefore, for a better definition of the evaluation procedure, future research is needed consisting in additional validation with test pits performed *in situ*, and in consideration of other materials present on the existing railway substructure, such as limestone ballast.

Regarding the proposed procedure, it is necessary to remember that other geometric parameters should be taken into account for a better definition of the stretch interval where to perform the maintenance action and also that test pits are fundamental for verifying track conditions.

For a quantification of the level of fouling in the ballast, analytical models can be developed or adapted and, for this purpose, the laboratory results obtained in this research represent valuable information for calibration.

Finally, more GPR monitoring campaigns should be collected for better understanding the variation of materials dielectric constant values along the track life cycle, together with the geometric parameters assessment. With more data available, it is possible to study the evolution of the dielectric constant of materials

in time and its sensitivity to season variation. The joint interpretation of GPR and geometric parameters it is important also in order to define trends for ballast fouling evolution and therefore to develop performance indexes for a better track management policy.

REFERENCES

AASHTO M 145, 1995. Classification of soils and soil-aggregate mixtures for highway construction purposes. Standard Specifications for Transportation Material and Methods of Sampling and Testing.

Al-Qadi, I., Xie, W., Roberts, R., 2010. Optimization of antenna configuration in multiple-frequency ground penetrating radar system for railroad substructure assessment. NDT E Int. 43, 20–28.

Al-Qadi, I.L., Lahouar, S., 2005. Measuring layer thicknesses with GPR – Theory to practice. Constr. Build. Mater. 19, 763–772. doi:10.1016/j.conbuildmat.2005.06.005

Al-Qadi, I.L., Xie, W., Roberts, R., 2008. Scattering analysis of ground-penetrating radar data to quantify railroad ballast contamination. NDT E Int. 41, 441–447.

Alani, A.M., Aboutalebi, M., Kilic, G., 2013. Applications of Ground Penetrating Radar (GPR) in Bridge Deck Monitoring and Assessment. J. Appl. Geophys.

Anbazhagan, P., Su, L., Indraratna, B., Rujikiatkamjorn, C., 2011. Model track studies on fouled ballast using ground penetrating radar and multichannl analysis of surface wave. J. Appl. Geophys. 74, 175–184.

Anders Ekberg, B.P., 2010. INNOTRACK: Concluding technical report.

Andersson, M., 2002. Strategic Planning of Track Maintenance. State Art Rep. CDU R. Inst. Technol. Stockh.

Annan, A., 1999. Practical processing of GPR data., in: Proceedings of Second Government Workshop on Ground Prenetrating Radar, Sensor and Software Inc.

Annan, A.P., 1992. Ground penetrating radar workshop notes. Sens. Softw. Inc Mississauga.

Audley, M., Andrews, J.D., 2013. The effects of tamping on railway track geometry degradation. Proc. Inst. Mech. Eng. Part F J. Rail Rapid Transit 227, 376–391.

Bailey, B., Hutchinson, D.J., Siemens, G., Ruel, M., 2011. Assessment of embankment fouling from geotechnical testing of railway ballast samples, in: Proceeding of the 2011 Pan-Am CGS Geotechnical Conference.

Berggren, E., 2009. Railway track stiffness: dynamic measurements and evaluation for efficient maintenance PhD Thesis). University West.

Berggren, E.G., 2010. Efficient track maintenance: methodology for combined analysis of condition data. Proc. Inst. Mech. Eng. Part F J. Rail Rapid Transit 224, 353–360.

Berthelot, C., Podborochynski, D., Saarenketo, T., Marjerison, B., Prang, C., 2010. Ground-Penetrating Radar Evaluation of Moisture and Frost across Typical Saskatchewan Road Soils. Adv. Civ. Eng. 2010. doi:10.1155/2010/416190

Budai-Balke, G., 2009. Operations research models for scheduling railway infrastructure maintenance. Rozenberg Publishers.

Carpenter, D., Jackson, P.J., Jay, A., 2004. Enhancement of the GPR method of railway trackbed investigation. NDT E Int. 37, 95–103.

Clark, M., Gordon, M., Forde, M.C., 2004. Issues over high-speed non-invasive monitoring of railway trackbed. NDT E Int. 37, 131–139. doi:10.1016/j.ndteint.2003.05.002

Clark, M., Gordon, M., Giannopoulos, A., Forde, M., 2004. Advanced analysis of ground penetrating radar signals on railway, in: Proceedings of the 7h International Conference on Railway Engineering. London, UK.

Clark, M.R., Gillespie, R., Kemp, T., McCann, D.M., Forde, M.C., 2001. Electromagnetic properties of railway ballast. NDT E Int. 34, 305–311.

Conyers, L.B., 2013. Ground-Penetrating Radar for Archaeology. AltaMira Press.

Daniels, D.J., 2004. Ground Penetrating Radar, 2nd Edition. IET.

Daniels, J.J., 2000. Ground penetrating radar fundamentals. Prep. Append. Rep. US EPA Reg. V Dep. Geol. Sci. Ohio State Univ.

De Bold, R.P., 2011. Non-destructive evaluation of railway trackbed ballast (PhD Thesis). University of Edinburgh.

De Chiara, F., Fontul, S., Fortunato, E., D'Andrea, A., 2013. Ground Penetrating Radar technique for railway track characterisation in Portugal, in: EGU General Assembly Conference Abstracts. Presented at the EGU General Assembly Conference Abstracts, p. 12196.

De Chiara, F., Fontul, S., Paixão, A., D'Andrea, A., 2011. Bituminous mixtures application in railway sub-ballast layer. Presented at the 5th International Conference Bituminous Mixtures and Pavements, Thessaloniki, Greece.

Del Conte, A., 2004. Georadar artemis: Il radar penetrante (GPR) [WWW Document]. URL https://www.google.it/search?newwindow=1&client=firefox-a&rls=org.mozilla%3Ait%3Aofficial&channel=fflb&biw=1366&bih=655&q=georadar+artemis+Il+radar+penetrante+%28GPR%29+Ing.+Antonio+del+Conte+&oq=georadar+artemis+Il+radar+penetrante+%28GPR%29+Ing.+Antonio+del+Conte+&gs_l=serp.12...79417.80660.0.84728.2.2.0.0.0.0.136.270.0j2.2.0....0...1c.1j2.37.serp..2.0.0.Uf39v3ozM2Q

Donohue, S., 2011. Geophysical and geotechnical assessment of a railway embankment failure. Surf. Geophys. doi:10.3997/1873-0604.2010040

Ebersohn, W., 1998. Implementing a railway infrastructure maintenance system, in: Conference on Railway Engineering Proceedings: Engineering Innovation for a Competitive Edge. Central Queensland University, p. 395.

EN 13848-5:2008, 2008. Track geometry quality – Geometric quality levels.

Eriksen, A., Gascoyne, J., Al-Nuaimy, W., 2004. Improved productivity & reliability of ballast inspection using road-rail multi-channel GPR. Proc. Railw. Eng. 6th–7th July Commonw. Inst. Lond. UK 1–5.

Esveld, C., 2001. Modern railway track, Ed. 2. ed, Zaltbommel. MRT-Productions.

Evans, R.D., Frost, M.W., Dixon, N., Stonecliffe-Jones, M., 2008. The response of ground penetrating radar (GPR) to changes in temperature and moisture condition of pavement materials.

Feldman, F., Nissen, D., 2002. Alternative testing method for the measurement of ballast fouling: percentage void contamination, in: Proceedings of the Conference on Railway Engineering,Wollongong, Australia. Railway Technical Society of Australia, Canberra, Australia., pp. 101–109.

Fisher, E., McMechan, G.A., Annan, A.P., Cosway, S.W., 1992. Examples of reverse-time migration of single-channel, ground-penetrating radar profiles. Geophysics 57, 577–586. doi:10.1190/1.1443271

Fontul, S., 2004. Structural evaluation of flexible pavements using non-destructive tests (PhD Thesis). Departamento de Engenharia Civil, Universidade de Coimbra.

Fontul, S., Antunes, M.L., Fortunato, E., Oliveira, M., 2007. Practical application of GPR in transport infrastructure survey. Presented at the International Conference on Advanced Characterisation of Pavement and Soil Engineering Materials.

Fontul, S., Fortunato, E., De Chiara, F., 2011. Non-Destructive Tests for Railway Infrastructure Stiffness Evaluation. Presented at the the Thirteenth International Conference on Civil, Structural and Environmental Engineering Computing, B.H.V. Topping, Y. Tsompanakis, Stirlingshire, UK. doi:10.4203/ccp.96.16

Fontul, S., Fortunato, E., De Chiara, F., 2012a. Non-Destructive Tests for Railway Infrastructure Stiffness Evaluation. doi:10.4203/ccp.96.16

Fontul, S., Fortunato, E., De Chiara, F., Paixão, A., 2012b. Non Destructive Tests for Evaluation of Railway Platforms: Application of Ground Penetrating Radar. Presented at the the First International Conference on Railway Technology: Research, Development and Maintenance", Civil-Comp Press, J. Pombo, Stirlingshire, UK. doi:10.4203/ccp.98.134

Forde, M.C., De Bold, R., O'Connor, G., Morrissey, J., 2010. New Analysis of Ground Penetrating Radar Testing of a Mixed Railway Trackbed, in: Transportation Research Board 89th Annual Meeting.

Fortunato, E., 2005. Renovação de Plataformas Ferroviárias. Estudos Relativos à Capacidade de Carga (Ph.D. (in Portuguese)). Departamento de Engenharia Civil; Porto: Faculdade de Engenharia da Universidade do Porto;

Fortunato, E., Pinelo, A., Lobo da Costa, J., Gonçalves, D., Pratas, A., 2007. Some results of performance indicators of a railway track obtained during its renewal process. Presented at the 4 th International SIIV Congress, Palermo , Italy.

Fortunato, E., Pinelo, A., Matos Fernandes, M., 2010. Characterisation of the fouled ballast layer in the substructure of a 19th century railway track under renewal. Soils Found. 50, 55–62.

Gallagher, G.P., Leiper, Q., Williamson, R., Clark, M.R., Forde, M.C., 1999. The application of time domain ground penetrating radar to evaluate railway track ballast. NDT E Int. 32, 463–468.

Göbel, C., Hellmann, R., Petzold, H., 1994. Georadar-model and in-situ investigations for inspection of railway tracks, in: Fifth International Conferention on Ground Penetrating Radar.

GSSI, 2008. BALLASTVUE module: RADAN software user's guide [WWW Document]. URL http://www.geophysical.com/Documentation/Brochures/GSSI-RADAN6Brochure.pdf (accessed 1.13.14).

Gunn, D.A., Reeves, H., Chambers, J.E., Pearson, S.G., Haslam, E., Raines, M.R., Tragheim, D., Ghataora, G., Burrow, M., Weston, P., 2007. Assessment of embankment condition using combined geophysical and geotechnical surveys, in: Proc. 9th Int. Conf. Railway Engineering, London.

Highways Agency, 2001. Design Manual for Roads and Bridges.

Hing, C., Halabe, U., 2010. Nondestructive Testing of GFRP Bridge Decks Using Ground Penetrating Radar and Infrared Thermography. J. Bridge Eng. 15, 391–398. doi:10.1061/(ASCE)BE.1943-5592.0000066

Hugenschmidt, J., 2000. Railway track inspection using GPR. J. Appl. Geophys. 43, 147–155.

Hyslip, J.P., 2002. Fractal analysis of track geometry data. Transp. Res. Rec. J. Transp. Res. Board 1785, 50–57.

Hyslip, J.P., 2007. Substructure Maintenance Management–Its Time Has Come, in: AREMA Conference, Chicago. pp. 9–12.

Hyslip, J.P., Chrismer, S., LaValley, M., Wnek, J., 2012. Track Quality From The Ground Up, in: AREMA Conference. Chicago, IL.

Hyslip, J.P., Olhoeft, G.R., Selig, E., Smith, S., 2007. Ground Penetrating Radar for Railroad Track Substructure Evaluation.

Hyslip, J.P., Smith, S.S., Olhoeft, G.R., Selig, E.T., 2003. Assessment of railway track substructure condition using ground penetrating radar, in: 2003 Annual Conference of AREMA.

IDS, 2013. Note tecniche IDS [WWW Document]. URL http://www.boviar.net/schede_georadar/NOTE%20TECNICHE%20IDS.pdf (accessed 12.27.13).

IDS, 2014. SRS.pdf [WWW Document]. URL http://www.drilline.com/files/SRS.pdf (accessed 1.13.14).

Indraratna, B., Su, L., Rujikiatkamjorn, C., 2011. A new parameter for classification and evaluation of railway ballast fouling. Can. Geotech. J. 48, 322–326.

Jol, H.M., 2008. Ground penetrating radar theory and applications. Access Online via Elsevier.

Jovanovic, S., 2004. Railway track quality assessment and related decision making, in: Systems, Man and Cybernetics, 2004 IEEE International Conference on. pp. 5038–5043.

Jovanovic, S., Pearce, M., 2000. Ecotrack: An overview of the system's functionality and implementation to date, in: AREMA Proceedings of the 2000 Annual Conference.

Kathage, A., Niessen, J., White, G., Bell, N., 2005. Fast Inspection of Railway Ballast By Means of Impulse GPR Equipped with Horn Antennas, in: Proceedings of Railway Engineering. Edinburgh, Scotland, p. 1.

Kim, J.-H., Cho, S.-J., Yi, M.-J., 2007. Removal of ringing noise in GPR data by signal processing. Geosci. J. 11, 75–81.

Lahouar, S., 2003. Development of Data Analysis Al gorithms for Interpretation of Ground Penetrating Radar Data (PhD Thesis). Faculty of the Virginia Polytechnic Institute and State University, Blacksburg, Virginia.

Lee, S., Milios, E., Greiner, R., Rossiter, J., 1992. An expert system for automated interpretation of ground penetrating radar data. Ground Penetrating Radar Geol. Surv. Can. Pap. N 90-4 125–131.

Leng, Z., Al-Qadi, I.L., 2009. Dielectric Constant Measurement of Railroad Ballast and Application of STFT for GPR Data Analysis. NDT&E International. Nantes, France. June 30th–July 3rd.

Leucci, G., 2008. Ground Penetrating Radar: The Electromagnetic Signal Attenuation and Maximum Penetration Depth. Sch. Res. Exch. 2008, 1–7. doi:10.3814/2008/926091

Leucci, G., 2012. Ground Penetrating Radar: A Useful Tool for Shallow Subsurface Stratigraphy Characterisation, in: Elitok, mer (Ed.), Stratigraphic Analysis of Layered Deposits. InTech.

Li, D., Read, D., Thompson, H., Sussmann, T., McDaniel, R., Railway, N.S., Roanoke, V.A., 2010. Evaluation of Ground Penetrating Radar Technologies for Assessing Track Substructure Conditions.

Li, D., Selig, E., 1998. Method for Railroad Track Foundation Design. I: Development. J. Geotech. Geoenvironmental Eng. 124, 316–322. doi:10.1061/(ASCE)1090-0241(1998)124:4(316)

Lichtberger, B., 2005. Track compendium: Formation, permanent way, maintenance, economics. Eurailpress.

Lichtberger, B., 2007. The Track System and Its Maintenance. RTR Spec. pp. 14–22.

Liu, J., Zhang, Q., 2012. Vehicle GPR in the maintenance of the high-speed railway, in: Ground Penetrating Radar (GPR), 2012 14th International Conference on. pp. 93–97.

LNEC E 196: 1967, 1967. Soils. Aggregate grading analysis.

LNEC E 197: 1966, 1966. Compactation test.

Loizos, A., Plati, C., 2007a. Accuracy of ground penetrating radar horn-antenna technique for sensing pavement subsurface. Sens. J. IEEE 7, 842–850.

Loizos, A., Plati, C., 2007b. Ground penetrating radar: A smart sensor for the evaluation of the railway trackbed, in: Instrumentation and Measurement Technology Conference Proceedings, 2007. IMTC 2007. IEEE. pp. 1–6.

Loizos, A., Silvast, M., Dimitrellou, S., 2007. Railway trackbed assessment using the GPR technique. Adv. Characterisation Pavement Soil Eng. Mater. Vols 1, 1817–1826.

Lopez-Pita, A., Teixeira, P.F., Casas, C., Bachiller, A., Ferreira, P.A., 2008. Maintenance costs of high-speed lines in Europe: State of the art. Transp. Res. Rec. J. Transp. Res. Board 2043, 13–19.

Maal, L., Carr, G., 2011. Heavy Axle Load Revenue Service Mud-Fouled Ballast Investigation. Res. Results.

Madejski, J., Grabczyk, J., 2002. Continuous geometry measurement for diagnostics of tracks and switches, in: International Conference on Switches: Switch to Delft.

Manacorda, G., Morandi, D., Sarri, A., Staccone, G., 2002. Customized GPR system for railroad track verification, in: Ninth International Conference on Ground Penetrating Radar (GPR2002). pp. 719–723.

Manacorda, G., Simi, A., 2012. Non-destructive inspection and characterisation of track bed with microwaves, in: Ground Penetrating Radar (GPR), 2012 14th International Conference on. pp. 805–810.

Moretti, M., Triglia, M., Maffei, G., 2004. ARCHIMEDE - the first European diagnostic train for global monitoring of railway infrastructure, in: 2004 IEEE Intelligent Vehicles Symposium. Presented at the 2004 IEEE Intelligent Vehicles Symposium, pp. 522–526. doi:10.1109/IVS.2004.1336438

Mundrey, J.S., 2010. Railway Track Engineering. Tata McGraw-Hill Education.

Norman, C., Farritor, S., Arnold, R., Elias, S.E.G., Fateh, M., El-Sibaie, M., 2006. Design of a system to measure track modulus from a moving railcar. US Department of Transportation, Federal Railroad Administration, Office of Research and Development.

NP EN 1097- 6: 2003, 2003. Tests for mechanical and physical properties of aggregates. Determination of particle density and water absorption. Portuguese Standard.

NP EN 13450: 2005, 2005. Aggregates for railway ballast. Portugues Standard.

NP EN 1936: 2001, 2001. Natural stone test methods. Determination of real density and apparent density and of total and open porosity. Portuguese Standard.

NP EN 581: 1969, 1969. Aggregates for mortars and concrete. Determination of specific density and water absorption of coarse aggregate. Portuguese Standard.

Okrasinski, T., Koerner, R., Lord, A., 1978. Dielectric Constant Determination of Soils at L Band Microwave Frequencies. Geotech. Test. J. 1, 134. doi:10.1520/GTJ10384J

Olhoeft, G.R., 2005. Working in a difficult environment: GPR sensing on the railroads, in: Antennas and Propagation Society International Symposium, 2005 IEEE. pp. 108–111.

Olhoeft, G.R., Selig, E.T., 2002. Ground-penetrating radar evaluation of railway track substructure conditions, in: SPIE, Vol 4758. Presented at the Ninth International Conference on Ground Penetrating Radar, S Koppenjan & H Lee, Santa Barbara, California. Proc., pp. 48–53. doi:10.1117/12.462264.

Parrillo, R., Roberts, R., 2006. Integration of FWD and GPR. Presented at the Geophysics NDE Conference, Saint Louis, MO, USA.

Pedrosa, M., 2009. Caracterização da fundação de infra-estruturas de transporte com recurso ao Georadar. Identificação das camadas de apoio (M.Sc.(in Portuguese)). Faculdade de Engenharia da Universidade do Porto, Porto.

Peters Jr, L.P., Daniels, J.J., Young, J.D., 1994. Ground penetrating radar as a subsurface environmental sensing tool. Proc. IEEE 82, 1802–1822.

Phillips, C., Balasundaram, A., Ahmed, Z., Kohlberger, R., Hoffman, D., 2006. The Integrated Use of GPR and Conventional Methods for Continuous Pavement Condition Investigations: A Case Study of the QEW Rehabilitation and Widening Project, in: Annual Conference & Exhibition of the Transportation Association of Canada, 2006. Congres et Exposition Annuels de l'Association Des Transport Du Canada, 2006.

Plati, C., Loizos, A., 2013. Estimation of in-situ density and moisture content in HMA pavements based on GPR trace reflection amplitude using different frequencies. J. Appl. Geophys.

Plati, C., Loizos, A., Papavasiliou, V., 2010. Inspection of railroad ballast using geophysical method. Int. J. Pavement Eng. 11, 309–317.

REFER, 2009. “Tolerâncias dos parâmetros geométricos da via.” IT.VIA.018.

RFI, 2013. Brochure Archimede, il treno misure [WWW Document]. URL http://www.rfi.it/cms-file/allegati/rfi/BrochureArchimedeIlTrenoMisura.pdf (accessed 1.9.14).

RFI, 2014. Dia.man.te, il nuovo treno diagnostico di Rete Ferroviaria Italiana - Notizie - FSNews [WWW Document]. URL http://www.fsnews.it/cms/v/index.jsp?vgnextoid=72c1ed0c531d7310VgnVCM1000008916f90aRCRD (accessed 1.9.14).

Roadscanners, O., 2000. Railway Doctor User’s guide. Rovaniemi, Finland.

Roberts, R., Al-Qadi, I., Tutumluer, E., 2008. Track Substructure Characterisation Using 500 MHz and 2 GHz Ground Penetrating Radar: Results from over 250 Miles of Track in Wyoming and Alaska. Urbana 51, 61801.

Roberts, R., Al-Qadi, I., Tutumluer, E., Boyle, J., 2008. Subsurface Evaluation of Railway Track Using Ground Penetrating Radar.

Roberts, R., Rudy, J., Al Qadi, I.L., Tutumluer, E., Boyle, J., 2006. Railroad Ballast Fouling Detection Using Ground Penetrating Radar–A New Approach Based on Scattering from Voids, in: Ninth European Conference on NDT.

Saaranketo, T., 2006. Electrical properties of road materials and subgrade soils and the use of ground penetrating radar in traffic infrastructure surveys (PhD Thesis). University of Oulu.

Saarenketo, T., 1997. Using Ground-Penetrating Radar and Dielectric Probe Measurements in Pavement Density Quality Control. Transp. Res. Rec. J. Transp. Res. Board 1575, 34–41. doi:10.3141/1575-05

Saarenketo, T., 1998. Electrical properties of water in clay and silty soils. J. Appl. Geophys. 40, 73–88.

Saarenketo, T., Matintupa, A., Varin, P., 2012. The Use of Ground Penetrating Radar, Thermal Camera and Laser Scanner Technology in Asphalt Crack Detection and Diagnostics, in: Scarpas, A., Kringos, N., Al-Qadi, I., A, L. (Eds.), 7th RILEM

International Conference on Cracking in Pavements, RILEM Bookseries. Springer Netherlands, pp. 137–145.

Saarenketo, T., Scullion, T., 2000. Road evaluation with ground penetrating radar. J. Appl. Geophys. 43, 119–138.

Sadeghi, J., 2010. Development of Railway Track Geometry Indexes Based on Statistical Distribution of Geometry Data. J. Transp. Eng. 136, 693–700. doi:10.1061/(ASCE)0733-947X(2010)136:8(693)

Scheers, B., 2001. Ultra-wideband ground penetrating radar with application to the detection of anti personnel landmines. Chapter 7, 867–871.

Schilling, R., 2005. Ballast Cleaning of Single-Track Railway Lines: A Strategic Analysis. Rail Eng. Int. 34.

Scullion, T., Saarenketo, T., 1998. Applications of Ground Penetrating Radar technology for network and project level pavement management systems, in: Fourth International Conference on Managing Pavements.

Scullion, T., Saarenketo, T., 2000. Integrating ground penetrating radar and falling weight deflectometer technologies in pavement evaluation. ASTM Spec. Tech. Publ. 1375, 23–40.

Sebesta, S., Scullion, T., Saarenketo, T., 2013. Using Infrared and High-speed Ground-penetrating Radar for Uniformity Measurements on New HMA Layers. Transportation Research Board.

Selig, E.T., Cantrell, D.D., Past President, A., 2001. Track Substructure Maintenance–From Theory to Practice, in: American Railway Engineering and Maintenance of Way Association Annual Conference.

Selig, E.T., Waters, J.M., 1994. Track geotechnology and substructure management. Thomas Telford.

Shangguan, P., Al-Qadi, I.L., Leng, Z., 2012. Development of Wavelet Technique to Interpret Ground-Penetrating Radar Data for Quantifying Railroad Ballast Conditions. Transp. Res. Rec. J. Transp. Res. Board 2289, 95–102.

Shao, W., Bouzerdoum, A., Phung, S.L., Su, L., Indraratna, B., Rujikiatkamjorn, C., 2011. Automatic classification of ground-penetrating-radar signals for railway-ballast assessment. Geosci. Remote Sens. IEEE Trans. On 49, 3961–3972.

Shihab, S., Zahran, O., Al-Nuaimy, W., 2002. Time-frequency characteristics of ground penetrating radar reflections from railway ballast and plant, in: High Frequency Postgraduate Student Colloquium, 2002.7 Th IEEE. p. 8–pp.

Silvast, M., Levomaki, M., Nurmikolu, A., Noukka, J., 2006. NDT techniques in railway structure analysis, in: Proceedings of the 7th World Congress on Railway Research, Montreal, Canada. pp. 4–8.

Silvast, M., Nurmikolu, A., Wiljanen, B., Levomaki, M., 2010. An inspection of railway ballast quality using ground penetrating radar in Finland. Proc. Inst. Mech. Eng. Part F J. Rail Rapid Transit 224, 345–351.

Slob, E.C., Groenenboom, J., Fokkema, J.T., 2003. Automated acquisition and processing of 3D GPR data for object detection and characterisation. Subsurf. Sens. Technol. Appl. 4, 5–18.

Smekal, A., Berggren, E.G., Silvast, M., 2006. Monitoring and substructure condition assessment of existing railway lines for upgrading to higher axle loads and speeds, in: Congress Proc. 7th World Congress on Railway Research.

Stenström, C., 2012. Maintenance performance measurement of railway infrastructure with focus on the Swedish network. Luleaa Univ. Technol. Luleaa.

Su, L.J., Indraratna, B., Rujikiatkamjorn, C., 2011. Non-destructive assessment of rail track condition using ground penetrating radar.

Sussmann, T., 1999. Application of Ground Penetrating Radar to railway track substructure maintenance management. University of Massachussets.

Sussmann, T.R., Maser, K.R., Kutrubes, D., Heyns, F., Selig, E.T., 2001. Development of Ground Penetrating Radar for railway infrastructure condition detection. Presented at the The 14th EEGS Symposium on the Application of Geophysics to Engineering and Environmental Problems (SAGEEP).

Sussmann, T.R., O'Hara, K.R., Selig, E.T., 2002. Development of material properties for railway application of ground-penetrating radar, in: Ninth International Conference on Ground Penetrating Radar (GPR2002). pp. 42–47.

Sussmann, T.R., Ruel, M., Christmer, S., 2012. Sources, Influence, and Criteria for Ballast Fouling Condition Assessment, in: Proceeding of the 91st Annual Meeting of the Transportation Research Board.

Sussmann, T.R., Selig, E.T., Hyslip, J.P., 2003. Railway track condition indicators from ground penetrating radar. NDT E Int. 36, 157–167.

The Finnish Geotechnical Society, 1992. Ground Penetrating Radar - Geophysical Research Methods. Tampere.

Tosti, F., Benedetto, A., 2012. Pavement pumping prediction using ground penetrating radar. Procedia-Soc. Behav. Sci. 53, 1045–1054.

TRB, 1998. Ground Penetrating Radar for evaluation subsurface conditions for transportation facilities. TRB.

Turtschy, J.C., Ooijen van, W.H., Fontul, S., Simonin, J.M., Ferne, B., Kokot, D., Sjögren, L., Hildebrand, G., Teng, P., 2004. Assessment of high speed monitoring equipment, Fully Optimised road Maintenance.

Tutumluer, E., Dombrow, W., Huang, H., 2008. Laboratory characterisation of coal dust fouled ballast behavior, in: Proceedings of the AREMA 2008 Annual Conference and Exposition. pp. 21–24.

Ulriksen, C.P.F., 1982. Application of impulse radar to civil engineering. Lund University of Technology, Lund.

Vale, C., Calçada, R., 2013. A dynamic vehicle-track interaction model for predicting the track degradation process. J. Infrastruct. Syst.

Van der Westhuizen, N.J., 2009. Optimisation of railway asset life cycle performance through a continuous asset improvement process as part of the maintenance management programme. SATC 2009.

Waite, A.H., Schmidt, S.J., 1962. Gross Errors in Height Indication from Pulsed Radar Altimeters Operating over Thick Ice or Snow. Proc. IRE 50, 1515–1520. doi:10.1109/JRPROC.1962.288195

Wenty, R., 2007. Plasser & Theurer machines and technologies applied for track maintenance of high-speed railway lines: a selection. Rail Eng. Int. 36.

Wenty, R., 2011. High speed precision tamping for high availability of track, in: Proceedings of the AREMA 2011 Annual Conference. Presented at the AREMA 2011, Minneapolis, MN.

Xu, P., Sun, Q., Liu, R., Wang, F., 2011. A short-range prediction model for track quality index. Proc. Inst. Mech. Eng. Part F J. Rail Rapid Transit 225, 277–285. doi:10.1177/2041301710392477

Yelf, R., 2007. Application of ground penetrating radar to civil and geotechnical engineering. Electromagn Phenom 7, 102–117.

Yilmaz, Ö., 2001. Seismic Data Analysis: Processing, Inversion, and Interpretation of Seismic Data. SEG Books.

Zhang, Q., Gascoyne, J., Eriksen, A., 2011. Characterisation of ballast materials in trackbed using ground penetrating radar: Part 1. IET, pp. 4A1–4A1. doi:10.1049/cp.2011.0593

Zhang, Y.-J., El-Sibaie, M., Lee, S., 2004. FRA track quality indices and distribution characteristics, in: Proc., AREMA Annual Conf.